The Stromal Ultrastructure of Normal and Pathologic Human Corneas

Thesis

The Stromal Ultrastructure of Normal and Pathologic Human Corneas.

ANDREW JAMES QUANTOCK, B.Sc.

Thesis submitted for the degree of Doctor of Philosophy in the Discipline of Biophysics.

The Biophysics Group,

Open University,
June, 1991.

Date of submission: 18th June 1991

Date of award: 2nd September 1991

ProQuest LLC.
789 East Eisenhower Parkway
P.O. Box 1346
Ann Arbor, MI 48106 – 1346

"The eye is the window of the human body through which it feels its way and enjoys the beauty of the world. Owing to the eye the soul is content to stay in its bodily prison, for without it such bodily prison is torture."

LEONARDO DA VINCI, 1452–1519.

Abstract

This thesis describes results and observations from an ultrastructural study of the stroma of various human corneo–scleral tissues. The major components of the stromal extracellular matrix are collagen fibrils and proteoglycan macromolecules. Their character and distribution in normal human cornea and sclera are first studied. The main thrust of the research then progressed to elucidating the ultrastructure in two pathologic conditions where proteoglycan anomalies were known to occur; macular corneal dystrophy and corneal oedema.

Transmission electron microscopical studies, employing the proteoglycan–specific stain Cuprolinic blue, demonstrated that the arrangement of proteoglycans, with respect to the collagen fibrils, in normal human cornea differs from other mammals in that there is more 'b' band association.

Meridional X–ray diffraction showed that the axial electron density of human scleral collagen was similar to rat tail tendon collagen. When used in conjunction with Cupromeronic blue–staining, it verified as non–artifactual the electron microscopical observation that proteoglycans associate with collagen near the 'd/e' staining bands in the gap zone.

Transmission electron microscopy revealed that macular dystrophy corneal stromas contain numerous collagen–free lacunae. Cuprolinic blue–staining further revealed that some of these lacunae contain congregations of various sized proteoglycan filaments. Enzyme digests identified these filaments as belonging to the chondroitin/dermatan sulphate population of proteoglycans. It was concluded that aggregation of chondroitin/dermatan sulphate proteoglycans often occurs in the macular dystrophy stroma. X–ray diffraction data supported the electron microscopical observation of normal collagen fibrils in the macular

dystrophy cornea. However, meridional X–ray data, from Cuprolinic blue–stained specimens, pointed to an abnormal distribution of proteoglycans along the collagen fibrils. Equatorial X–ray diffraction results indicated heterogeneous close packing of normal diameter collagen fibrils throughout the macular dystrophy stroma, this effect was deemed responsible for the central corneal thinning *in vivo*; a clinical feature of macular dystrophy. By using fresh tissue in the X–ray experiments, it was shown that that cryostorage of excised corneal buttons had no effect on the fibril dimensions. A collaboration was set up to analyse serum and corneal tissue immunochemically from the macular dystrophy patients, to characterise the type of macular dystrophy under investigation. There were no specific ultrastructural differences between type I and type II macular dystrophy stromas; an overall structural heterogeneity exists which indicates that the classification system is not, as yet, complete. High–angle X–ray patterns from macular dystrophy corneas contained two "extra reflections" not obtained from other human corneas, normal or pathologic. The reflections arise from 4.61Å and 9.62Å periodic structures which are considered to be glycosaminoglycan in origin.

Electron microscopy revealed the presence of "wavy" lamellae and various sized collagen free "lakes" in the stroma of the oedematous human cornea, with the posterior portion containing by far the largest "lakes". The existence of stromal "lakes" was further supported by the equatorial X–ray diffraction data. Cuprolinic blue–stained transmission electron micrographs demonstrated a D–periodic association of proteoglycans with collagen, which suggested a depletion of keratan sulphate in the oedematous stroma; this was backed–up by immunochemical evidence. Large proteoglycan filaments (possibly chondroitin/dermatan sulphate) were observed in some parts of the extracellular matrix. Scheie's syndrome corneal stromas, which contain no α–L–iduronidase, also contained dense Cuprolinic blue–stained deposits. The possibility exists that aggregation of corneal chondroitin/dermatan sulphate is a common factor of several corneal pathologies.

Acknowledgements

By far the biggest vote of thanks, in the production of this thesis, must go to my supervisor, and Chairman of the Biophysics Group, Dr. Keith Meek. His guidance and friendship have been of great value, and his enthusiasm a constant source of encouragement during my attacks of apathy. It has been a pleasure to work alongside him. Professor Gerald Elliott, Director of the Oxford Research Unit, is warmly thanked for encouraging and looking after the interests of, not just myself, but all the Ph.D. students.

I owe a debt of gratitude to my colleagues, especially Dr. Rita Wall and Mr. Nigel Fullwood; Rita for all the help, especially biochemical, that she has extended and also for managing to remain cheerful and pleasant whilst sharing an office with me for the past four years; Nigel for showing me how the scanning electron microscope works and for freely offering criticism (some of it constructive) about all aspects of everything.

The collaboration with Professor Eugene Thonar (Rush–Presbyterian–St. Luke's Medical Center, Chicago) was essential for publication of the macular dystrophy work. The participation of the clinicians, Mr. Alan Ridgway, Mr. Andrew Tullo (both Royal Eye Hospital, Manchester), Professor Anthony Bron (Nuffield Department of Ophthalmology, Oxford), Dr. Paul Brittan (Wolverhampton Eye Infirmary) and Dr. Ralph Zabel (Ottawa General Hospital), in this project was invaluable.

I thank Mrs. Naomi Williams (Open University) for introducing me to the transmission electron microscopes; Dr. Wim Bras, Dr. Liz Towns–Andrews and Dr. Colin Jackson, plus my colleagues in the Biophysics group Nageena Malik and Ian Rawe, for their assistance at the Daresbury Synchrotron over the past three and a half years; Mr. Boris Marcynuik (Manager, Manchester Eye Bank) for corneal storage facilities; Dr. Bruce Caterson (University of North Carolina) for providing the

anti-keratan sulphate monoclonal antibody; Dr. Alan Horwitz and Dr. Martin Mathews (University of Chicago) for supplying the international standard for keratan sulphate.

I deeply appreciate the encouragement/nagging of my family and friends. Thanks go out to Màire for giving me two weeks of relaxation and space in Belfast in which to start to "write up", to Harj. for his infectious enthusiasm, to Rachel for help with the manuscript and to all the other friends who, unknown to them, encouraged me in ways too trivial to mention.

Contents

List of Figures

List of Tables

Chapter 1

Introduction

Corneal transparency is of vital importance to the function of the eye. This transparency, unique to the cornea amongst all other bodily connective tissues, is occasionally affected by injury or disease processes which alter the corneal ultrastructure. Preservation of the stromal architecture therefore seems to be essential to the maintenance of corneal transparency. In this thesis human sclera, normal human corneas and pathological human corneas will be studied in order to elucidate their structures, observe the differences and contemplate implications for transparency.

1.1 Anatomy of the Eye

The eyeball, whose diameter is on average 24mm, has three main layers each of which is further divided (figure 1.1). The outer supporting coat consists of the transparent cornea, the opaque sclera and the junction of the two, the corneo-scleral limbus. It is constructed principally from collagen, a fibrous protein with high tensile strength and low extensibility. This outer coat is inflated by the compressed intraocular fluid into a shape resembling the segments of two spheres. The radius of curvature is about 13mm for the sclera and about 7.5mm for the cornea. The white sclera

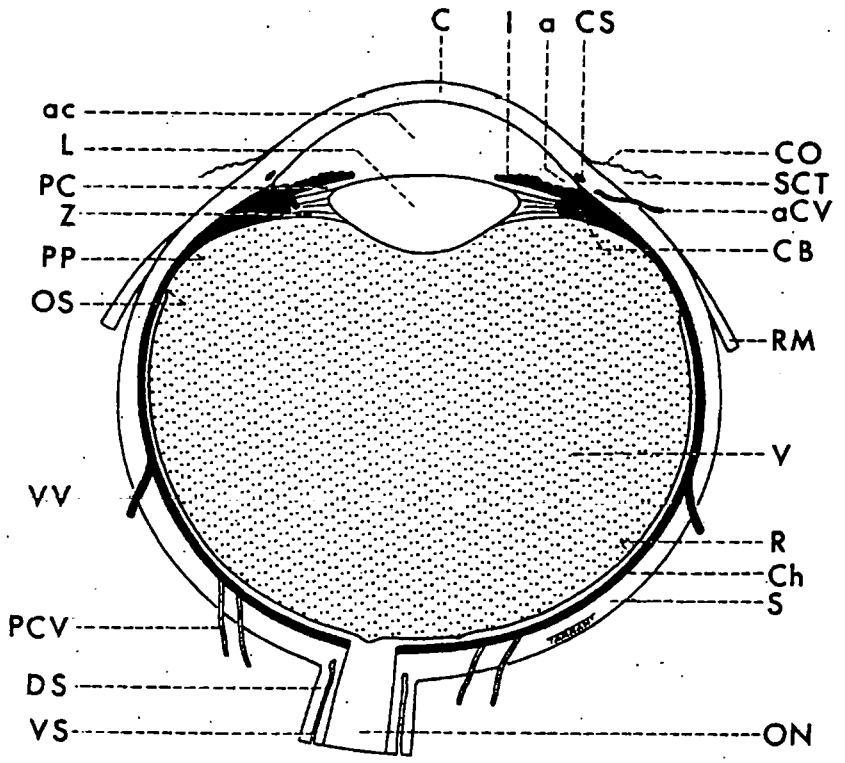

Fig. 1.2 Diagram of a longitudinal section of the eyeball: a, angle of anterior chamber; ac, anterior chamber; aCV, anterior ciliary vessel; C, cornea; CB, ciliary body; Ch, choroid; CO, ocular conjunctiva; CS, canal of Schlemm; DS, dural sheath; I, iris; L, lens; ON, optic nerve; OS, ora serrata; PC, posterior chamber; PCV, posterior ciliary vessel; PP, pars plana; R, retina; RM, rectus muscle; S, sclera; SCT, sub-conjunctival tissue; V, vitreous; VS, vaginal sheath; VV, vortex vein; Z, zonule

Figure 1.1 Anatomy of the eye. Reproduced from Miller, 1990.

constitutes the posterior five sixths of the eyeball with the transparent cornea contributing the anterior one sixth. The sclera has a particularly firm consistency at the limbus and is capable of determining the shape of the eye without the help of the cornea (Newell, 1982; Maurice, 1988).

1.2 Anatomy of the Cornea and Sclera

The cornea, a transparent, avascular, membranous tissue, is the main refracting structure of the eye. Its central area supports the air/tear film interface which contributes four fifths of the eye's refracting power. The

cornea in humans measures 10.8mm vertically and 11.7mm horizontally at its anterior surface; its posterior surface is circular with a diameter of 11.7mm. The central area in humans is about 0.52mm thick, gradually increasing up to about 0.65mm at the periphery (Buckley, 1987; Newell, 1982). The human cornea has five layers as shown in figure 1.2.

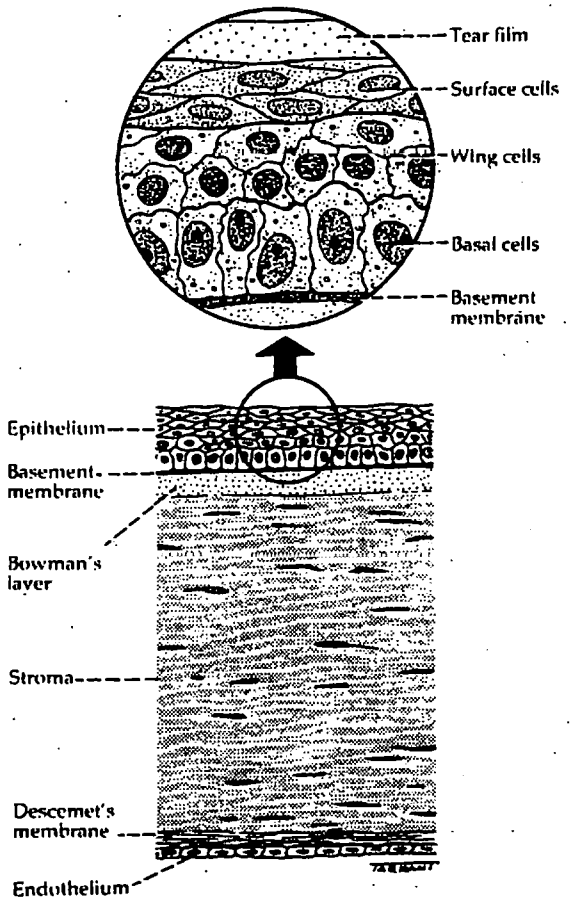

Figure 1.2 Anatomy of the cornea. Reproduced from Kanski, 1984.

The epithelium accounts for 10% of the corneal thickness and is made up of three types of cell. A single layer of basal cells are attached to the basement membrane by hemidesmosomes, a lack of which may be responsible for recurrent corneal erosions. Adjacent to the basal cell layer

are two or three rows of wing-shaped cells, then two layers of surface cells. Both these types of cell derive from the basal cells. The outermost surface cells have their surface area increased by the presence of microvilli and microplicae in order to facilitate interaction with the tear film. After a lifespan of a few days the surface cells are shed into the tears, giving an epithelial turnover time of about 7 days. Because of the epithelium's excellent ability to regenerate (surrounding cells spread within hours to fill a defect in a traumatised basement membrane) the epithelium itself does not scar. However scarring can develop immediately below the epithelium (Buckley, 1987; Kanski, 1984).

Bowman's layer constitutes about 2% of the corneal thickness and is an acellular condensation of collagen, a superficial layer of the stroma. It is mechanically very resistant to tensile deformation but does not regenerate when damaged. Its mechanical resilience restrains the cornea anteriorly, ensuring that stromal swelling proceeds in a posterior direction (Buckley, 1987; Kanski, 1984).

The stroma is bounded posteriorly by Descemet's membrane which, in an adult, represents about 3% of the total corneal thickness. It is the basement membrane secreted by the endothelium through life, and from birth to old age it increases in thickness from about 20μm to 200μm. Descemet's' membrane consists of amorphously arranged collagen and glycoproteins including fibronectin. It is very resistant to trauma and pathological processes (Buckley, 1987; Kanski, 1984).

The endothelium, which forms the posterior 1% of the cornea, consists of a single layer of hexagonal cells. It plays a vital role in maintaining the state of hydration of the stroma by acting as a metabolic pump which opposes the osmotic properties of the hydrophilic stromal proteoglycans (Mishima & Kudo, 1967). The endothelial cells are not regenerated so there is a gradual decrease in their numbers with age. Neighbouring cells spread in order to fill any vacant gaps. The endothelium has a considerable functional reserve and it is likely that up to 80% of the cells

may be lost before corneal stability is affected (Buckley, 1987; Kanski, 1984).

The stroma constitutes the bulk of the corneal thickness, about 84% (Buckley, 1987). It consists of collagen fibrils, regularly arranged and of uniform diameter, which lie parallel to the surface of the cornea in wide thin lamellae (figure 1.2). The thickness of the stroma is made up from about 200 of these lamellae, each one of which seems to run uninterrupted from limbus to limbus (Maurice, 1988). The fibrils within adjacent stromal lamellae run at angles to each another and in the human cornea it has been demonstrated that they are preferentially oriented at right angles to one another, tending to a medial–lateral, inferior–superior organisation (Meek et al., 1987a,b). A basic analogy can be drawn with the structure of plywood. Corneal fibrils extend to the limbus where they tend to curve around and run circumferentially, either forming a belt around the limbus or following a circular course from one point on the limbus to another (Maurice, 1988; Meek et al., 1987a,b). The major stromal component is collagen; its contribution to the dry weight of the cornea has been variously reported as 65% in bovine cornea (Maurice, 1969), as 71% (Newsome et al., 1981) and 90–95% in normal human cornea (Winterhalter et al., 1988), although this last figure may be an over–estimate. The fibrils are embedded in a matrix which consists mainly of proteoglycans. The stroma is populated by keratocytes, lying in and between the lamellae, which have long, slender, branching communication processes. These keratocytes are involved in proteoglycan synthesis and secondary collagen fibrillogenesis (Birk & Trelstad, 1984), the primary stroma seemingly being laid down by the epithelium (Hay & Revel, 1969). The keratocytes are not static but are free to move through the stroma in response to a number of stimuli (Buckley,1987).

The fibrous bands seen in microscopical images of the scleral stroma are a continuation of the corneal lamellae which run uninterrupted across the limbus (Maurice, 1969). The scleral lamellae contain collagen fibrils with a diameter range from 30nm to 300nm (Schwartz, 1953). The matrix of

predominantly proteoglycans is also different to that found in the adjacent cornea.

1.2.1 Molecular Collagen Structure

The most prevalent collagen in the human cornea is type I collagen, one of the family of fibril forming collagens. Each type I collagen molecule consists of three left-handed helical polypeptides, mutually staggered by one residue, which form into a triple helix. Each type I polypeptide contains about 1000 residues, there are 3.27 residues per turn and the molecule itself is about 300nm long. Due to steric restrictions every third residue has to be glycine, the polypeptide can therefore be represented by $[\text{Glycine–X–Y}]_n$ where X and Y are commonly proline and hydroxyproline respectively. This Glycine–proline–hydroxyproline triplet forms about 10% of the polypeptide. Each polypeptide is stabilized by the steric repulsion of the pyrrolodine rings of the proline residues. The triple helix is cross-linked by hydrogen bonds between the three polypeptides which involve the lysine and hydroxylysine residues (Nimni & Harkness, 1988). The triple helical molecule is bounded by small non–helical N– and C–domains called telopeptides. The intramolecular cross–links occur mainly via the telopeptides due to their high content of hydroxylysine residues (Bailey, 1975). The molecule is also stabilised by ionic interactions between charged residues on adjacent polypeptides (Parry, 1988).

Along with type I collagen, the human corneal stroma also contains lesser proportions of other collagen types, in particular types III and V, both of which are of the the fibril forming variety (Newsome et al., 1982). The collagen types are distinguished by differences in the amino acid sequence of the polypeptide helices. Type I collagen consists of two α1(I) chains and one α2(I) chain with the triplet region extending for 1014 residues in each case (Parry, 1988). Type III collagen is made up of three α1(III) chains and type V collagen contains three chains classified as α1(V), α2(V) and α3(V). The amino acid sequence of the α1(I), α2(I) and

α1(III) chains has revealed the presence of four repeat units of 234 residues in each of the chains (Miller, 1988); this is an important condition for collagen fibril formation. Immunolocalisation studies on chick cornea found that type I and type V collagens could be co-distributed within the same fibril (Birk et al., 1986). Nakayasu et al. (1986) concluded that type V collagen is located on or close to the stromal fibrils in human cornea and that type III collagen may well form hybrid fibrils with type I collagen. The proportion of type III collagen included with type I collagen effects the diameter of the hybrid fibrils formed *in vitro* (Lapiere et al., 1977). This could bear some relation *in vivo* to the occurrence of large heterogeneous fibril diameters in human sclera where the proportion of type III collagen rises to 35% compared to about 10% in the human cornea (Newsome et al., 1981). The axial distribution of charged amino acid residues in type V collagen molecules has been shown to be similar to that of type I molecules. Furthermore the electron microscopical D-periodic banding pattern of type I/type V hybrid fibrils is identical to that of pure type I fibrils (Adachi & Hayashi, 1987). Type VI collagen is present in the bovine corneal stroma (Murata et al., 1989) and has also been located in the human cornea where it is considered to be one of the major extracellular components (Zimmerman et al., 1986). Unlike the molecules of types I, III and V collagens which contain the characteristic $[\text{Glycine–X–Y}]_n$ repeat, the amino acid sequence of type VI collagen, along with some other minor corneal collagens, possess interruptions at various positions along its polypeptide chain. These collagens, therefore, do not form fibrils but do self-assemble in specific ways to form biological networks (Veis & Payne, 1988).

The cornea also contains small quantities of other minor collagens. Type IV collagen is present in the basement membrane of the corneal epithelium in human cornea (Newsome et al., 1981; Nakayasu et al., 1986) although some has been detected in the murine corneal stroma (Pratt & Madri, 1985). In human cornea type VII collagen forms globular domains and anchoring fibrils which play a role in epithelial adhesion. The fibrils

interact with type IV collagen in the epithelial basement membrane and on average extend only 0.6 μm into the human stroma (Gipson et al., 1987).

In conclusion the human corneal stroma is predominantly composed of type I collagen with considerably lesser amounts of types III and V; these species are able to associate with each other in the form of cross-banded fibrils which are visualised in the transmission microscope by heavy metal stains. Type VI collagen is also present in considerable amounts, but is a non-fibril forming collagen.

1.2.2 Fibrillar Collagen Structure

Collagen fibrils are formed by the lateral packing of collagen molecules, axially staggered by the repeat unit of about 234 amino acid residues (see figure 1.3). The axial stagger is equal to approximately a quarter of the length of the helical portion of the molecule. This particular conformation is due to the tendency of charged and hydrophobic residues to occur in groups (Chapman et al., 1990). This quarter–stagger theory of molecular packing was prompted by electron-microscopical observations of collagen fibrils by Hodge & Petruska (1963) (see chapter 1.5). The fibrils are stabilized by the formation of covalent intermolecular cross-links involving hydroxylysine residues in the telopeptides, with the exception of the C-terminus of the α2(I) chain (Parry, 1988).

1.2.3 Proteoglycan Structure

Proteoglycans are macromolecules which consist of a protein core or backbone to which one or more glycosaminoglycan side chains are covalently bound via a linkage region. The glycosaminoglycan side chains which give the proteoglycans their classification consist of repeating disaccharide units (figure 1.4) and are named after the tissue from which

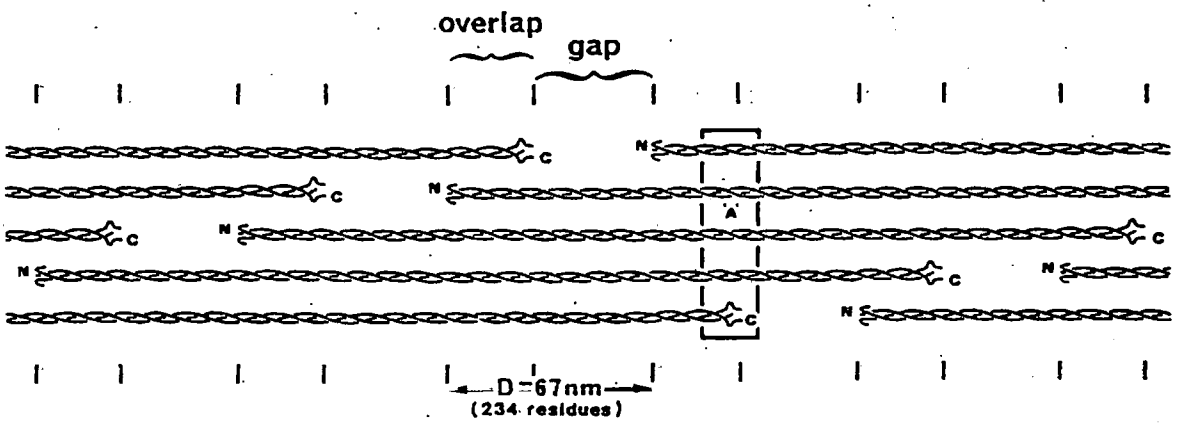

Figure 1.3 A schematic representation of the axial relationships in a collagen fibril based on the quarter–stagger theory of Hodge & Petruska (1963). At the end of each molecule (made up of three helically wound polypeptide chains) the N and C telopeptides are labelled. Reproduced from Chapman et al., 1990.

they were first extracted (Poole, 1986). Proteoglycans occur in a wide variety of tissues and exhibit a heterogeneity both in size and content. Cartilage, for example, contains "very large", space-filling proteoglycans with 150-200 KD core proteins and up to 200 glycosaminoglycan side chains of both the keratan sulphate and chondroitin sulphate variety (Hardingham et al., 1986).

Chondroitin sulphate glycosaminoglycans by definition contain glucuronic acid and do not contain iduronic acid. The chondroitin sulphate glycosaminoglycans in the cornea, however, do contain some iduronic acid (about 10% for bovine (Axelsson & Heinegard, 1975)) which qualifies the glycosaminoglycan as dermatan sulphate (Stuhlsatz et al., 1972). Hence

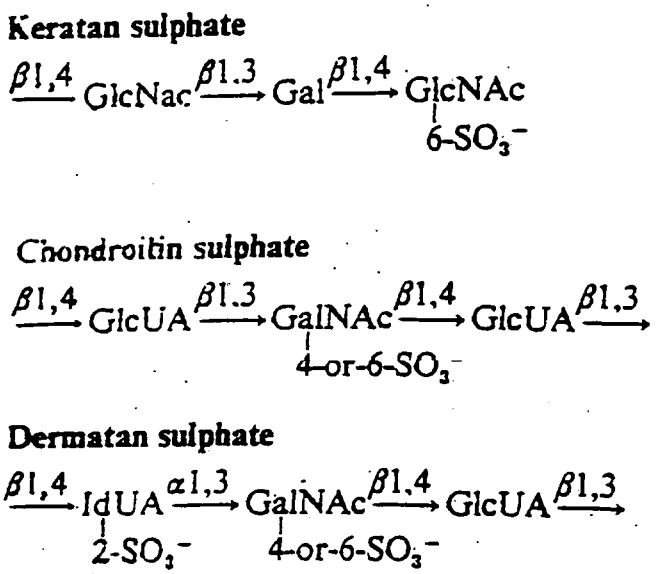

Figure 1.4 The chemical structure of the main corneal glycosaminoglycans. Reproduced from Poole, 1986.

the classification of these corneal proteoglycans varies and seems to depend on what proportion of the uronic acid is iduronic or glucuronic. This classification in the literature appears to be interchangeable and varies between chondroitin sulphate (Bansal et al., 1989), glucuronic-rich dermatan sulphate (Poole, 1986), proteodermatan sulphate (Gregory et al., 1988), dermatan sulphate (Scott, 1988a) and chondroitin/dermatan sulphate (Scott & Haigh, 1988). If referring I will use the nomenclature quoted in the relevant publication, otherwise I will use the term chondroitin/dermatan sulphate.

The rabbit corneal stroma contains two main classes of proteoglycan. Keratan sulphate proteoglycans (molecular weight~100KD) consist of a

protein core to which either one or two keratan sulphate side chains are linked (Gregory et al., 1982). Dermatan sulphate proteoglycans from bovine cornea have one dermatan sulphate glycosaminoglycan (molecular weight~55KD) linked to a 40KD protein core (Axelsson & Heinegård, 1975). The glycosaminoglycan chains consist of 10–100 repeating disaccharide units (Scott, 1988b). No detailed study of human ocular proteoglycans has been published but from parallels with other mammalian species it is expected that the human ocular tissues investigated in this thesis contain "small" proteoglycans with only one or two side chains.

Two types of proteoglycan have been isolated from bovine sclera (Cöster & Fransson, 1981). The"large" one (molecular weight~160–410 KD) contained several side chains with approximately 10% iduronic acid whereas the "small" one (molecular weight~70–100KD) had between one and three side chains which were rich in iduronic acid. Comparison with two similar dermatan sulphate proteoglycans found in tendon (Vogel & Heinegård, 1983) led to the conclusion that the "small" dermatan sulphate proteoglycan associates with the gap zone of the collagen fibril whilst the "large" one is interfibrillar (Scott & Orford, 1981; Scott & Haigh, 1985b). The "small" dermatan sulphate proteoglycan in sclera shows immunological identity and peptide pattern similarity to those in bone, tendon and cornea (Hardingham et al., 1985).

1.3 Electron Microscopy

Transmission electron microscopy has been extensively employed, along with specific staining methods for collagen and proteoglycans, in the determination of scleral and corneal ultrastructure. Scanning electron microscopy has not been so widely employed but can yield information about the lamellar structure of the tissues.

1.3.1 Staining of Collagen Fibrils

Collagen fibrils stained with heavy metal salts exhibit a characteristic banding pattern due to the preferential attachment of heavy metal ions to charged amino acid residues (Hodge & Schmitt, 1960). The staining pattern repeats itself every 65nm for corneal collagen (67nm for tendon), due to the fact that the molecules are axially staggered by multiples of 65nm, i.e. 234 residues (see chapter 1.3). The repeat distance is referred to as the D-period. For type I collagen, since the molecules have length ~4.4D, the architecture of the fibril is constrained to include a "gap–overlap" system as seen in figure 1.3 (Hodge & Petruska, 1963). The length of the collagen molecule has more recently been put at 4.47D (Parry, 1988). The overlap zone (length~0.47D) and the gap zone (length~0.53D) contain laterally packed molecules in the ratio 5:4. Amino acid sequence data from the α1(I) and α2(I) chains have allowed the distribution of residues to be correlated with the banded staining pattern of type I collagen fibrils (Meek et al., 1979).

Figure 1.5 shows the conventional notation for the positive staining bands (Hodge & Schmitt, 1960). From right to left;

(a) The four evenly spaced 'a' bands,'a_1', 'a_2', 'a_3' and 'a_4'; 'a_4' is slightly weaker than the others.

(b) The 'b' doublet, 'b_1' and'b_2'.

(c) A weak 'c_1', a strong 'c_2' and a very weak 'c_3'.

(d) A strong broad 'd' band.

(e) A diffuse 'e' doublet, 'e_1' and 'e_2' tending to merge together.

The boundaries of the gap and overlap zones are around the bands 'c_2' and 'a_3', the 'd/e' bands being at the centre of the gap and the 'b' doublet being within the overlap. The electron microscopical appearance of the type I collagen-rich fibrils will not be affected by the presence of varying amounts of type V molecules within the fibril (Adachi & Hayashi, 1987).

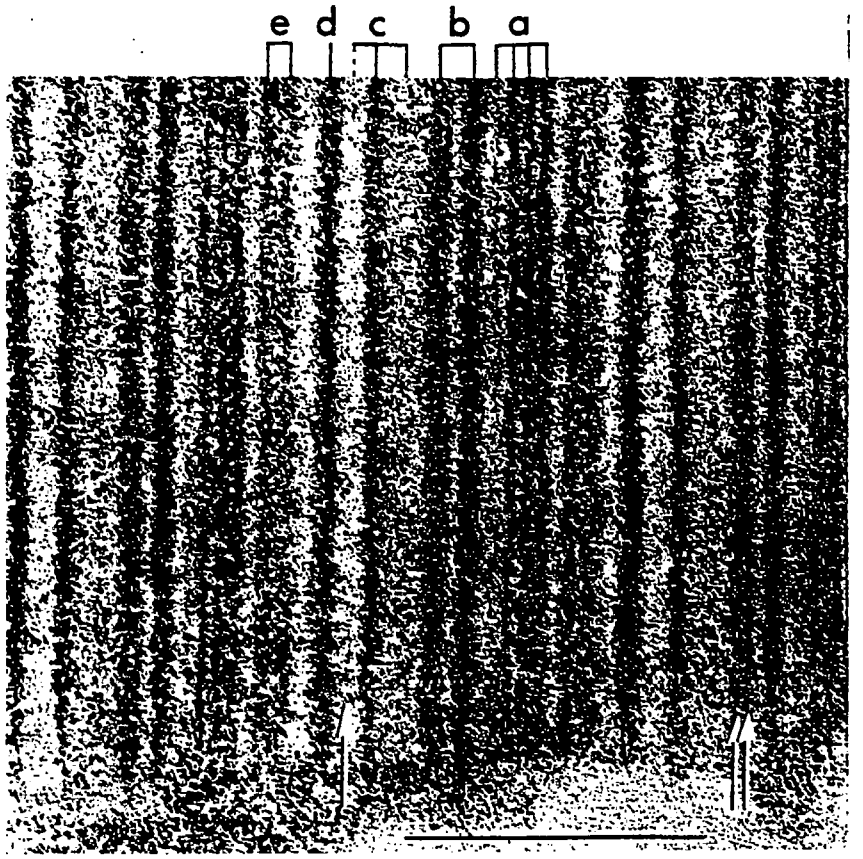

Figure 1.5 The banding pattern of a collagen fibril positively stained with metal containing anions and cations. The very weak c_3 band is indicated by a single arrow; the doublet character of the b_2 band is indicated by twin arrows. Bar=1 D–period (67nm in the native state). Reproduced from Chapman, 1974.

1.3.2 Staining of Proteoglycans

The electron density of proteoglycans is very low so if their distribution is to be observed in the electron microscope their contrast must be enhanced. This can be achieved by staining the proteoglycans with the cationic copper based dye Cuprolinic blue, or its isomer Cupromeronic blue,[1]in the "critical electrolyte concentration" mode (Scott, 1980; Scott et al., 1981). The concentration of the electrolyte (typically $MgCl_2$) included in the staining solution influences the extent to which the stain is taken up by the polyanionic glycosaminoglycans. Anions from the electrolyte (i.e. Cl^-) attached to some of the positive charges on the dye lead to a more intense staining pattern. However, if there is an excess of anions they compete with the proteoglycans for the attention of the dye. Hence for optimum staining the concentration of the electrolyte is critical. Cuprolinic blue enables predominantly sulphated glycosaminoglycans to be stained and brings about a partial collapse of the glycosaminoglycan side chains onto the proteoglycan protein core. The electron density of the Cuprolinic blue/dye complex is greatly enhanced by replacing the Cl^- anion with one with a higher electron density e.g. tungstate (Scott, 1980).

1.4 X–Ray Diffraction

X-ray diffraction is a non–invasive technique which can successfully be used to yield information about the distribution of periodic structures within connective tissues. The amount of information extractable from a connective tissue X–ray pattern depends upon the extent of order within the tissue. In a perfect crystal the X–ray information can lead to a direct determination of structure. However, since a connective tissue is much less ordered than a crystal structure, the X–ray information is used to suggest or refine structural models (Brodsky et al., 1988). The order in

[1]The stains behave identically except that Cupromeronic blue is thought to have a slightly higher specificity and appears to produce finer filaments in the electron microscope.

connective tissues occurs at various levels; order in the axial form of the triple helix, order in the lateral packing of the collagen molecules, order in the diameters and lateral packing of the collagen fibrils and order in the D–periodic repeat along each fibril axis. Orientation of collagen fibrils is another factor which affects the diffraction pattern.

The X-ray diffraction pattern consists of two components, parallel and perpendicular to the collagen axis, called meridional and equatorial reflections respectively. The meridional reflections arise from the periodic distribution of matter along the collagen fibrils whilst the equatorial reflections represent the lateral order in packing and diameter of the fibrils. A reduction in the lateral order of the fibrils will lead to a smearing of the equatorial maxima (Brodsky et al., 1988). Collagen fibrils run approximately parallel to one another within a single lamella but where there is little or no preferential orientation of lamellae the net effect throughout a specimen is to have no preferred fibrillar orientation. When this occurs, as in the case of bovine cornea, the scattered intensity is spread over 360° and the pattern becomes more circular and diffuse. This phenomenon enables the extent of collagen orientation within a tissue to be estimated; this type of analysis has been carried out on articular cartilage (Aspden & Hukins, 1981) and human corneal stroma (Meek et al., 1987a,b).

Contributions to an X-ray diffraction pattern obtained from a whole native tissue come solely from the periodic ordered structures, the unordered ones merely serve to increase random background scatter. Derivation of a structural model of a tissue by X-ray diffraction is often complemented by direct observation techniques such as electron microscopy. X-ray diffraction has the advantage over electron microscopy in that specimens can be examined in a hydrated, unprocessed state thus nullifying the risk of assuming that electron microscopical preparative artifacts represent actual *in vivo* tissue components.

All the X–ray work to be described in this dissertation, along with some

previous studies already discussed, has been carried out on the very high intensity S.E.R.C. synchrotron X–ray source at Daresbury, U.K. This is advantageous since corneal organisation is weak compared to other fibrous tissues, such as tendon or muscle, which have been studied by X–ray diffraction. X–ray patterns which require exposures of at least 24 hours on conventional laboratory X–ray sets can be obtained with an exposure time of several minutes. For short exposures the increased X–ray intensity has negligible detrimental effect on the corneal tissue due to the comparative energetics of the two systems which produce a much better signal to noise ratio. The reduced time span in the X–ray beam also has a beneficial effect on the tissue; hydration is more easily controlled and any *in vitro* distortions greatly reduced to obtain a more representative non–dynamic, steady–state picture.

1.4.1 Equatorial X–Ray Diffraction of the Cornea and Sclera

High–angle X-ray diffraction elucidates periodic structures on the nanometer scale and can therefore be used to calculate the intermolecular packing within collagen fibrils (Ramachandran, 1967). The only modern high–angle study has been carried out on bovine cornea (Meek et al., in press). Synchrotron X-ray diffraction studies on the corneas, equilibrated to various hydrations, show that around physiological hydrations the intermolecular spacing is 1.8 nm. The intermolecular spacing remains fairly constant with hydration around the physiological value. The high–angle intermolecular pattern for scleral tissue has not been previously obtained.

The low–angle equatorial X-ray diffraction pattern from the corneal stroma gives a measure of the interfibrillar packing of the collagen fibrils (Sayers et al., 1982; Worthington & Inoyue, 1985). It has been analysed for a wide range of mammals, fish and birds with the discovery that fish

and aquatic mammals have more densely packed fibrils in the stroma. Mammalian corneas were shown to contain a species–dependant variation in the packing of their fibrils. There is also a range of spacings within each cornea, greater in some species than others. The collagen interfibrillar spacing for human cornea at about physiological hydration was calculated to be 61.9nm (±4.5nm) (Gyi et al., 1988). The low–angle equatorial pattern also contains information about the diameters of the collagen fibrils. The diameter can be obtained from analysis of the dimensions of the equatorial pattern outside the first order interfibrillar reflection (Worthington & Inoyue, 1985). Fibril diameters have been calculated from frog cornea to be 37nm (Worthington & Inoyue, 1985) and from rabbit cornea to be 39nm (Brodsky et al., 1988). The interspecies variation of fibril diameters and interfibrillar spacings has led to the postulation that the all–important feature of the transparent cornea could be the surface to surface separation of the collagen fibrils (Gyi et al., 1988).

A transmission electron microscope study of corneal collagen fibril diameters from various species, unlike the X-ray diffraction study of Gyi et al. (1988), found no variation between species (Craig & Parry, 1981). However, the fibrils observed microscopically were all of the dehydrated, fixed and embedded tissue. Indeed, using a low–temperature protocol, which goes some way towards preserving structure, substantially larger fibril diameters have been noticed in the electron microscope (Craig et al., 1986). Comparing data demonstrates that conventional electron microscopy of cornea (Craig & Parry, 1981) represents a more or less uniform shrinkage of fibril diameters and interfibrillar spacings by about 25% from the X-ray diffraction values (Gyi et al., 1988). It seems, therefore, that the equatorial X-ray diffraction data from the fresh tissue give a better *in vivo* representation of the lateral corneal architecture. As mentioned in chapter 1.2 the preferred orientation of collagen fibrils in the central zone of human corneal stroma is in a medial–lateral, inferior–superior orthogonal arrangement (Meek et al., 1987a,b). This has the affect of producing four symmetrical lobes in two orthogonal

directions in the equatorial X-ray diffraction rings. It is not understood why this affect is so pronounced in the human cornea.

No low–angle equatorial X-ray diffraction pattern can be obtained from sclera because the variation in the diameters and the packing of the fibrils is too great (Borcherding et al., 1975).

1.4.2 Meridional X–Ray Diffraction of the Cornea and Sclera

The meridional X-ray diffraction pattern from cornea can be used to deduce the axial electron density, i.e. the distribution of matter, along the collagen fibrils (Meek et al., 1981a). In addition to the intensities of the meridional orders, the phase of each reflection is required in order to calculate the axial electron density distribution. The phase of each reflection is related to the relative time of arrival of each each X–ray photon at the photographic plate. It is not measurable in the experiment. Phases for an X-ray diffraction pattern can be obtained, for example, from models derived from known amino acid sequences (Hulmes et al., 1977) or from isomorphous replacement techniques (Bradshaw et al., 1989). Alternatively a model of assumed structure can be constructed from data obtained by other methods such as electron microscopy. Phases determined using this model are combined with the observed meridional intensities to form a representation of the axial electron density (Tomlin & Worthington, 1956; Meek et al., 1983). In most collagen–containing tissues, the most intense meridional reflection is the first order, which arises mostly from the step in electron density between the gap and overlap regions of the characteristic 67nm (65nm in cornea) repeating D–period (Tomlin & Worthington, 1956). This, however, was noticed to be absent in X-ray diffraction patterns obtained from bovine cornea, probably due to the presence of some material occupying a large proportion of the gap zone of the fibril (Goodfellow et al., 1978; Meek et

al., 1981a,b). Bovine corneas contain proteoglycans in the gap zone of the collagen fibrils but there is uncertainty as to whether or not their electron density is sufficient to affect the X-ray diffraction pattern (Meek et al., 1986). When a structural glycoprotein (molecular weight~135KD) was extracted from bovine corneal stroma, the first order meridional reflection was rendered visible, thus suggesting that the glycoprotein was removed from the gap zone (Wall et al., 1988). The meridional first order reflection is present, however, in X-ray diffraction patterns obtained from the human corneal stroma, and the axial electron density distribution differs significantly from that obtained from the bovine corneal stroma (Meek et al., 1983). These differences were attributed to different collagen/proteoglycan arrangements, of unknown function, between the species. Any periodic binding of non–collagenous matrix components to collagen fibrils results in alterations in the relative intensities of the meridional reflections provided the components are sufficiently electron dense. Non–specific binding would merely increase the levels of background scatter. Treatment of bovine cornea with the proteoglycan stain Cupromeronic blue in conjunction with meridional X-ray diffraction has enabled the extra electron density due to the proteoglycans to be located in relation to the collagen fibrils. The proteoglycans occur at the 'a','c', 'd' and 'e' collagen staining bands (Meek et al., 1986).

1.5 Proteoglycan/Collagen Interactions in Connective Tissues

Connective tissue collagens co-exist in intimate contact with proteoglycans and there is a long history of speculation related to the possible influence that proteoglycans have on the structure and function of collagen fibrils. The use of the proteoglycan dyes, Cuprolinic blue and Cupromeronic blue, in conjunction with uranyl acetate staining of collagen and electron microscopy, has enabled the proteoglycans to be

located in various connective tissues (Scott & Haigh, 1985a). Since cornea contains more than one type of proteoglycan, enzyme digestion of glycosaminoglycans within a population of proteoglycans, prior to staining, allows the remaining undigested proteoglycans containing the other glycosaminoglycans to be located. Hence the organization of a specific type of proteoglycan can be observed (Scott & Orford, 1981; Scott & Haigh, 1985a,b). Dermatan sulphate proteoglycans have been located at the 'd' and 'e' staining bands of type I collagen-rich tissues such as tendon (Scott, 1980; Scott & Orford, 1981), skin (Scott & Haigh, 1985a), heart valve (Nakao & Bashey, 1972), intervertebral disc (Scott & Haigh, 1986) and articular cartilage (Orford & Gardner, 1984). Meridional X-ray diffraction techniques have also located proteoglycans at the 'd/e' bands in fresh rat tail tendon, thereby supporting the electron optical observations (Meek et al., 1985).

1.5.1 Proteoglycan/Collagen Arrangement in Sclera

Using the aforementioned electron microscopical techniques dermatan sulphate proteoglycans have been located at the 'd/e' staining bands in the gap zone of collagen fibrils from mouse sclera (Scott & Haigh, 1985b). Similar methods have also led to reports of their presence at the 'd' band in both rabbit and human sclera. This specific association was evident throughout all levels of the sclera despite considerable variations in fibril diameter (Young, 1985). Depletion of scleral proteoglycans has been reported to precede the degradation of scleral collagen in an inflammatory disease of the human sclera called necrotizing scleritis (Young et al., 1988).

1.5.2 Proteoglycan/Collagen Arrangement in Cornea

Proteoglycan binding in the cornea is more complex than in the sclera since the corneal stroma contains keratan sulphate proteoglycans along

with chondroitin/dermatan sulphate proteoglycans (see chapter 1.23). Unlike sclera, a proportion of the gap zones ('d/e' bands) in the cornea remain unoccupied by proteoglycans (Scott & Haigh, 1985a).

Early microscopical studies suggested the existence of a regular association between proteoglycans and collagen fibrils in rabbit cornea (Smith & Frame, 1969). More recently Cuprolinic blue and Cupromeronic blue have been employed demonstrating association of keratan sulphate and chondroitin sulphate with collagen fibrils in the adult rat cornea (Velasco & Hidalgo, 1988). Proteoglycans in the rabbit cornea were noticed to be arranged orthogonally to the fibrils and after incubation of corneal samples with keratanase the remainder appeared to associate in the gap zone of the fibrils at the 'd' band (Scott & Haigh, 1985a). Further observations of keratanase and chondroitinase ABC rabbit corneal digests demonstrated that keratan sulphate proteoglycans associate with the collagen at the 'a' and 'c' bands, whilst chondroitin/dermatan sulphate proteoglycans are located at the 'd' and 'e' bands. This 'd/e' band association of chondroitin/dermatan sulphate proteoglycans has been seen in all other connective tissues so far studied (Scott & Haigh, 1985b). Rabbit cornea contains two types of dermatan sulphate proteoglycan and two types of keratan sulphate proteoglycan varying in their protein cores (Gregory et al., 1982). A similarity existed between the percentage of keratan sulphate proteoglycans at a certain binding site and the percentage with a certain type of protein core. A similar relationship was evident for the chondroitin/dermatan sulphate proteoglycans. This indirectly implied that each proteoglycan bound specifically to one of the four binding sites (Scott & Haigh, 1985b). This implication was confirmed using specific enzyme digestions (Scott & Haigh, 1988a).

The keratan sulphate proteoglycan content of the corneal stroma shows remarkable interspecies variation (Scott & Haigh, 1988a). The ratio of keratan sulphate content to total glycosaminoglycan content increases with increasing size of the cornea. Keratan sulphate is absent from mouse cornea with proteoglycans associating with collagen mainly at the 'd'

band. Rat and rabbit demonstrated 'a','c','d' and 'e' band occupancy (Scott & Haigh, 1988b) supporting the proposal that keratan sulphate proteoglycans associate with the 'a' and 'c' collagen bands in these species. Hence keratan sulphate content was noticed to be directly proportional to corneal thickness. This work led to the hypothesis that keratan sulphate proteoglycan is a "stand in" for chondroitin/dermatan sulphate proteoglycan in conditions of oxygen lack. In contrast to the interspecies variation in the relationship of the keratan sulphate proteoglycan with the collagen, the chondroitin/dermatan sulphate proteoglycans are found in all corneas and retain a constant relationship with the fibrils (Scott & Haigh, 1988b).

All the structural information so far mentioned about the intimacy of collagen and proteoglycans has been gained from the location of Cuprolinic blue in electron microscope prepared tissue. The collagen fibrils shrink axially by about 10% during preparation for electron microscopy, however the relative axial location of structures is valid (Chapman et al., 1990). Meridional X-ray diffraction patterns (see chapter 1.42) can be used to deduce the axial distribution of electron density along the collagen fibrils (Meek et al., 1981b). The axially bound proteoglycans have been identified by analysis of these meridional reflections obtained from Cuprolinic blue treated bovine cornea. They locate at the 'a','c','d' and 'e' staining bands (Meek et al., 1986). Binding of proteoglycans at specific sites along the collagen fibril has also been demonstrated using X-ray diffraction in the normal human cornea. This distribution of proteoglycans along the fibril axis is noticed to be altered in the disease keratoconus (Meek et al., 1987b).

Further support for the architecture described above comes from a freeze–etching and rotary–shadowing technique applied to rabbit corneal stroma (Hirsch et al., 1989). Micrographs demonstrated major cross–banded collagen fibrils which frequently were orthogonally linked by regularly spaced interfibrillar bridges. The architecture strongly resembles the Cuprolinic blue staining of cornea, and although the fast–freezing

technique does not provide chemical identification of these bridges it is assumed that they represent proteoglycans.

1.5.3 Functions of the Proteoglycans

The absence of dermatan sulphate proteoglycan at the 'd' band has been noted in demineralized bone collagen (Scott & Haigh, 1985a). Since the gap zone contains the probable site of nucleation of calcification (Fitton-Jackson, 1957) it has been suggested that the presence of dermatan sulphate proteoglycans in non–calcified tissues sterically inhibits the nucleation of calcification (Scott & Orford, 1981; Scott & Haigh, 1985a).

The gap zone, in which the 'd' band is centred, contains the non–helical telopeptides of the laterally packing collagen molecules (see chapter 1.3). The presence of dermatan sulphate proteoglycans in the gap zone could prevent access to potential cross–linking sites on the telopeptides and it has been suggested that this process hinders accretion of collagen molecules and thus restricts the fibril diameter (Scott & Orford, 1981; Scott, 1984). Indeed dermatan sulphate proteoglycans can inhibit the *in vitro* fibrillogenesis of type I collagen (Vogel et al., 1984). In developing rat tail tendon there is an inverse relationship between collagen fibril diameter and the amount of dermatan sulphate proteoglycans present on the surface of the collagen fibrils (Scott et al., 1981).

Proteoglycans in cornea are thought also to play a role in maintaining the regular spacing of the uniform diameter collagen fibrils (Balazs, 1965; Borcherding et al., 1975; Meek et al., 1986). Maurice, in 1957, suggested that this regularity in the collagen/extracellular matrix architecture was the basis of the tissue's transparency. The light scattered by the regular collagen lattice is cancelled out by destructive interference in all directions except the straight through one, thus causing transparency. This model is generally preferred over the uniform refractive index theory of

transparency (Maurice, 1957, 1984). Theoretical calculations demonstrate that this preferred theory for transparency holds even if the regular arrangement of collagen fibrils is less than perfect (Hart & Farrell, 1969). Consistent with Maurice's hypothesis is the fact that in opaque corneal scars the interfibrillar spaces between normal diameter fibrils are abnormally large (Cintron et al., 1978). The opaque scar tissue contains unusually large dermatan sulphate proteoglycans with normal size glycosaminoglycans but no keratan sulphate proteoglycans (Hassell et al., 1983). This type of result strengthens the case for implicating proteoglycans in the regulation of the stromal architecture.

1.6 Objectives of this Thesis

I will endeavour to highlight the type of structural information able to be gathered from a specific connective tissue by the use of two fundamentally distinct but complementary physical methods; electron microscopy and X–ray diffraction. The collaboration of these approaches leads to an ultrastructural model that is more reliable than either could attain independently. For example, the concern about electron microscopic preparative artifacts is diluted if the same information is obtained from X–ray studies on fresh, unprocessed tissue. On the other hand, electron microscopy can be employed to identify localised structural abnormalities not extensive enough to affect the X-ray diffraction pattern.

The connective tissues which have been studied in this project are the normal human corneal stroma and the normal human sclera. The collagen architecture was observed in the fresh tissue by X–ray diffraction, and staining of the processed tissue was carried out to visualise collagen in the electron microscope. Specific stains were employed, in conjunction with both X-ray diffraction and electron microscopy, to locate proteoglycans in the tissues. The aim was to understand the arrangement of collagen and proteoglycans in human ocular tissues.

These techniques, employed to study the normal human cornea, offer a new and exciting opportunity to gain an insight into the collagen/proteoglycan architecture in pathological human corneas (an electron microscopical study of the proteoglycan abnormalities in pathologic human sclera is being carried out elsewhere (Young et al., 1988)). To this end, three pathologic corneal conditions were chosen for the investigation; macular corneal dystrophy, corneal oedema and Scheie's syndrome. All were selected because they involved different types of proteoglycan abnormalities. Basically, macular corneal dystrophy patients lack, or have severely reduced levels of, keratan sulphate; the influx of stromal water in corneal oedema effects the proteoglycan content; Scheie's syndrome patients are deficient in α–L–iduronidase. A more extensive description of each pathology is given in chapter 2. Because of the nature of the techniques employed in this study, and the restricted supply of pathological human tissue, the data are obtained from a relatively small number of samples. Hence reproduciblity of the results is limited. Nevertheless, the information obtained should throw some light on the stromal requirements for corneal transparency, whilst at the same time identifying the abnormal stromal architecture, be it a primary or secondary effect, which presumably results in reduced visual acuity in specific ocular disorders.

Chapter 2

Clinical Details

In this chapter a clinical description of macular corneal dystrophy, corneal oedema and Scheie's syndrome will be given along with a review of the current ultrastructural knowledge concerning each condition. The available medical history of each patient will also be included.

2.1 Macular Corneal Dystrophy

Macular corneal dystrophy is an autosomal recessive, inherited disorder, clinically characterized by central corneal thinning (Ehlers & Thorkild, 1978; Donnenfeld et al., 1986) and progressive clouding of the cornea. Stromal clouding usually begins superficially between the ages of 5 and 9 years and as a rule spreads to involve the full extent of the stroma in the second decade. Small, scattered, white macular opacities appear, initially at the centre of the cornea at around puberty, and with time increase in number and size (Klintworth 1980, 1982). The pre–keratoplasty, clinical appearance of the eye of macular dystrophy patient 1 is shown in figure 2.1. Visual impairment is such that penetrating keratoplastic surgery is normally required by the third to fifth decade . Figure 2.2 shows the post–operative clinical appearance of the eye of macular dystrophy patient 2 with the radial sutures still in place. There is a sharp

Figure 2.1 The pre–operative clinical appearance of the eye of macular dystrophy patient 5. The cornea is obviously cloudy and white opacities are evident.

distinction between the clear central donor button and the cloudy outer host cornea. Due to its recessive mode of inheritance, unlike the other corneal dystrophies which are inherited as dominant traits, it is rare with a higher prevalence in populations with a relatively small gene pool such as Iceland (Jonasson et al., 1989). The disease is histologically characterized by an accumulation of glycosaminoglycan deposits within the stromal matrix (Klintworth & Vogel, 1964; Garner, 1969).

Macular dystrophy corneas do not produce a normal keratan sulphate proteoglycan (Klintworth & Smith, 1980, 1983; Hassell et al., 1980, 1982; Nakazawa et al., 1984; Klintworth et al., 1986) but synthesize an unusual

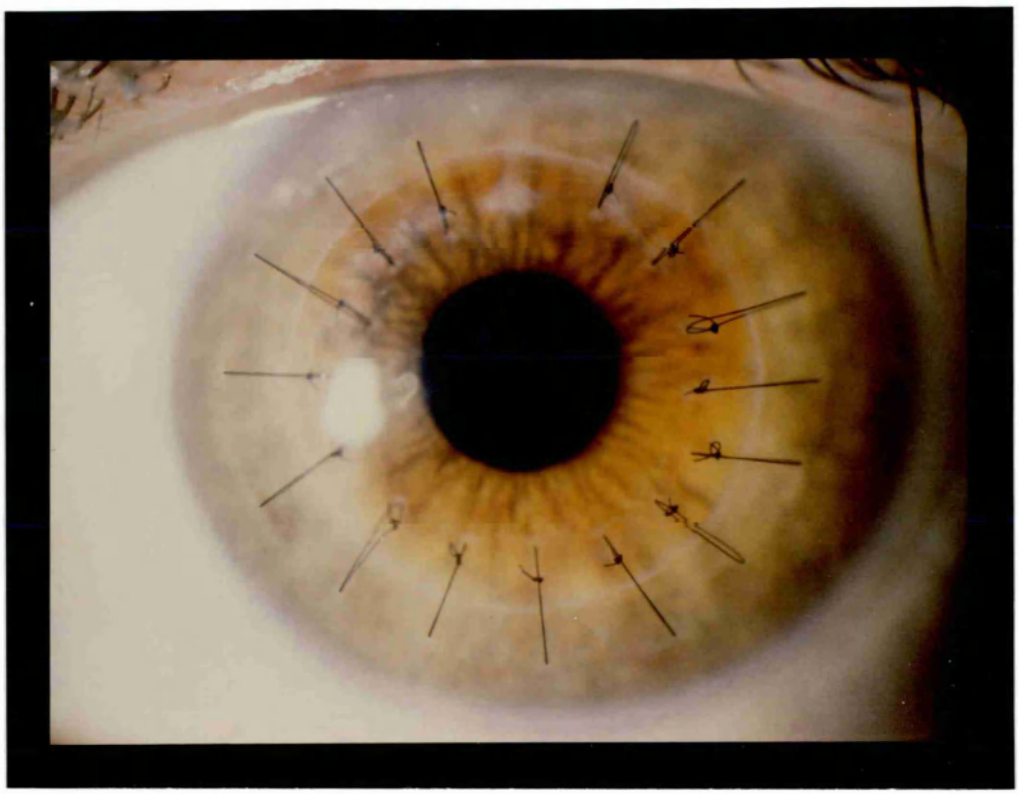

Figure 2.2 The post–operative clinical appearance of the eye of macular dystrophy patient 2. The radial sutures are still in place, grafting the clear donor button to the cloudy host cornea.

glycoprotein not found in normal human corneas (Klintworth & Smith, 1977, 1980, 1983; Hassell et al., 1980). This glycoprotein has an immunologically identical protein core to the keratan sulphate proteoglycan (Hassell et al., 1982; Nakazawa et al., 1984) but is slightly smaller than normal (Klintworth & Smith, 1980; Hassell et al., 1980, 1982). In their respective corneas both are synthesized in similar amounts (Hassell et al., 1982). Until recently the glycosaminoglycan moities of the abnormal keratan sulphate proteoglycan were thought to be unsulphated (Nakazawa et al., 1984; Hassell et al., 1984), a defect which could be the result of an error in the action of the specific sulphotransferases involved

in the sulphation of the molecule (Nakazawa et al., 1984). Monoclonal antibodies that recognize sulphated keratan sulphate have been used to demonstrate its presence in the serum of healthy individuals. The keratan sulphate is thought to exist mostly on fragments of the degradation of the large cartilage proteoglycans (Thonar et al., 1985). This method has also been used to demonstrate the absence of sulphated keratan sulphate in both the cornea and serum of patients with macular corneal dystrophy (Klintworth et al., 1986; Thonar et al., 1986). However, recent immunohistochemical evidence (Yang et al., 1988) has shown that sulphated keratan sulphate is present in the corneas of some individuals with macular corneal dystrophy. The serum of these patients also contains detectable levels of keratan sulphate. Together the immunohistochemical and serum findings suggest that at least two varieties of macular corneal dystrophy exist, namely keratan sulphate negative (type I) and keratan sulphate positive (type II). However the presence of keratan sulphate in the cornea of a patient showing negligible levels in the serum suggests that further groupings may be necessary (Edward et al., 1988).

Efforts to identify the abnormal keratan sulphate proteoglycan have largely overshadowed the biochemical characterization and location of chondroitin/dermatan sulphate proteoglycans. The cells in corneas with macular dystrophy synthesize more chondroitin-6-sulphate than normal (Klintworth & Smith, 1977); the chondroitin/dermatan sulphate proteoglycans are larger than normal and are oversulphated (Nakazawa et al., 1984). These chondroitin/dermatan sulphate proteoglycans may be incorporated into the extracellular deposits of abnormal keratan sulphate proteoglycans (Nakazawa et al., 1984) although there has been no conclusive evidence to support this suggestion.

Corneas with macular dystrophy appear under the transmission electron microscope, to have a disrupted lamellar structure (Klintworth & Vogel, 1964; Morgan, 1966; Garner, 1969; Klintworth 1980, 1982; Newsome et al., 1982) and to contain both intracellular and extracellular deposits (Klintworth & Vogel, 1964; Morgan, 1966; Teng, 1966; Garner, 1969;

Ghosh & McCulloch, 1973; Klintworth & McCracken, 1979; Klintworth, 1980, 1982; Newsome et al., 1982). These deposits of abnormal keratan sulphate proteoglycan (Nakazawa, 1984), were seen in the cytoplasm of the keratocytes by Klintworth and Vogel, 1964. These authors suggested that the deposits form intracellularly and are stored prior to their migration out into the extracellular matrix. The individual collagen fibrils appear well preserved (Klintworth & Vogel, 1964; Morgan, 1966; Ghosh & McCulloch, 1973), and they exhibit an apparently normal banding pattern (Klintworth & Vogel, 1964).

Results presented in this thesis show that the structural interactions, character and distribution of proteoglycans in macular dystrophy stromas are abnormal. Also presented are data from the first X-ray diffraction study of macular dystrophy corneas.

2.1.1 Macular Dystrophy Case Histories

Nine macular dystrophy corneal buttons, either 7mm or 7.5mm in diameter, were obtained at penetrating keratoplasty from nine different patients with this rare disorder. The excisions, which remained within the area of diseased cornea in each case, were studied by various ultrastructural techniques. The patients (1–9), three females and six males, were from seven distinct pedigrees within the United Kingdom. They underwent penetrating keratoplasty, performed by one of three ophthalmic surgeons, at either Manchester Royal Eye Hospital or Oxford Eye Hospital between March, 1986 and September, 1990. The two pairs of corneas obtained from within the same pedigrees were from two similarly affected brothers (patients 2 and 4) and a brother and sister (patients 3 and 9). In this thesis the corneas are numbered chronologically from the date of surgery. As only one button was obtained from each macular dystrophy patient the number of the cornea corresponds to the number of the patient. In some cases, extensive case histories were not available.

Patient 1: Corneal button 1 (7.5mm diameter) was from the left eye of a 32 year old female with typical corneal features of macular dystrophy. She was the only affected member of her family. She has a history of back and neck ache dating back to the age of 8 years and, at 20 years old, she was diagnosed as having cervical spondylosis. X-rays at Oxford Eye Hospital revealed a modelling abnormality of both humeral heads which showed a broad articular curvature and were subluxed from the glenohumeral joint. She was investigated for mucopolysaccharidosis but no abnormalities were identified on the axial skeleton which were classical of the disorder. The urine mucopolysaccharidosis screening (glycosaminoglycan:creatine ratio) proved negative. Vision at the time of surgery was 6/24. Histochemistry of the corneal button showed stromal, subepithelial and epithelial deposits which were positive for Alcian blue (pH 2.5) and colloidal iron, but negative for periodic acid Schiff. These features are typical of macular dystrophy.

Patient 2: This half button (whole button diameter=7mm) was obtained from the left eye of a 36 year old male. Visual acuity prior to surgery was 6/60. His right eye had previously been grafted and had shown the same characteristic macular dystrophy histology as was observed in the half button of the left graft which was examined histologically. He is the younger of two affected brothers of an otherwise normal pedigree. His older brother is patient 4.

Patient 3: Button 3 (7mm diameter), was from a 25 year old male who was originally diagnosed as having macular corneal dystrophy at the age of 7 years. Both of his corneas were similarly affected, this is his left one, with the visual acuity reduced to 6/24 in each eye. There is one sister with macular corneal dystrophy making two out of four siblings affected.

Patient 4: Corneal button 4 was excised from the left eye of a 42 year old male who had previously had his right eye grafted. He is the older brother of patient 2.

Patient 5: Patient 5 is the second of the two females, she underwent penetrating keratoplasty at the age of 41 years.

Patient 6: Corneal button 6 was obtained from a male who was 63 years old at the time of surgery. The whole cornea was irregular in thickness. Bowman's layer was found to be incomplete and lost in places and there was a deposition of amorphous material between the basal epithelium and anterior stroma/Bowman's layer. This appeared to be a hyaline material and did not have the characteristics of amyloid. Also present were areas in which there were deposits of a foamy/granular material within keratocytes and apparently loose within the stroma. There were extensive deposits of this material which extended throughout the stroma as well as the pannus beneath the epithelium. Similar accumulations were present within some epithelial cells. These deposits stained positively with the PAS stain and the high iron diamine stain (HID) for sulphated mucopolysaccharides. Alcian blue staining was not eliminated after prior hyaluronidase digestion. These findings are consistent with the features in macular corneal dystrophy. The patient's right eye was unsuccessfully grafted three times in the 1960's. A successful graft was carried out in February 1988 and the donor tissue transplanted at that time remains clear (May 1990). Only one of the previous biopsies (1988) was available. The findings were of a scarred dystrophic graft with no evidence of the glycosaminoglycan deposits characteristic of macular corneal dystrophy. It seems therefore that the 21 year period between the third rejected graft in 1968 and the successful 1988 graft of the right eye resulted in no reoccurrence of macular corneal dystrophy.

Patient 7: Diagnosis; macular corneal dystrophy. Male, aged 17 years.

Patient 8: Diagnosis; macular corneal dystrophy. Female.

Patient 9: Diagnosis; macular corneal dystrophy. Female, sister of patient 3.

2.2 Corneal Oedema

Oedema, or swelling, of the cornea is often associated with damage to the endothelial cells which permits aqueous humour to gain entrance to the stroma. It can be basically divided into epithelial oedema and stromal oedema. The most frequent clinical circumstance, however, is when they occur in conjunction with one another (Goldman & Kuwabara, 1968), both being the result of the same primary physiological defect. Advanced stromal oedema can result in the appearance of large blebs, or bullae, due to local detachments of the epithelium from the underlying Bowman's layer. This condition is given the term bullous keratopathy. These bullae, caused by the influx of fluid, can rupture causing extreme pain. Another clinical manifestation is the thickening of the stroma. These changes cause visual loss.

The oedema is invariably associated with damage to the endothelial cells which allows aqueous humour to gain entrance to the stroma. This endothelial damage is often a complication of cataract surgery and bullous keratopathy caused by surgical trauma can be variously classed as pseudophakic or aphakic, depending whether or not an intraocular lens has been inserted during the cataract surgery. This subdivision of bullous keratopathy is irrelevant to this study which details the effect of the stromal oedema on the collagen/proteoglycan organization.

Electron microscopic observations of the oedematous corneal stroma

demonstrate non–uniform separation of normal diameter collagen fibrils within the lamellae, along with separation of the lamellae from one another. Swelling is normally associated with loss of transparency in that portion of the cornea where oedema is present (Goldman & Kuwabara, 1969). These ultrastructural stromal deformations are typical of human oedematous corneas. The occurrence of collagen–free "lakes" and wavy lamellae has been reported in cases of hereditary corneal oedema (Kanai et al., 1971) and bullous keratopathy (Kanai & Kaufman, 1973). Electron microscopic studies of oedematous rabbit cornea showed an increase in collagen fibril diameter (Kaye et al., 1982). It was suggested that the increase was due to lateral aggregation of fibrils rather than to swelling of individual fibrils.

Biochemical studies have shown that surgically induced transient oedema in rabbit corneas results in a reduction of both keratan sulphate and chondroitin sulphate proteoglycans by about 50% (Anseth, 1969). Also corneas which have undergone endothelial cell damage by perfusion in a calcium–free medium become swollen and selectively lose keratan sulphate proteoglycans to the medium (Kangas et al., 1990; Cintron, 1989). Corneas treated in this way, when compared with controls, demonstrate reduced Cuprolinic blue staining after removal of the chondroitin/dermatan sulphate proteoglycans from the cornea by incubation with chondroitinase ABC. This indicates a loss of keratan sulphate proteoglycans from the stroma of the corneas with endothelial damage (Cintron, 1989).

Immunohistochemical studies have revealed a decreased corneal keratan sulphate:chondroitin sulphate ratio in a number of diseases of the cornea including bullous keratopathy and Fuch's dystrophy (Klintworth et al., 1986); corneas in both of these conditions contain oedematous stromas. However it was not possible to attribute this ratio change to either a keratan sulphate decrease or a chondroitin/dermatan sulphate increase. Results described in this thesis extend the previous immunohistochemical observations of oedematous corneas and attempt to distinguish between

the anterior and posterior sections of the corneal stroma.

2.2.1 Corneal Oedema Case Histories

Ten corneal buttons from eight unrelated patients with various forms of corneal oedema were examined. The study of each button employed as many electron microscopical and X-ray diffraction techniques as was possible. The restrictions included availability of beam time on the synchrotron and the amount of tissue available. Four oedematous corneas and one normal control were analysed for glycosaminoglycan content. Transmission electron microscopy, with Cuprolinic blue staining, was carried out on eight buttons with two of those further undergoing prior incubation with glycosaminoglycanases. Scanning electron microscopy was performed on one oedematous specimen (plus a normal control). Low–angle equatorial X-ray diffraction was performed on three buttons to obtain values for the collagen fibril diameters (in two of the cases) and spacings (in the three cases). Low–angle meridional data were obtained from three of the buttons to provide information about the periodic binding of proteoglycans to the collagen. High–angle X–ray work was carried out on eight of the oedematous buttons. The buttons, obtained during penetrating keratoplasty, were collected in a frozen state from either Oxford, Manchester or Wolverhampton Eye Hospitals. Wherever possible, depending on the amount of tissue available, a portion of the button was dissected and its hydration calculated. The hydration could not be obtained for several of the smaller samples since a dissected portion with a wet weight below about 2mg would lead to unrepresentative and slightly inaccurate values for the hydration. In some cases, extensive case histories were not available.

Patient 1: Female, diagnosis; bullous keratopathy.

Patient 2: Diagnosis; bullous keratopathy.

Patient 3: Female, diagnosis; bullous keratopathy.

Patient 4: Male, aged 72 years, left eye. Presented with visual acuity 6/24 due to decompensated Fuch's dystrophy with lens opacities. Apical pachymetry was 0.89mm with 12mm/Hg tension. Underwent penetrating keratoplasty with extracapsular cataract extraction and primary lens implantation.

Patient 5: Right button from patient 4. Visual acuity 6/36 at 72 years of age due to decompensated Fuch's dystrophy with lens opacities. Apical pachymetry was 0.84mm with 10mm/Hg tension. At the age of 73 years he was submitted to penetrating keratoplasty, extracapsular cataract extraction and lens implantation.

Patient 6: Male, age 49 years, right eye. At the age of 46 years a penetrating keratoplasty resulted in a clear graft six months post–operatively, but with a visual acuity of only 6/60. The graft began to decompensate but settled during a fortnight of intensive treatment giving an acuity of 6/18 a year after the operation. However two years later the graft again was beginning to decompensate and another penetrating keratoplasty was carried out 3.5 years after the previous one.

Patient 7: Female, aged 84 years, left eye. Underwent an intracapsular cataract extraction and insertion of an iris–supported intraocular lens at the age of 76 years and 5 years later developed bullous keratopathy. The graft was performed 3 years after the diagnosis of bullous keratopathy. The right eye has a similar ocular history.

Patient 8: Female, aged 64 years, right eye. Endothelial dystrophy noted at the age of 62 years along with corneal oedema, blurred vision and raised intraocular pressure. Worsening endothelial dystrophy was treated by a penetrating keratoplasty at the age of 65 years.

Patient 9: Diagnosis; bullous keratopathy.

Patient 10: Male, aged 67 years, left eye. Underwent a left cataract extraction and insertion of an iris–supported intraocular lens at the age of 59 years and a left trabeculectomy for post–operative glaucoma 4 month later. At the age of 65 years corneal decompensation and corneal oedema were noted; a penetrating keratoplasty was performed two years on.

2.3 Scheie's Syndrome

Scheie's syndrome is a very rare (1:500,000) autosomal recessive mucopolysaccharidosis (type IS) similar to, but not as severe as the Hurler syndrome (mucopolysaccharidosis type IH). Skin fibroblasts from patients with both disorders show a deficiency in an enzyme required for the catabolism of mucopolysaccharides, once called the "Hurler corrective factor" but now known to be α–L–iduronidase (Bach et al., 1972). Due to this enzyme defect the glycosaminoglycan side chains of heparan sulphate and dermatan sulphate proteoglycans are not degraded. It is possible that storage of chondroitin/dermatan sulphate proteoglycans in the cornea results in collagen abnormalities (Zabel et al., 1989).

Clinically the Scheie's syndrome patient suffers from mild skeletal and facial changes and a cloudy cornea. Unlike the Hurler syndrome, intelligence and lifespan are normal. To date very little corneal tissue from patients with Scheie's syndrome has been available for evaluation. The specimen investigated in this study was previously the subject of an electron microscopical study of all layers of the cornea including the

stroma (Zabel et al., 1989). Stromal abnormalities included the deposition of proteoglycan storage material along the lamellae and within the cells, a typical finding of all systemic mucopolysaccharidoses. The occurrence of a type of fibrous long spacing collagen in the corneal stroma seemed, however, to be unique to patients with Scheie's syndrome. In the conventionally embedded electron microscope images there seemed to be two populations of collagen fibrils. The first had a diameter in the range 21–24nm, which is the range quoted for the diameter of dehydrated adult human corneal fibrils by Craig and Parry (1981). The second population existed in areas that contained large amounts of extracellular fibrillogranular material; the fibril diameter in these regions was approximately 39nm (Zabel et al., 1989). The study of the Scheie's syndrome cornea by Zabel and colleagues (1989) involved no X-ray diffraction analysis or Cuprolinic blue staining of proteoglycans.

2.3.1 Scheie's Syndrome Case History

This corneal button was obtained from a female in her early twenties who suffers from Scheie's syndrome. She was initially seen in ophthalmic consultation at 7 years of age. Visual acuity was 6/9 in the right eye and 6/30 in the left, improved to 6/12 by occlusion therapy. Corneal clouding was noted at the time. At 18 years of age she was re–examined due to progressively deteriorating vision over the preceding 6 months. The best corrected visual acuity was 6/24 in both eyes and bilateral corneal clouding occurred with mainly stromal involvement. She had various mild skeletal abnormalities. The α–L–iduronidase activity was dramatically reduced in skin fibroblasts and absent altogether in leucocytes. Based on these clinical and biochemical findings a diagnosis of Scheie's syndrome was made. The degree of vision was adequate until the age of 20 years when she was referred for corneal transplantation.

Macular dystrophy patient	Electron microscopy	Low–angle X–ray diffraction	High–angle X–ray diffraction	Glycosaminoglycan analysis
1	√	√		√
2	√			√
3	√	√		√
4	√	√	√	√
5	√		√	√
6	√	√	√	√
7	√		√	√
8	√	√	√	√
9	√		√	√
Oedema patient				
1	√	√		
2	√		√	
3	√			
4	√	√	√	
5	√	√		
6	√	√	√	√
7	√	√	√	√
8	√	√	√	√
9	√	√	√	√
10	√	√	√	
Scheie	√			

This table lists the techniques performed on each pathologic human cornea during the course of this study.

Chapter 3

Materials and Methods

3.1 Clinical Sources and Specimen Storage

The human corneal and scleral tissue examined in this work was obtained post–mortem or post–operatively from a number of ophthalmic surgeons, namely:

Professor Anthony J. Bron, FRCS, Nuffield Laboratory of Ophthalmology, University of Oxford, Walton Street, Oxford OX2 6AW.

Mr. Alan E.A. Ridgway, FRCS, Manchester Royal Eye Hospital, Oxford Road, Manchester M13 9WH.

Mr. Andrew B. Tullo, FRCS, Manchester Royal Eye Hospital, Oxford Road, Manchester M13 9WH.

Dr. Paul Brittain, FRCS, Wolverhampton and Midland Eye Infirmary, Compton Road, Wolverhampton WV3 9QR.

Dr. Ralph W. Zabel, FRCS, Department of Ophthalmology, Ottawa General Hospital, 501 Smyth, Ottawa, Ontario, Canada K1H 8L6.

On resection the samples were wrapped in clingfilm to control evaporation, were frozen and stored at –20°C prior to collection.

Occasionally it was possible to examine specimens fresh; this enabled an assessment to be made of the effects of freezing upon the tissue. In two cases I was fortunate enough to be present in theatre at the time of surgery, armed with the electron microscopy fixative/staining solution. Small pieces were dissected from specific regions in the button and immersed in the solution a matter of minutes after excision. For the X-ray diffraction experiments it was again fortuitous that two corneal grafts were being performed just prior to our experimental time on the synchrotron X–ray facility. On these occasions the buttons were wrapped in either clingfilm or muslin and suspended in a saturated atmosphere (H_2O) and stored at 4°C until exposure to the X–ray beam either 36 hours or 48 hours later. The corneas were then frozen in clingfilm for storage.

3.2 Hydration Measurements

In most cases, especially for the oedema work, a small piece of cornea was dissected at the time of experiment, weighed and dried down over several days in a desiccator containing silica gel. The hydration, defined as the ratio of water to dry material, is calculated using:

$$H = \frac{\text{wet weight} - \text{dry weight}}{\text{dry weight}}$$

The hydration of human corneas has been calculated, using a variety of methods, to be in the range H=3.5–3.68 (Fatt, 1978; Mishima, 1978). The method used here, due to the fact that the cornea is not heated during drying, produces slightly lower values than those quoted. A corneal thickness–hydration correlation of human cornea carried out by Ytteborg and Dohlman (1965) yielded the empirical equation relating the two quantities;

$$H = 7.0q - 0.64$$

where q is the corneal thickness in mm. Since the thickness from central cornea to limbus increases from about 0.52mm to about 0.65mm, in the adult human cornea, we expect the hydration within the cornea to vary from about H=3.0 to H=3.98 with a mean value of H=3.46.

It was not possible to obtain the hydration for several of the smaller samples since, due to measurement errors, a dissected portion with a wet weight below about 2mg would lead to unrepresentative and slightly inaccurate values for the hydration.

3.2.1 Scleral Hydration

Human scleral tissue was required at several different hydrations for a study of the effect of hydration on collagen intermolecular spacing. This experiment has previously been carried out on cornea (Meek et al., 1991).

Three corneo–scleral rings were obtained, post–mortem, minus the 7mm diameter central corneal buttons which had been used for a penetrating keratoplasties. The donors were all young males with normal vision. Each ring, which consisted of approximatly 4–5mm of tissue either side of the limbus, was dissected into eight equal portions. In order to produce tissue covering a range of hydrations the samples were equilibrated by immersion in eight different concentrations of polyethylene glycol (PEG, mol. wt.=20,000) in a saline at about physiological concentration. The saline was 0.15M NaCl and the PEG percentages (w/v) were 0%, 0.5%, 2%, 7.5%, 10%, 15%, 20% and 25%. Three samples, one from each donor, were immersed in each PEG concentration. Prior to immersion the samples were placed in dialysis tubing in order to preserve their physiological components. Equilibration was carried out at 4°C for 4.5 days. As with cornea, the wet and dry weights were obtained to calculate the hydration.

3.3 Electron Microscopy

3.3.1 Transmission Electron Microscopy

Small pieces were dissected from various locations in each specimen of donated tissue. Each small sample ($\sim$1mm^2) was then fixed and simultaneously stained for proteoglycans. This was achieved by immersion overnight in 0.05% Cuprolinic blue (BDH Ltd, Atherstone, Warwickshire, U.K.) containing 2.5% (w/v) glutaraldehyde and 0.1M $MgCl_2$ in 25mM sodium acetate buffer, pH 5.7 (Scott et al., 1981). They were rinsed 3 times each for 5 minutes in the the buffer solution containing glutaraldehyde and $MgCl_2$. The pieces were then stained 'en bloc' in three changes of 0.5% aqueous sodium tungstate for a total time of 15 minutes followed by three 5 minute washes in 0.5% sodium tungstate in 50% ethanol. Dehydration through a graded ethanol series was completed with two 1/2 hour washes in 100% ethanol. The samples were embedded in either Spurr, Epon 812 or Polarbed. Prior to infiltration by the resin, in the case of Epon and Polarbed, the samples were bathed twice in propylene oxide. For all resins, infiltration occurred overnight in pure resin after which the samples were placed in blocks and polymerisation took place over the following 48 hours, 24 hours at 60°C and 24 hours at 40°C. Where proteoglycan staining was not required, samples were treated identically with Cuprolinic blue omitted from the fixative.

Thin sections of the embedded tissue were cut on a Reichert–Jung Ultracut E ultramicrotome (Reichert–Jung, Wien, Austria) using either a Dupont 5mm edge diamond knife (Dupont Company, Wilmington, Delaware, USA) or a Diatome 2.4mm edge diamond knife (Diatome Ltd., Bienne, Switzerland). The reflected light from the ribbon of twin sections was silver/gold indicating a thickness of the order of 70nm. The sections were picked up on either G200, G300 or G400 copper /palladium mesh grids (Bio-Rad Microscience Ltd., Hemel Hempstead, Herts, UK). If positive staining of collagen was required, the thin sections were floated

on either 1% or 2% aqueous uranyl acetate for about 40 minutes at 37°C followed by a brief wash in distilled water. This was occasionally preceded by positive staining for about 40 minutes at 37°C with aqueous phosphotungstic acid (1% or 2%) and an aqueous wash. The thin sections of the embedded tissue were examined on a Phillips 301 transmission electron microscope operating routinely at 80KV calibrated with a 2160 lines/mm grating replica. The microscope was loaded with Ilford technical EM film (Ilford Ltd, Knutsford, Cheshire, UK). Very occasionally a Jeol 2000FX transmission electron microscope running at 80KV was used to obtain micrographs.

3.3.2 Proteoglycan Location in Normal Cornea

The proteoglycans from a normal human post–mortem cornea were stained for electron microscopy as described in section 3.2. Ultrathin sections on four different grids (4–6 sections per grid) were examined in the Phillips 301 transmission electron microscope. Seven of the micrographs obtained from the grids were suitably stained, for both proteoglycans and collagen, to allow identification of the binding sites. In all, seventeen areas from these micrographs were analysed to establish the arrangement of proteoglycans with collagen.

In each area the number of proteoglycan filaments which could be seen to associate with a specific region of the collagen fibril were recorded. Specific regions were assumed to mean either a certain band or the area between two adjacent bands. Due to the resolution in the micrographs and the finite thickness of the proteoglycan filaments, it was not possible to draw intra–band distinctions, i.e. location of a proteoglycan at any of the four 'a' bands was listed as 'a' band association. Proteoglycans which were not uniquely in contact with any one area were not recorded. Frequently, proteoglycans appeared to be attached to the fibrils, but poor take–up of uranyl acetate by the collagen resulted in an inferior fibrillar banding pattern which precluded identification of the attachment sites.

3.3.3 Scanning Electron Microscopy

Corneal samples were immersed in a solution containing 3% glutaraldehyde and 0.1M phospate buffer (pH 7.2) for 4 hours at room temperature. They were then subjected to three washes, each for 8 minutes, in the buffer without the glutaraldehyde. The samples were post–fixed in 2% osmium tetroxide and 0.1M phospate buffer for 1–2 hours, again at pH 7.2. Following dehydration the corneas were placed in 100% acetone. Using a Bio-Rad critical point dryer (Bio-Rad Microscience Ltd., Hemel Hempsted, Herts, UK) the acetone was replaced by CO_2, the CO_2 heated and the samples critical point dried. The corneas were suitably mounted onto aluminium stubs and coated with gold using an Emscope sputter coater. They were examined on a Jeol 820K scanning electron microscope and images were recorded on Kodak TMX 120 film (Kodak, Hemel Hempsted, Herts, U.K.).

3.4 Enzymatic Proteoglycan Digestion

Enzyme digestion of glycosaminoglycan side chains, within a population of proteoglycans in a cornea, was achieved by incubating small ($\leq 1mm^2$) corneal samples with specific enzymes. The small samples were first lightly fixed for 30 minutes at 4°C in 2.5%(w/v) formaldehyde in a 25mM sodium acetate buffer. They were washed in the buffer to remove unbound fixative before being immersed for about 4 hours at room temperature in the enzyme solution. The enzyme used was either keratanase (*Pseudomonas* sp.), chondroitinase AC (*Arthrobacter aurescens*) or chondroitinase ABC (*Proteus vulgaris*), all of which were obtained from Sigma Chemicals, Poole, Dorset, U.K. The enzymes were included in a Tris buffer at concentrations of 5 units/ml for keratanase and 2.5 units/ml for the chondroitinases. The Tris buffer (0.25M) at pH 8.0 contained 0.5 mg/ml bovine serum albumin, 0.33M sodium acetate and 0.5M sodium chloride. Protease inhibitors (soybean trypsin inhibitor, EDTA and

benzamidine) were included in the solution (Scott & Haigh, 1985b). After digestion the samples were washed in the buffer without the enzyme. Enzyme digest controls were treated identically, through the solutions deficient only in the enzymes. The samples were stained for proteoglycans with the Cuprolinic blue procedure described in section 3.31.

3.5 Keratan Sulphate Analysis

Various corneal and serum specimens were analysed for the presence of sulphated keratan sulphate using a monoclonal antibody (1/20/5–D–4) specific for a very highly sulphated epitope on the keratan sulphate chain. The technique, developed by Professor Eugene Thonar, employs an enzyme–linked immunosorbent assay (ELISA) (Thonar, et al., 1985; Klintworth et al., 1986). This analysis was carried out by Professor Eugene J–M.A. Thonar[1]. The anti–keratan sulphate antibody was a gift from Dr. Bruce Caterson[2] and the international standard of keratan sulphate was provided by Dr. Martin Mathews and Dr. Alan Horwitz[3].

3.5.1 Serum Analysis

It was possible to obtain blood samples from the macular dystrophy patients 1, 2, 3, 4, 5, 6, 8 and 9. Control blood was obtained from myself (24 year old male) and my supervisor, Dr Keith Meek (37 year old male) to be included in the first batch of sera to be analysed. In four cases (patients 1–4), blood was spun down and ~2 ml of serum was frozen to -40°C. The samples were packed in an insulating box containing dry ice and delivered to Chicago within 36 hours of collection by Federal Express, (Federal Express International Section, Abingdon, Oxon., U.K.) In the

[1]Departments of Biochemistry and Internal Medicine, Rush—Presbyterian–St. Luke's Medical Center, Chicago, Illinois, U.S.A.

[2]University of North Carolina, Chapel Hill, NC, U.S.A.

[3]The University of Chicago, Chicago, Illinios, U.S.A.

case of macular corneal dystrophy patients 5, 6 and 8 the whole blood was sent frozen as described. Serum was analysed without previous knowledge of the histological corneal data. The serum keratan sulphate was quantified using a previously described ELISA (Thonar, 1985) modified as outlined below to permit more accurate quantification of keratan sulphate. The anti-keratan sulphate monoclonal antibody (1/20/5-D-4) used in this study has been well characterised and has been shown to be specific for a sulphated carbohydrate moiety on keratan sulphate chains (Thonar et al., 1985). All serum samples were analysed in triplicate. Preliminary studies established that the conditions previously described (Thonar et al., 1985, 1986) yielded inhibition curves for samples of normal human serum that were not always parallel in their entirety to the curves generated for the international standard of keratan sulphate purified from pig costal cartilage. This problem was circumvented by changing the pH of the buffer used as the diluent for all incubations (phosphate buffered saline) from pH 6.0 to pH 5.3. All other conditions remained as previously described (Thonar et al., 1985).

3.5.2 Corneal Analysis

Corneal tissue from macular corneal dystrophy patients 4, 5, 6, 7 and 8, from oedematous corneas 6, 7, 8 and 9 and post-mortem from a 37 year old female with no history of ocular problems were analysed for the presence of keratan sulphate. Samples were fixed for half an hour at 4°C in 2.5% formaldehyde in a 25 mm sodium acetate buffer, pH 5.7. They were frozen in dry ice and shipped to Chicago within 36 hours by Federal Express. The corneal sample was digested with papain to solubilise the glycosaminoglycans. The concentration of chondroitin/dermatan sulphate in the papain digest was obtained by measuring the uronic acid (Klintworth et al., 1986). The concentration of keratan sulphate was measured using the previously described ELISA. The distribution of sulphated keratan sulphate in the oedematous corneas and the normal

control was investigated by analysing three small ($\sim$2mm^2) specimens from each button; one full thickness sample and one sample dissected in the plane of the cornea. As the corneal sample could not be cut along its plane in the unfrozen state, the dissection into approximately anterior and posterior halves was performed on a frozen and hence rigid cornea. It was carried out fairly quickly, in a dish containing solid CO_2, using a scalpel and tweezers which had been cooled in dry ice. The specimens were thawed, fixed and shipped to Chicago as before.

3.6 X–Ray Diffraction

3.6.1 Obtaining the Patterns

X-ray patterns were obtained at the SERC synchrotron source at Daresbury, U.K. Corneas were taken out of the freezer, weighed and placed in air–tight cells enclosed by mylar windows which were then mounted on a mobile computer–controlled stage in the path of the X–ray beam. The specimen was positioned by temporarily attaching some X–ray sensitive, adhesive, "green paper" to the cell. The low-angle patterns were recorded using the long camera (between 2.5m and 4m depending on the experimental run) on station 8.2. The high-angle patterns were obtained using the short ($\sim$ 12 cm) camera arrangement on station 7.2b. After the exposure the corneas were re–weighed, wrapped in clingfilm, and frozen. The specimen–film distance of the long camera, apart from a few cms between the backstop and the film, was evacuated to avoid air–scatter. The position of the lead backstop, required to stop the "straight–through" beam, was computer adjustable. Alignment of the backstop was required so as not to obscure the first order equatorial reflection. This was achieved by obtaining a rat tail tendon exposure on PolaPan 4 x 5 Instant Sheet Film (Fabriqué aux EU par Polaroid Corporation, Cambridge, MA, USA).

The specimen–film distance on the short camera was, apart from a few

centimeters between the backstop and film, filled with helium to reduce air–scatter. The camera set–up required the specimen cell to be inserted inside the camera housing, and it would have been difficult to pumpout the camera to vacuum for each exposure. The specimen was placed a matter of only a few millimeters from the end of the collimator through which the beam emerged and the lead backstop was situated about 10cm further on. The short distances involved enabled the specimen and backstop positions to be fixed. The wavelength of the radiation was either 1.602 Å or 1.54 Å on station 8.2 and 1.488 Å on station 7.2b. The beam dimensions on the long camera were typically 0.5mm x 4mm apart from when unfrozen macular corneal dystrophy cornea 4 and the normal control were scanned with the beam to find the interfibrillar spacings at various positions. In those cases the beam dimensions were cut down to 1mm x 0.5mm and 1mm x 2mm respectively. The X-ray beam used on the short, high-angle camera was produced through a 4-dot collimator to give a circular beam of 1mm diameter. Patterns were recorded on Ceaverken AB photographic film (Ceaverken, Strängnäss, Sweden) and were scanned using an Ultrascan XL laser microdensitometer (LKB Instruments Inc., Gaithersburg, MD, USA).

The exposure times were dependent on the intensity of the beam, they were not always constant. Low–angle equatorial patterns were recorded in about 45 seconds (1^{st} order) and 10–20 minutes (two subsequent orders). Low–angle meridional patterns were recorded with exposure times of 30 seconds–2 minutes (1^{st} and 3^{rd} orders) and 25–45 minutes (up to the 10^{th} order). High–angle patterns were obtained in 4–5 minutes. A suitably exposed film was dependent on several, not totally predictable, variables including beam intensity, camera length, specimen thickness, specimen staining etc. The actual exposure time was, therefore, an estimate and to ensure a useful exposure with "one take',' two X–ray films separated by a sheet of black paper were placed in the film holder. Thus two patterns were recorded for each specimen, one being more heavily exposed than the

other.

A meridional pattern can be analysed to produce an electron density profile along one D–period of the fibril. To locate extra electron density along corneal or scleral collagen due to the presence of proteoglycans, half of the specimen was stained and fixed for at least 6 hours in 2.5% glutaraldehyde, 0.1M $MgCl_2$ in 25mM sodium acetate buffer (pH 5.7) containing 0.05% Cuprolinic blue. The control half was treated identically with Cuprolinic blue omitted from the solution. The samples were then enhanced with sodium tungstate as in the electron microscopy preparation (section 3.2). The electron densities for both halves were obtained and a subtraction enabled the stain to be located.

3.6.2 Analysis of the Equatorial Patterns

In the corneal stroma the 1^{st} order Bragg spacing, d, is related to the mean centre-to-centre interfibrillar spacing i by i = 1.12 d (Worthington and Inouye, 1985). A comparison of the diameter of the 1^{st} order equatorial ring from cornea with the diameter of the 67nm reflection from rat tail tendon (which arises from the axial periodicity of collagen) allowed d to be obtained (Goodfellow et al., 1978; Gyi et al., 1988). The dimensions of the respective reflections were measured from a linear scan across the ring. This method is valid because the long camera length leads to very small scattering angles where $\sin\theta \simeq \theta$. It does not hold for high–angle scattering. Experimentally, the comparison was only valid when both the cornea and tendon X–ray patterns were obtained on the same camera and when the densitometer calibration was taken into account.

The two subsidiary maxima on the equatorial pattern are thought to be due to scattering from the individual cylindrical collagen fibrils (Worthington and Inouye, 1985) and would be expected to occur at:

$$R = \frac{5.14}{2\pi r_o} \qquad 1^{st} \text{ subsidiary}$$

and

$$R = \frac{8.42}{2\pi r_o} \qquad 2^{nd} \text{ subsidiary}$$

where R is the reciprocal space co–ordinate of the reflections, r_o is the fibril radius and the numerical factors derive from Bessel functions (see Vainshtein, 1966). The positions of these reflections in the diffraction pattern may therefore be used to find R and hence calculate r_o.

3.6.3 Analysis of the Meridional Patterns

The relative intensities of the equally spaced meridional diffraction rings were obtained by scanning the pattern with the laser microdensitometer and measuring the area under each peak (above the background scatter) in the trace. The full scale deflection setting of the densitometer was the same for each scan. Due to the large spread in the range of intensities encountered, a pattern on which the 10^{th} order was intense enough to be scanned would be saturated at the 3^{rd} order. To overcome this problem the 1^{st} and 3^{rd} orders were obtained on a short exposure pattern, the 3^{rd} and 5^{th} on a slightly longer one and the 5^{th} to the 10^{th} on the longest. The area under each peak was obtained by overlaying the trace on graph paper on a light box and counting squares. Since the same 3^{rd} and 5^{th} orders both appeared on two densitometer scans a full set of relative intensities (1^{st} through 10^{th}) could be obtained. Additional scaling of the meridional intensities from different specimens is further discussed in the appropriate results section.

A statistical test employing the R–factor was used to assess the extent of agreement between two sets of intensities. The R–factor is given by:

$$R = \frac{\sum || F_S | - | F_T ||}{\sum | F_S |}$$

where F_S and F_T are the structure factor amplitudes, taken as the square roots of the observed intensities, for sclera and tendon respectively.

Where appropriate phases were availible for the intensities, a Fourier analysis was carried out to obtain an axial electron density profile over a collagen D–period (Meek et al., 1985) using existing laboratory software.

3.6.4 Analysis of the High–Angle Patterns

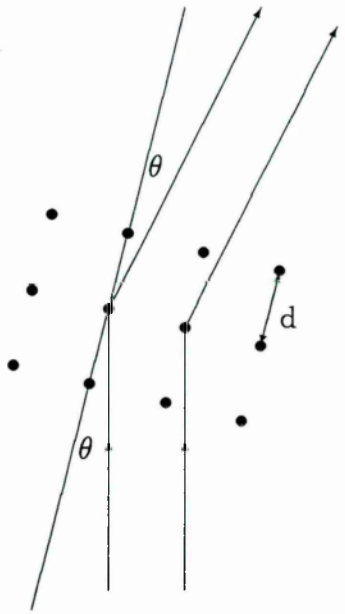

Figure 3.1 A schematic representation of the theoretical basis for Bragg's equation in a perfect crystal lattice. Lattice points are represented by black dots with the distance between them equal to the Bragg spacing, d. The X–ray beam is represented by the arrowed lines.

The theoretical basis behind constructive interference of waveforms and the production of diffraction patterns is embodied in Bragg's equation:

$$n\lambda = 2d \sin\theta$$

where n is the order of the reflection, λ is the wavelength of the radiation (in this case X–rays), θ is half the angle between the 'straight through' beam and the n^{th} order reflection and d is the Bragg spacing for collagen molecules within a fibril (see figure 3.1). Assuming "pseudo–hexagonal" packing of molecules, which is the most common arrangement for an assembly of rod–like molecules, allows the Bragg spacings to be multiplied by a factor of 1.11 to give values for the intermolecular separation (Klug & Alexander, 1974). In these high–angle experiments the wavelength, λ, of the X–rays is 1.488 Å. Observing the 1^{st} order diffraction ring of the high–angle pattern gives the following expression for the Bragg spacing, d.

$$d = \frac{1.488}{2\sin\theta}$$

To obtain a value for d, a value for θ, i.e. half the angle through which the 1^{st} order reflection is deflected, is required. This can only be obtained if the specimen–film distance is known. It could be physically measured on the experimental equipment but is more accurately obtained by analysis of a diffraction ring produced by ground calcite crystals, a diffracting structure with a periodic repeat of 3.04Å. Since n, λ, and d are known for calcite Bragg's equation can be used to calculate θ.

The geometry of the diffracting set–up is shown in figure 3.2. The specimen–film distance can be calculated from

$$\text{Specimen} - \text{film distance} = \frac{\text{radius of ring}}{\tan 2\theta}$$

Using the reverse argument for a ring of known radius produced by a periodic diffracting structure (cornea or sclera) of unknown d, θ can be calculated using

$$2\theta = \tan^{-1} \frac{\text{radius of ring}}{\text{specimen} - \text{film distance}}$$

and hence a value for d can be obtained.

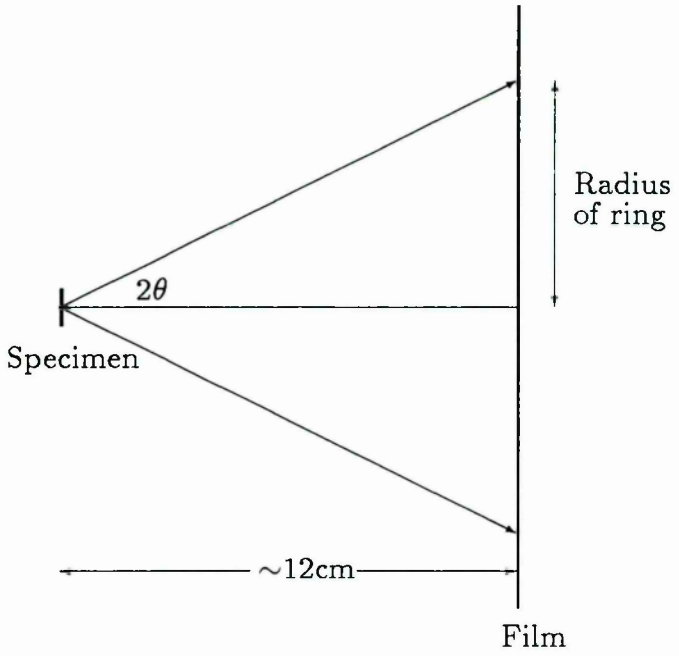

Figure 3.2 A schematic representation of the camera set–up for the high–angle X-ray diffraction experiments

The 1st order high–angle ring from cornea or sclera is fairly small ($\sim$ 1cm on a 12cm camera) and diffuse, hence its radius is calculated by scaling its densitometric trace to the trace of the calcite diffraction pattern. This contains a relatively large and sharp ring whose diameter ($\sim$ 6.5cm on a 12cm camera) can be more accurately measured on the film.

Chapter 4

Results

4.1 Human Sclera

4.1.1 Electron Microscopy

Figure 4.1 is an electron micrograph of normal human sclera stained for proteoglycans with Cuprolinic blue and for collagen with uranyl acetate. The proteoglycans associate regularly with the collagen fibrils, predominantly at the 'd/e' staining bands. This is consistent with other work on normal human sclera (Young,1985; Young et al., 1988).

4.1.2 Meridional X–Ray Diffraction

The low–angle meridional X-ray diffraction pattern from fresh human sclera is shown in figure 4.2. The X–ray beam was passed perpendicular to the plane of the sclera, i.e at right angles to the surface of the eyeball.

The collagen fibrils occur in all possible orientations within the plane of the sclera, this results in a diffraction pattern which consists of a series of concentric circles of which the fifth and ninth orders are numbered (figure 4.2). The integrated intensities of the reflections, above background scatter, are presented in table 4.1 where they are compared

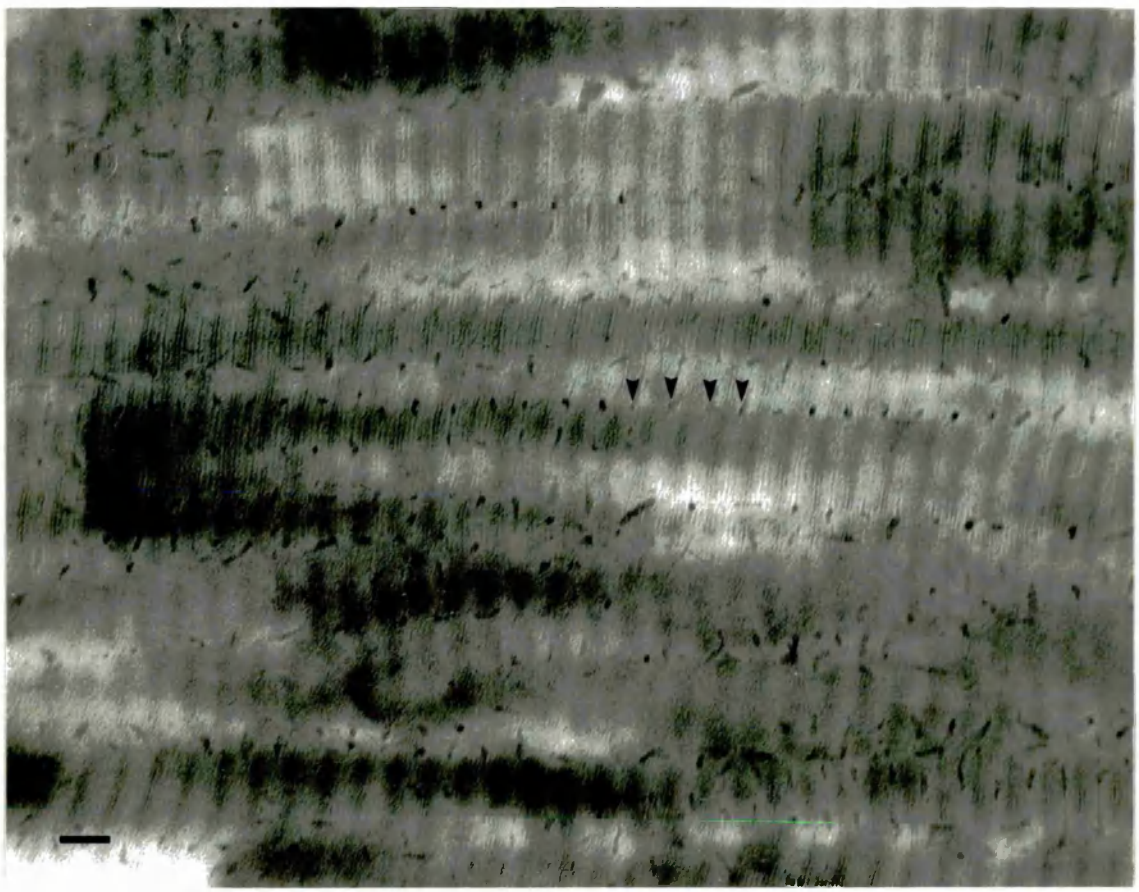

Figure 4.1 A micrograph of normal human sclera showing the collagen/proteoglycan organisation. The proteoglycans are arrowed. Bar=100nm.

with the corresponding intensities obtained from fresh rat tail tendon collagen (Hulmes et al., 1977).

The first order scleral intensity is arbitrarily assigned the value 1000 and the tendon data are scaled to this by equating the summed scattered intensities of the two sets of data using:

$$\sum_{n=1}^{10} I_{\text{sclera}} = \sum_{n=1}^{10} I_{\text{tendon}}$$

Order (n)	I_{sclera}	I^{*}_{tendon}	$Phase^{\dagger}_{tendon}$
1	1000	1034	66.7
2	23	28	95.6
3	143	113	346.2
4	10	11	83.4
5	80	56	279.1
6	19	18	255.6
7	32	22	184.3
8	16	6	336.1
9	46	73	31.8
10	11	20	193.1

* Hulmes et al., 1977; †Hulmes et al., 1980.

Table 4.1 Integrated X-ray intensities (I) from fresh human sclera and rat tail tendon. The first order scleral intensity is arbitrarily given the value 1000 and the tendon data are scaled to the sclera data by equating summed scattered intensities. The phases are with respect to a zero origin.

where n is the order of the reflection. This scaling process assumes that the number of electrons per unit cross-sectional area coherently scattered from a D-period is the same in both structures (Meek et al., 1981a). The close agreement between the intensities from sclera and tendon (table 4.1) suggests that at low resolution the corresponding electron densities are similar, and this allows the approximation to be made that the phases are also similar. Phases for rat tail tendon have been published (Hulmes et al., 1980) and are quoted in table 4.1.

Figure 4.3 shows the axial electron density, above water background, along one D-period of the collagen fibrils from sclera and tendon. Both electron densities are plotted on the same, arbitrary, vertical scale and the gap and overlap regions are shown approximately. The plots confirm that the axial electron density of scleral collagen is very similar to that in rat tail tendon collagen. This implies that the collagen axial structures, including the effects of natural cross-linking, are homologous in the two tissues. Although scleral collagen is known to have nearly twice as many

hydroxylysine-linked glycosides as tendon (Harding et al., 1980) these do not appear to contribute significantly to the X–ray diffraction.

In fresh cornea, the presence of some of the extra electron density along the collagen fibrils as compared with fresh tendon (Meek et al., 1981b) has been attributed to the periodic attachment of proteoglycans (Meek et al., 1986). Any proteoglycan attachment which occurs in sclera, however, does not appear to contribute to the X–ray scattering. This is possibly due to the fact that proteoglycans would be associated with the surface of collagen fibrils with a larger average circumference than is found in cornea (Meek et al., 1983; Scott, 1984). Due to the similarity of the electron densities from sclera and tendon (figure 4.3) a subtraction of one from the other to identify the location of any "extra", possibly proteoglycan, material is not possible. Such a plot would be highly dependent on the choice of scaling and hence would be meaningless. In order to locate any collagen bound proteoglycans, X-ray diffraction was performed on sclera whose proteoglycans had been stained with Cupromeronic blue. This stain is an isomer of Cuprolinic blue and, as shown by Professor John Scott (Scott & Haigh, 1988a), will produce specific staining similar to that shown in figure 4.1.

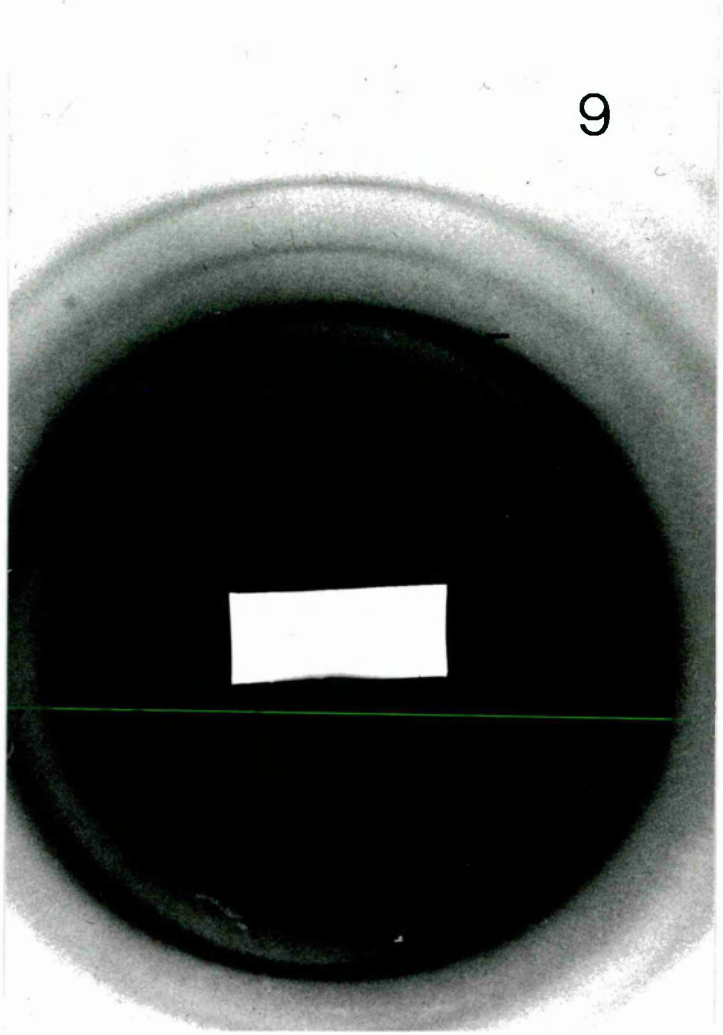

Figure 4.2 The low–angle meridional pattern from normal human sclera. The fifth and ninth orders of the pattern are indicated. Due to the range of intensities encountered in the X–ray patterns it is not possible to reproduce all the orders on a single photographic print.

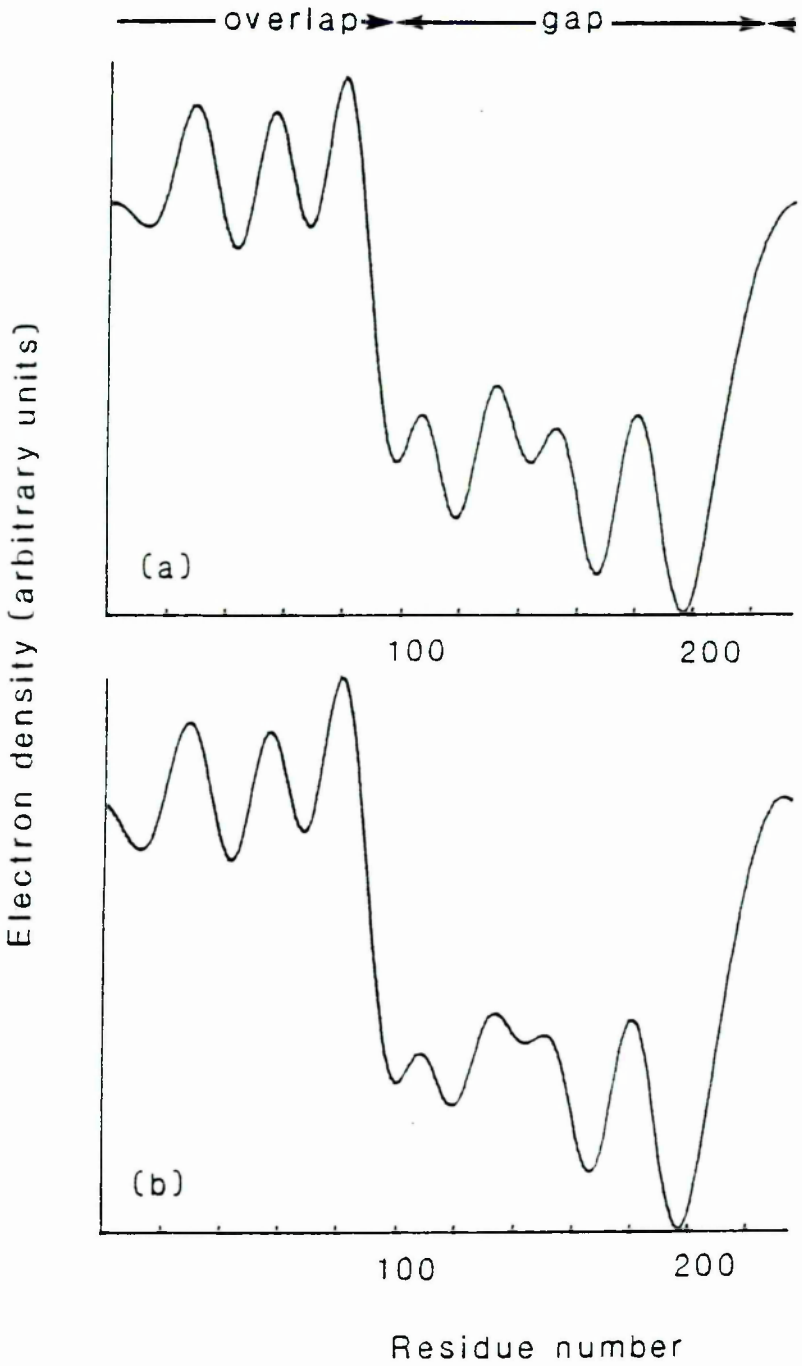

Figure 4.3 The axial electron density along one D–period of the collagen fibrils from (a) rat tail tendon and (b) human sclera. Both electron densities are plotted on the same (arbitrary) vertical scale and the gap and overlap regions are shown approximately.

4.1.3 Meridional X–Ray Diffraction of Cupromeronic blue Stained Sclera.

	CUPROMERONIC BLUE			CONTROL		
Order (n)	I_{sclera}	I^*_{tendon}	Phase*	I_{sclera}	I^*_{tendon}	Phase*
			degrees			*degrees*
1	1422	1574	301.6	1000	1151	66.2
2	136	88	161.8	43	39	90.6
3	116	187	5.0	201	144	353.5
4	103	31	6.3	59	6	56.0
5	132	162	297.6	209	166	290.1
6	154	36	228.1	85	59	236.8
7	121	54	199.6	113	120	194.0
8	33	48	343.8	91	98	341.4
9	112	169	39.7	173	169	39.5
10	54	34	195.6	34	56	195.0

*Taken from Meek et al., 1985.

Table 4.2 Integrated X–ray intensities (I) of human sclera stained with Cupromeronic blue. The first order scleral control intensity was arbitrarily given the value 1000 and the Cupromeronic blue–stained scleral data are scaled to the control data by matching out the details of the overlap zones in the electron density profiles. The phases are given with respect to a zero origin.

Human sclera was stained for X-ray diffraction using Cupromeronic blue as previously described. The integrated intensities of the first nine meridional intensities are shown in table 4.2, where the first order intensity from the control is arbitrarily assigned the value 1000. The scaling of the intensities derived from sclera, which had been stained with Cupromeronic blue, to the control data cannot be achieved by equating summed scattered intensities. This method of scaling would be unsuitable since, in this case, the presence of extra scattering from the stain electrons would invalidate the underlying assumption that the number of electrons per unit cross–sectional area coherently scattered from a D–period is the same in the two structures to be scaled together. First order intensities,

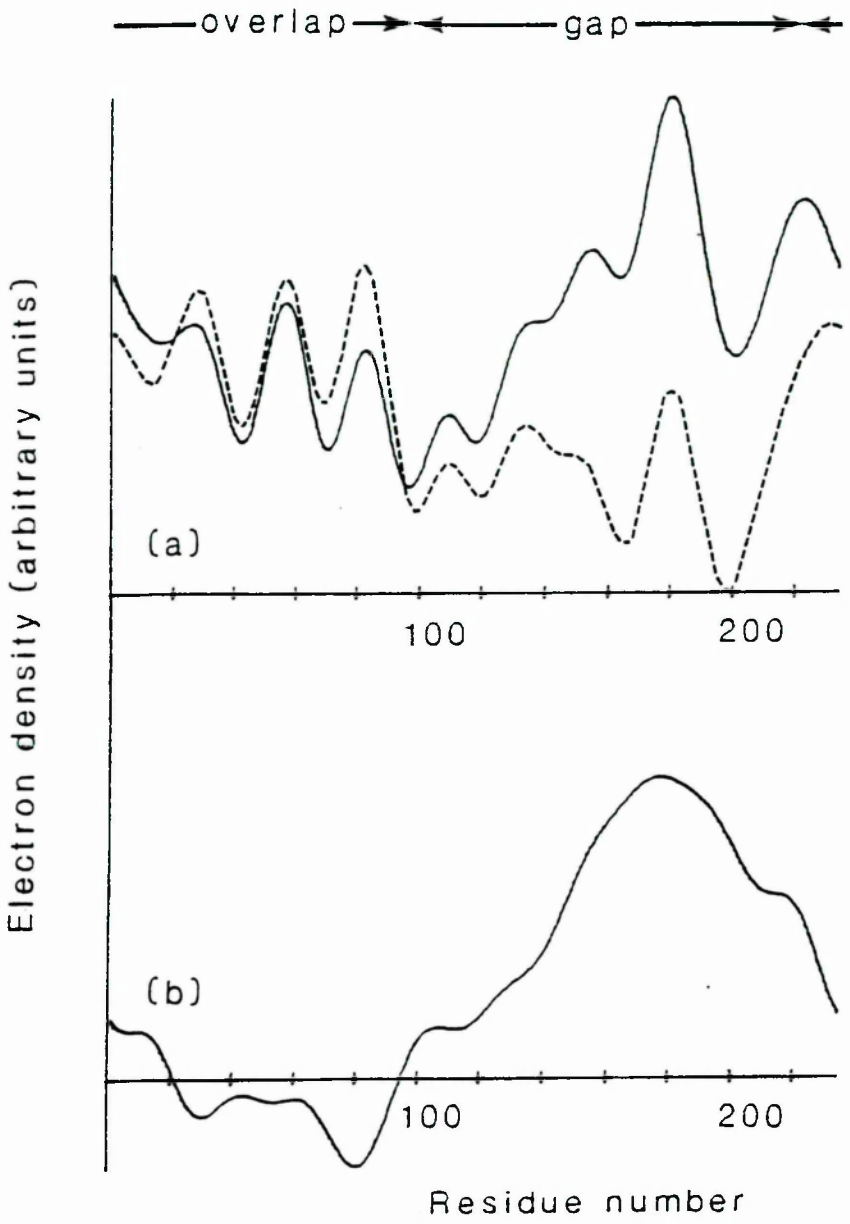

Figure 4.4 *a*. Axial distributions of electron density along one D–period of the collagen fibrils in human sclera treated with Cupromeronic blue (*solid line*) and its control (*dashed line*). *b*. Difference electron density distribution between Cupromeronic blue–treated human scleral collagen and its control, *a* and *b* are plotted on the same (arbitrary) vertical scale. The gap and overlap regions are shown approximately.

which arise mainly from the ratio of electron density in the overlap and gap zones, have been equated in several studies (Chandross & Bear, 1973; Tomlin & Worthington, 1956; Hulmes et al., 1977). However, since Cupromeronic blue staining would affect this ratio, equating the first orders can not be justified. Integrated intensities are often scaled to each other by equating a certain order (Stinson et al., 1979; Eikenberry & Brodsky, 1980; Brodsky et al., 1982). The data sets in table 4.2 could not be scaled by equating a particular order of the pattern since there was no reason to suppose that any diffraction order would remain the same after staining. To overcome the scaling dilemma a procedure that had previously been employed in an analysis of rat tail tendons was adopted (Meek et al., 1985). On examining the electron density profiles it was noticed that the density of the overlap region was barely altered after Cupromeronic blue staining. This prompted the assumption that the major changes caused by Cupromeronic blue–staining occur in the gap region. The data of Cupromeronic blue–stained sclera and its unstained control were therefore scaled so that the overlap details in the electron densities matched out as far as possible.

Producing the axial electron density profiles which correspond to the intensities given in table 4.2 requires the use of suitable phases. Scleral collagen exhibits a close similarity to rat tail tendon collagen as is demonstrated by the similarity of the electron density plots in figure 4.3. The changes in the electron density, caused by treatment with the control solution containing glutaraldehyde, were assumed to be comparable in rat tail tendon and sclera (Meek & Chapman, 1985; Meek et al., 1985).

The sets of intensities from the control sclera and the identically treated mature rat tail tendon (figure 4.2) were scaled to each other by equating the summed scattered intensities. These two sets of data were then compared and their agreement, represented by an R–factor of 0.13, was found to be good. It was, therefore, considered acceptable to assume that the phases for these tendons (given in table I; Meek et al., 1985) would be close to those for the control sclera. Using the same arguments, electron

microscopy suggests that proteoglycan binding is similar in tendon and sclera so that staining with Cupromeronic blue might be expected to produce phase changes in sclera not unlike those observed in tendons. The comparison between stained sclera and stained tendon (table 4.2) resulted in an R–value of 0.21 which, for ten orders of the diffraction pattern, is considered to be sufficiently low to make the approximation that the phases are, within experimental resolution, the same (Chandross & Bear, 1973; Meek et al., 1985). The relevant phases are shown in table 4.2 and are used to calculate the electron density profiles for Cupromeronic blue–stained sclera and its unstained control. These plots are shown in figure 4.4.

The difference between the Cupromeronic blue–treated sclera and its control indicates the extra electron density due to the presence of the dye. The prominent feature of this plot is a peak centred near residue 180 (the 'd' band). This peak is broad and extends the complete width of the gap zone. Smaller superimposed peaks are probably artifacts of the scaling process.

4.1.4 High Angle X–Ray Diffraction

H	Patient 1 intermolecular distance (nm)	H	Patient 2 intermolecular distance (nm)	H	Patient 3 intermolecular distance (nm)
0.6	1.53	0.8	1.54	0.7	1.49
0.8	1.49	0.8	1.56	1.1	1.55
1.2	1.54	1.3	1.66	1.1	1.56
1.7	1.60	1.4	1.59	1.4	1.61
2.4	1.70	2.8	1.64	1.8	1.66
2.6	1.67	4.1	1.70	2.5	1.68
3.4	1.70	5.0	1.71	3.6	1.75
				4.6	1.65

Table 4.3 The intermolecular distances in the scleras of three eye donors with no ocular defects as a function of hydration (H)

Table 4.3 shows data for the collagen intermolecular spacing in normal human sclera as a function of hydration. The swelling curves derived from these data are shown, for each of the three donors, in figure 4.5. The data demonstrate how the intermolecular separation increases from below 1.5nm, when the hydration is below 1, to a maximum value of 1.75nm. The intermolecular spacings increase only marginally at hydrations above about 2.5. The hydration range obtained by equilibriation of the scleras in 0% to 25% polyethylene glycol solutions rises from 0.6 to above 5.

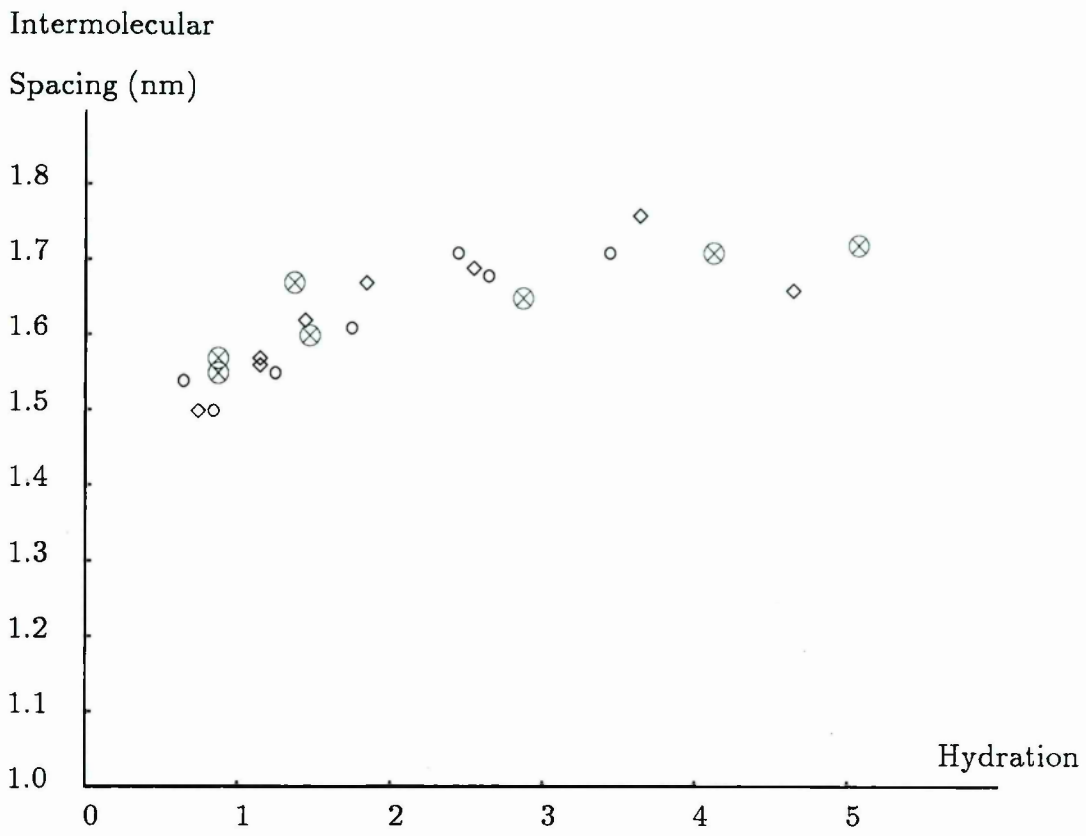

Figure 4.5 Swelling curves for the intermolecular spacing of three normal human scleras (data in table 4.3). Patient 1 (open circles), patient 2 (crossed circles) and patient 3 (diamonds).

4.2 Normal Human Cornea

4.2.1 Transmission Electron Microscopy

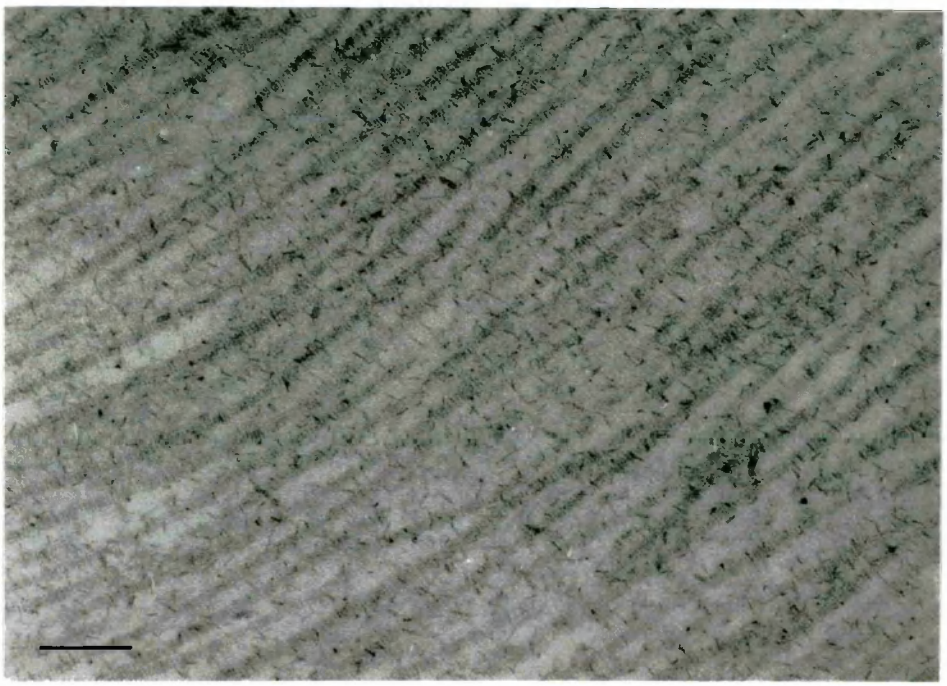

Figure 4.6 A micrograph of normal human cornea stained for proteoglycans with Cuprolinic blue and for collagen with uranyl acetate. The proteoglycans run predominantly transverse to the fibrils forming a mesh–like structure. Bar=150nm.

Cuprolinic blue was employed to locate proteoglycans in normal human cornea and to compare the results with the distribution of proteoglycans in corneas of other species (Scott & Haigh, 1985a,b, 1988a,b).
Understanding and recognising the proteoglycan/collagen arrangement in

Staining Band	Proteoglycan Frequency
'a'	3
'a/b'	4
'b'	16
'b/c'	5
'c'	7
'c/d'	2
'd'	5
'd/e'	2
'e'	1
'e/a'	6

Table 4.4 The frequency of occupation of collagen staining bands by proteoglycans in normal human cornea.

normal human cornea would also provide a control with which to compare the structures observed in pathological corneas. It is, therefore, a necessary starting point for the ultrastructural study of pathological human corneas.

The stromal macromolecular architecture, as can be seen from figure 4.6, consists of uniform diameter collagen fibrils running approximately parallel to one another (within a single lamella) with the proteoglycan filaments lying predominantly perpendicular to the fibrillar axes. Basically, this structure is typical of the stromal organisation from several other mammalian species (Meek et al., 1986; Velasco & Hidalgo, 1988). However, the corneal proteoglycan composition and the sites of proteoglycan association with the collagen have been shown to be species dependent (Scott & Haigh, 1985a,b, 1988a,b).

Analysis of micrographs from Cuprolinic blue–stained normal human corneas yielded data for the frequency of occupation of a particular staining band, or inter–band (table 4.4).

These data can be represented on a histogram (figure 4.7) with the x–axis representing one D–period along the collagen fibril and the y–axis

representing the occupation frequency of the particular staining band. The staining bands do not represent equal axial distances within a D–period and the y–dimensions in the histogram have been weighted to account for this. The weighting was achieved be dividing the number of proteoglycans attached to a particular band by the axial proportion of a D–period which that band occupies. It is the *area* under each histogram bar that is therefore representative of the occupation frequency. The main feature of the histogram seems to be a strong, broad bar in the vicinity of the 'b' doublet.

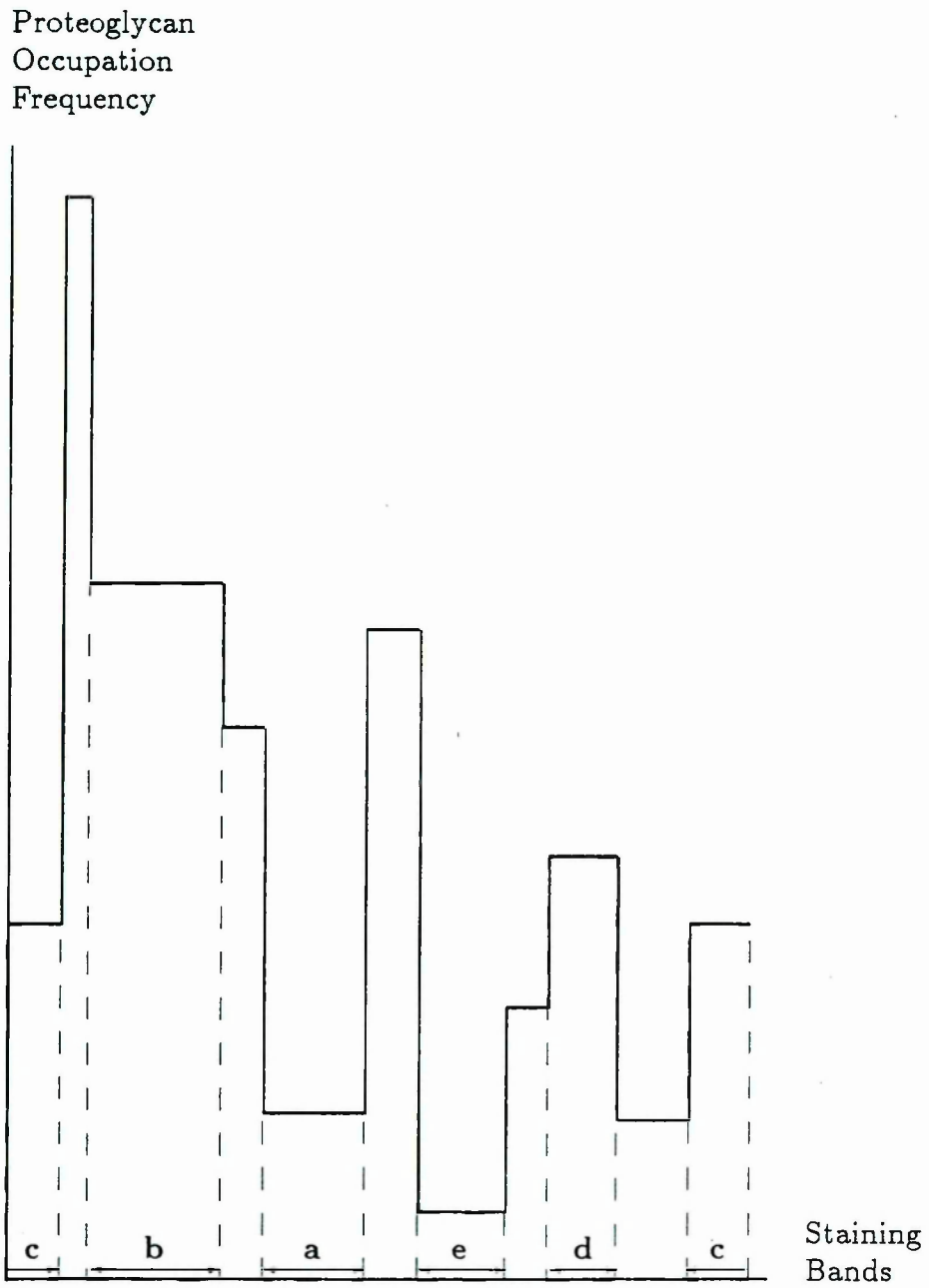

Figure 4.7 A histogram representing the relative occupation frequency of collagen bands by proteoglycans. There are no absolute units on the vertical axis as the number of proteoglycans associated with a particular staining band is represented by the area under the respective histogram bar and the axial extent of the bands is not equal. The horizontal axis represents one complete D-period; 10cms=65nm.

4.3 Macular Corneal Dystrophy

4.3.1 Scanning Electron Microscopy

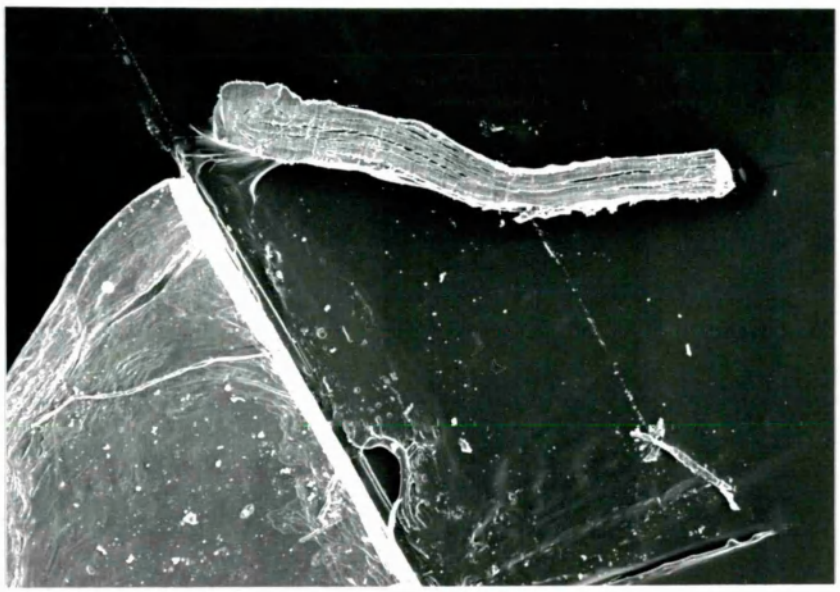

Figure 4.8 A scanning electron micrograph of a macular dystrophy cornea in cross section. A quarter segment of the stroma (diameter ~7mm) was prepared for scanning electron microscopy and mounted, epithelium facing upwards, on an aluminium stub. A thin section from the edge of the corneal segment was cut, turned through 90°, and gold coated to obtain an 'edge on' view of the macular dystrophy stroma

A scanning electron micrograph of a quarter macular corneal dystrophy button from patient 6 in cross–section (figure 4.8) clearly demonstrates how the stroma becomes progressively thinner towards the centre. The stroma is about 30% thicker at 7mm from the centre than it is at the

centre. This gives an overall view of the situation in macular corneal dystrophy. Due to preparative artifacts, actual measurements from this micrograph are fairly meaningless with respect to the *in vivo* stromal thickness.

4.3.2 Immunohistochemical Analysis

Patient	Serum KS (ng/ml)	Corneal KS(μg/ml)
1	41	–
2	<3	–
3	<3	–
4	<4	<0.07
5	<13	<0.02
6	161	1.11
7	–	<0.09
8	<6	<0.08
9	<6	–
Normal*	282	–
Normal**	448	–
Normal	–	10.24

Table 4.5 The levels of antigenic keratan sulphate in the corneas and serum of patients with macular corneal dystrophy. The normal sera were obtained from a 24 year old male* (myself) and a 37 year old male** (Keith Meek) both of whom are healthy with normal vision. The normal corneal tissue was obtained post–mortem from an individual with no history of ocular disease.

The immunohistochemical analysis of both serum and corneal tissue is required to ascertain what variety of macular corneal dystrophy is being studied. The distinction between the two main types so far documented (type I and type II) is based on immunohistochemical evidence and cannot be made clinically (Yang et al., 1988). From the data (table 4.5) it can be seen that patients 4, 5 and 8 are suffering from keratan sulphate–negative (type I) macular corneal dystrophy due to the

Patient	Type of Macular Dystrophy
1	II
2	I
3	I
4	I
5	I
6	II
7	I
8	I
9	I

Table 4.6 The table documents whether the patients had keratan sulphate negative (type I) or keratan sulphate positive (type II) macular corneal dystrophy. The classification was based on analysis of cornea and serum in four cases (4, 5, 6 and 8), of serum in four cases (1, 2, 3 and 9) and cornea in one case (7).

negligible amounts of antigenic keratan sulphate in both their corneas and sera. Although no corneal tissue from patients 2, 3 and 9 was available for the immunohistochemical analysis the fact that their sera contained no antigenic keratan sulphate suggested that they too had developed type I macular corneal dystrophy. Similarly, it seems that patient 7 is suffering from type I macular corneal dystrophy due to the lack of antigenic corneal keratan sulphate (no serum was obtained from this patient). Patient 6 demonstrates near normal levels of antigenic keratan sulphate in his serum and detectable (if reduced) levels in his cornea. This classifies him as suffering from keratan sulphate negative (type II) macular corneal dystrophy. Keratan sulphate was also present in the serum of patient 1, although at a level much lower than normal. Even though her corneal tissue was unable to be analysed for the presence of antigenic keratan sulphate it seems that she also has type II macular corneal dystrophy. Table 4.6 lists the macular dystrophy patients along with the type of disease under investigation.

4.3.3 Transmission Electron Microscopy

The transmission electron microscopical images of all the macular dystrophy corneas examined demonstrated the presence of many intra– and inter–lamellar electron transparent holes or lacunae (figures 4.9, 4.11, 4.12 and 4.13). This type of distinct space within the collagen matrix is not observed in normal human corneas. The lamellar structure of the macular dystrophy corneas varied from being slightly to grossly disrupted, with some lamellae observed to be only a single fibril wide. The individual collagen fibrils exhibited an apparently normal, positively stained, banding pattern.

The cross–sectional images suggest some variation in the packing of the collagen fibrils within the specimens. In cornea 1 a large majority of the fibrils were closely packed with many actually in contact with one or more of their neighbours (figure 4.9). Corneas 2 and 3 showed fewer regions with such close–packing. Cornea 4, when examined in this way, demonstrated the heterogeneous nature of the interfibrillar spacings, exemplified by the difference in fibril packing between figures 4.10(a) and 4.10(b). The diameter of the fibrils, measured from micrographs taken of corneas 1, 2 and 3, was found to be 24±3nm. The diameter of collagen fibrils in the human corneal stroma, as measured by two independant observers using conventional transmission electron microscopy, was reported as 22.5nm (S.D.=1.9nm) and 23.8nm (S.D.=1.5nm) respectively (Craig & Parry, 1981).

Proteoglycans in normal human cornea, visualised using Cuprolinic blue, run predominantly transverse to the direction of the collagen fibril axis forming a mesh–like structure (figure 4.6). All the macular dystrophy corneas analysed by transmission electron microscopy in conjunction with Cuprolinic blue staining, contained areas with a collagen–proteoglycan arrangement similar to that of normal human cornea. However, in other areas, the proteoglycans were seen to be highly aligned running in the same direction as the collagen (figures 4.11 and 4.13).

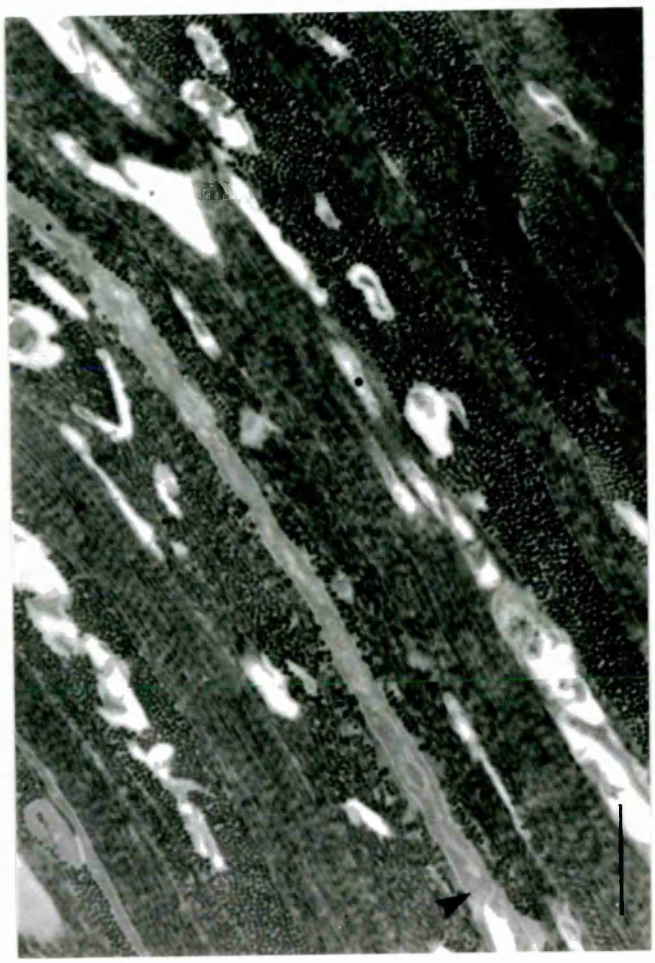

Figure 4.9 A transmission electron micrograph of macular dystrophy cornea 1 stained for collagen with 1% phosphotungstic acid and 1% uranyl acetate. Lacunae are present within and between disrupted lamellae and a keratocyte is arrowed. Close–packing of fibrils is evident in cross–section. Bar=500nm.

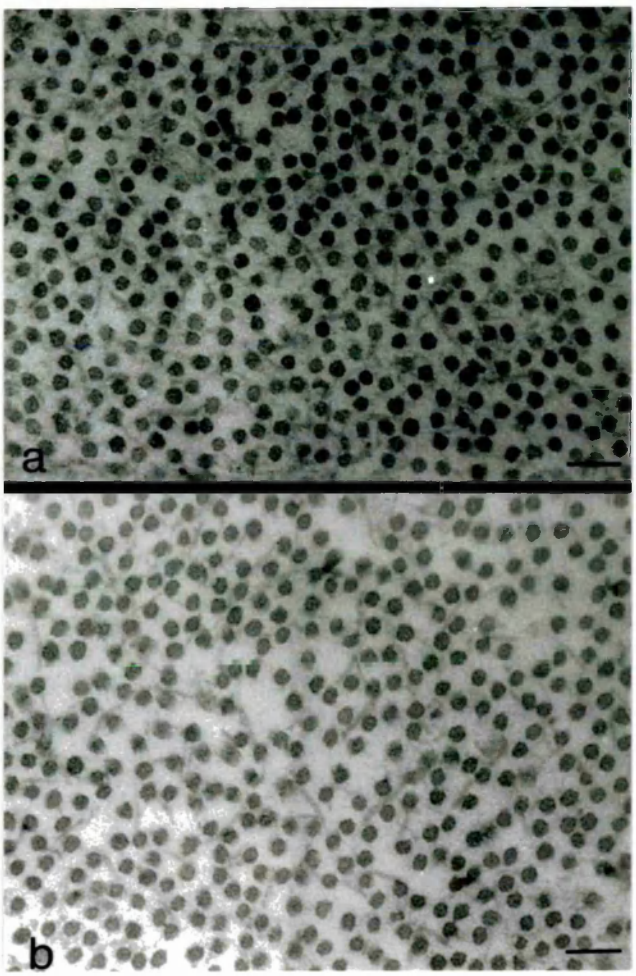

Figure 4.10 Two cross-sectional areas from macular dystrophy cornea 4 stained for collagen with 1% phosphotungstic acid and 2% uranyl acetate and for proteoglycans with Cuprolinic blue. The packing of the fibrils varies within the specimen. Proteoglycans are in evidence between the fibrils. Bar=100nm.

Figure 4.11 A transmission electron micrograph of macular dystrophy cornea 1 stained with 1% phosphotungstic acid and 1% uranyl acetate demonstrates the presence of a large congregation of various–sized electron dense Cuprolinic blue–stained filaments. Matrix proteoglycans are seen to run parallel with the collagen fibrils. Bar=300nm.

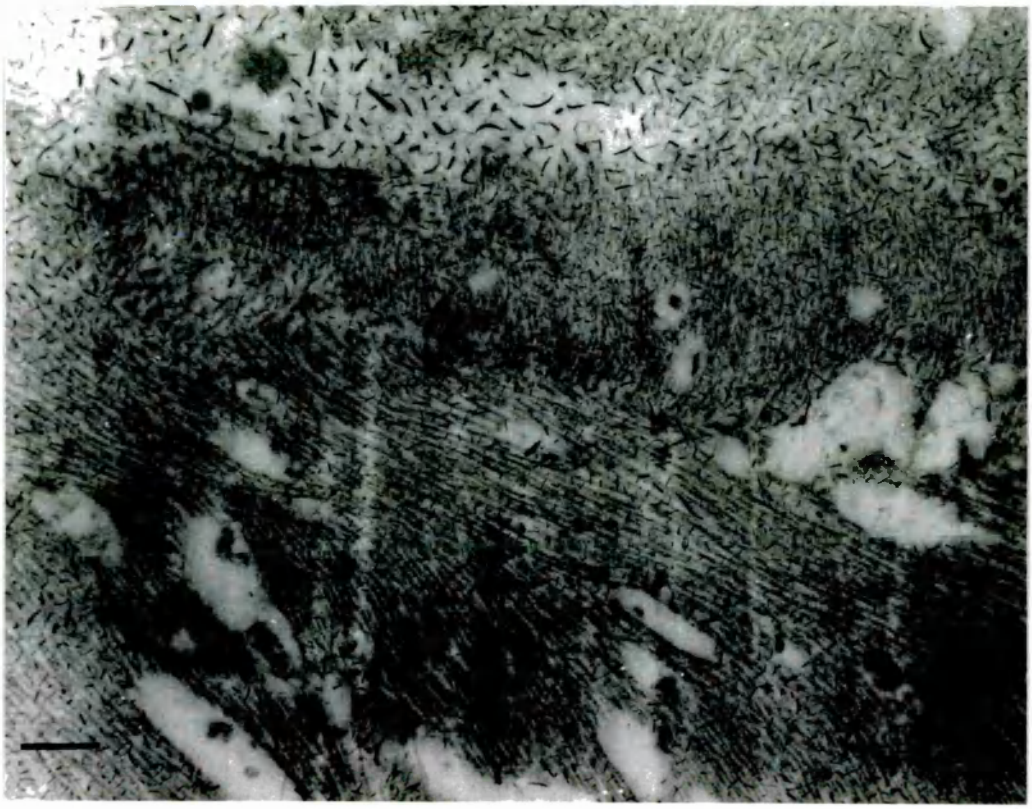

Figure 4.12 A transmission electron micrograph of macular dystrophy cornea 4 stained with 2% uranyl acetate demonstrates the presence of electron transparent lacunae, normal collagen–proteoglycan arrangement in some parts of the matrix and a deposit of variously–sized Cuprolinic blue–stained filaments. Bar=500nm.

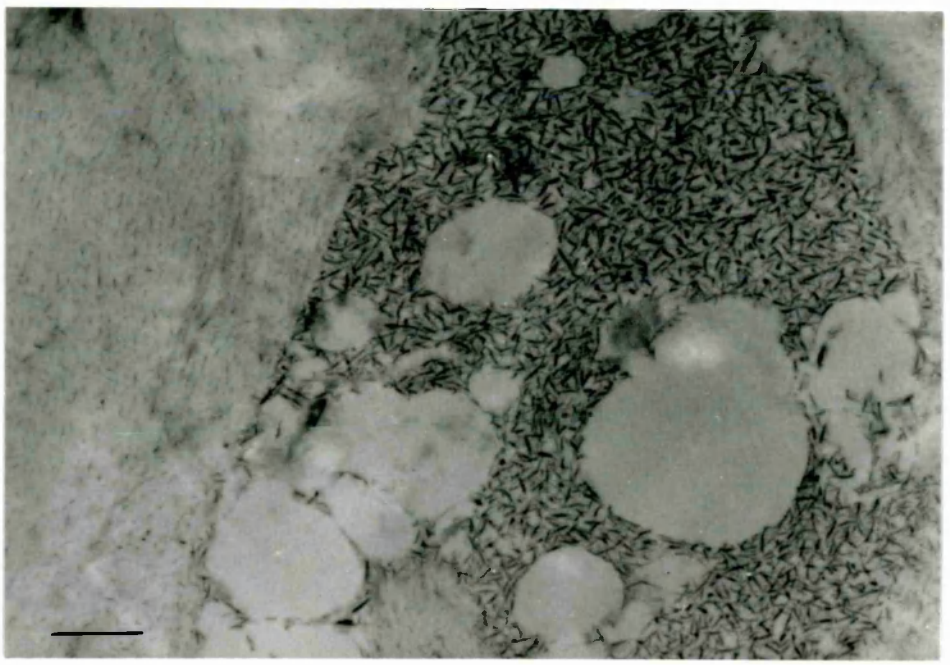

Figure 4.13 Macular dystrophy specimen 1 stained with Cuprolinic blue and 2% uranyl acetate. Matrix proteoglycans run mainly parallel to the lightly stained collagen. Several lacunae are present within the deposit of abnormal proteoglycans. Bar=500nm.

A striking feature of the macular dystrophy corneas, when stained with Cuprolinic blue, was the occurrence of congregations or deposits of various–sized electron dense filaments (figures 4.11, 4.12 and 4.13). There were basically two types of sulphated proteoglycan present in the macular dystrophy stroma. One type was similar in size ($\sim$ 50nm long) and arrangement (orthogonal to the collagen fibril axis) to the "small" proteoglycans which exist in normal cornea (compare areas of figure 4.12 with figure 4.6). These were also observed, interspersed with larger filaments, within the proteoglycan deposits. The other type was several times larger than normal (up to $\sim$ 600nm long) and tended to congregate in the lacunae, although occasionally an isolated one could be observed in the collagen matrix (figure 4.12).

The structural features just described are typical of all the macular dystrophy corneas examined. There was some variation in the extent of stromal disruption between and within corneas but it was not possible to quantify this using the electron microscope. Several corneal samples were taken from known positions across a meridian of macular dystrophy button 3 but exhibited no obvious structural differences arising from their position. The structural abnormalities observed in macular dystrophy cornea 4, which had not been frozen prior to electron microscopy processing, were not noticeably different from those observed in the other macular dystrophy corneas which had been stored at $-40°C$ for some time before their electron microscopy preparation.

The enzyme digests were carried out on macular dystrophy cornea 1 (keratanase and chondroitinase ABC) and cornea 4 (chondroitinase AC and chondroitinase ABC). Keratanase will not digest unsulphated keratan sulphate proteoglycans so it was used only on macular dystrophy cornea 1; the others were classed as keratan sulphate–negative (type I) macular corneal dystrophy. The control and keratanase digests performed on cornea 1 produced electron microscopical images similar to those in figures 4.11, 4.12 and 4.13. However, the micrographs obtained from the

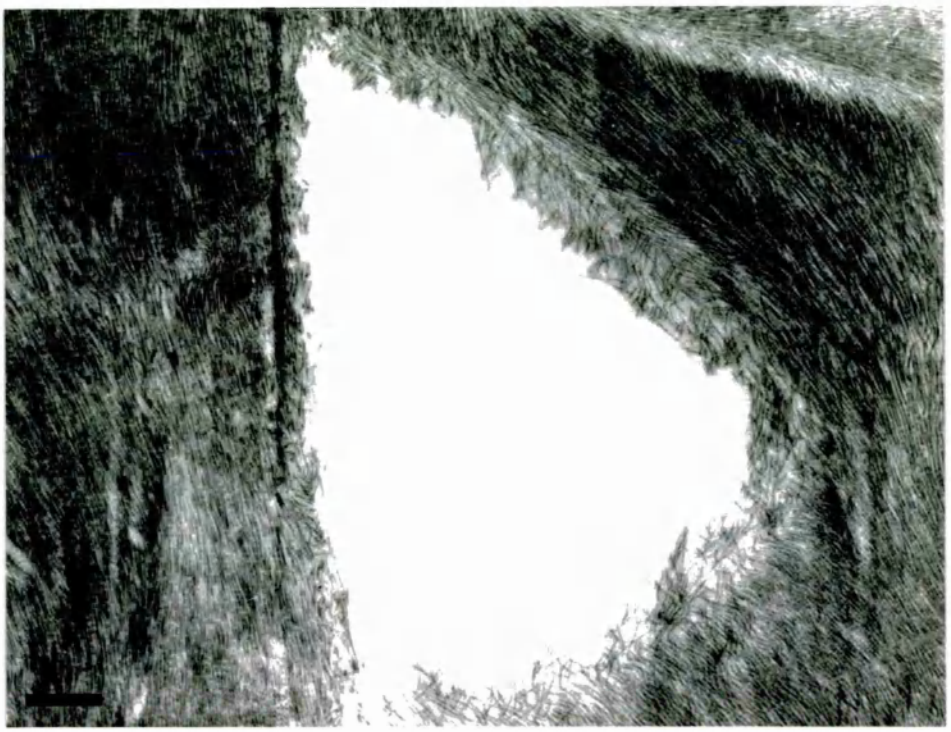

Figure 4.14 A chondroitinase ABC digest of macular dystrophy cornea 1 stained with 1% phosphotungstic acid, 1% uranyl acetate and Cuprolinic blue. No proteoglycans are present within the matrix and the deposit contains a structureless lightly stained material. Bar=600nm.

Figure 4.15 A chondroitinase ABC digest of macular dystrophy cornea 4 stained with 2% uranyl acetate and Cuprolinic blue. The distinct lack of proteoglycan filaments clearly indicates that the majority were susceptible to the action of the enzyme. A large proteoglycan filament is present within the matrix. Bar=100nm.

chondroitinase ABC digest (figure 4.14) showed distinct differences. The fibrillar organisation was disrupted and and there were no proteoglycans in the matrix between the collagen fibrils. The proteoglycan filaments in the deposits were also digested, so it seems that, whatever their size, they were predominantly varieties of a chondroitin sulphate or dermatan sulphate proteoglycan. The areas vacated by these digested proteoglycans were occupied by a structureless, lightly stained material. This is probably the protein cores of the proteoglycans remaining after most of the glycosaminoglycan side chains had been digested off and washed away. It may also contain some abnormal unsulphated keratan sulphate proteoglycans which would not take up the Cuprolinic blue stain.

Incubation of macular dystrophy cornea 4 with chondroitinase ABC digested almost all of the proteoglycan filaments, both small and large (figure 4.15), although a few very large filaments did appear to resist the action of the enzyme. The enzyme digest control and chondroitinase AC digest produced images similar to those of the untreated macular dystrophy cornea.

4.3.4 Equatorial X–Ray Diffraction

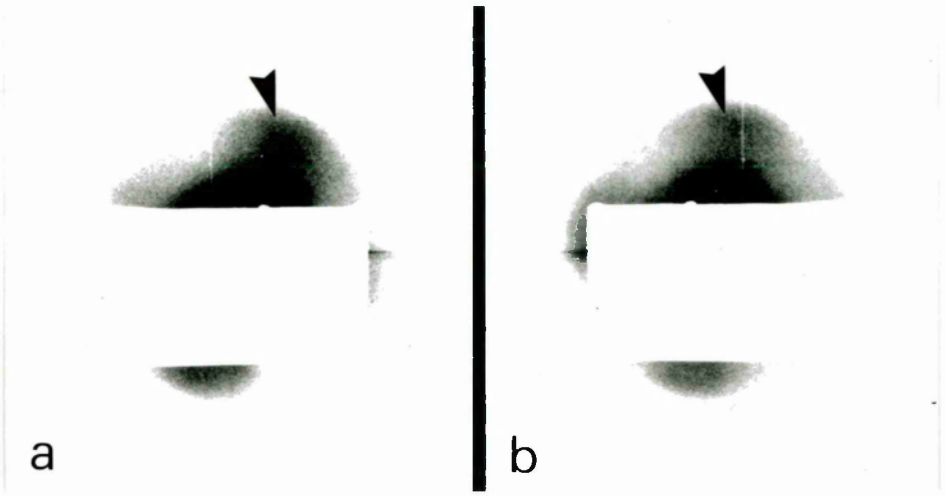

Figure 4.16 The first order equatorial diffraction ring (arrowed) from macular dystrophy cornea 1 at hydrations of (a) 2.0 and (b) 3.5. The mean centre–to–centre collagen fibril spacing is calculated from analysis of this ring.

The first order equatorial X-ray diffraction reflection from macular dystrophy cornea 1 is shown at two different hydrations (figure 4.16). The rings show maxima in two orthogonal directions which have been shown for normal human corneas to arise from a preferred orientation of collagen in the inferior–superior and medial–lateral directions (Meek et al., 1987a,b). A densitometric scan across an equatorial ring enables the diameter of the ring to be measured. Using X-ray diffraction patterns from various macular dystrophy corneas, data were obtained for the macular dystrophy interfibrillar spacings (table 4.7). The value quoted for macular dystrophy cornea 4 is the mean of 20 interfibrillar spacings throughout 1mm x 0.5mm areas the dystrophic stroma (see later: figure 4.20). The other spacings are derived from the pattern produced by a 4mm x 0.5mm beam passing through an area near the centre of the button.

Specimen	Type	Hydration	Interfibrillar spacing (nm)
1	II	2.0	43±2
1	II	3.5	43±2
3	I	–	52±3
4	I	–	48±4.7
6	II	–	52±2
8	I	–	49±2
Normal	–	–	60.8±2.9
Normal*	–	3.2	61.9±4.5

* Taken from Gyi et al., 1988.

Table 4.7 The mean interfibrillar spacings in 5 macular dystrophy corneas (type I and type II) and one normal control as derived from analysis of the first order equatorial reflection. The normal value was the mean of 20 different 1mm x 0.5mm areas within the normal stroma. The data taken from Gyi et al., (1988) are an average of 4 specimens, all near physiological hydration.

The first order equatorial reflection, produced by diffraction from the central cornea is shown in figure 4.17 for areas from (a) the macular dystrophy cornea and (b) the normal adult human cornea. The peak–to–peak distance in a linear densitometric trace through the centre of each ring (figure 4.19 and figure 4.18) represents the most frequently occurring interfibrillar spacing within that portion of the cornea through which the X–ray beam passes. The diameter of each ring is inversely proportional to the magnitude of the interfibrillar spacing, and the reflections shown in figure 4.17 (a) and (b) represent most frequent spacings of 45.4nm and 63.2nm respectively. The interfibrillar reflections from macular dystrophy and normal corneas also have different radial intensity distributions; this is evident from the difference in the shape of the peaks in the densitometer scans. The peaks in the scan across the normal human interfibrillar ring (figure 4.18) are fairly symmetrical about their centre. However, the peaks in the scan across the macular dystrophy cornea (figure 4.19) are skewed outwards, i.e. their peaks lie outside their centres. If the low–angle patterns are assumed to be esentially linear over

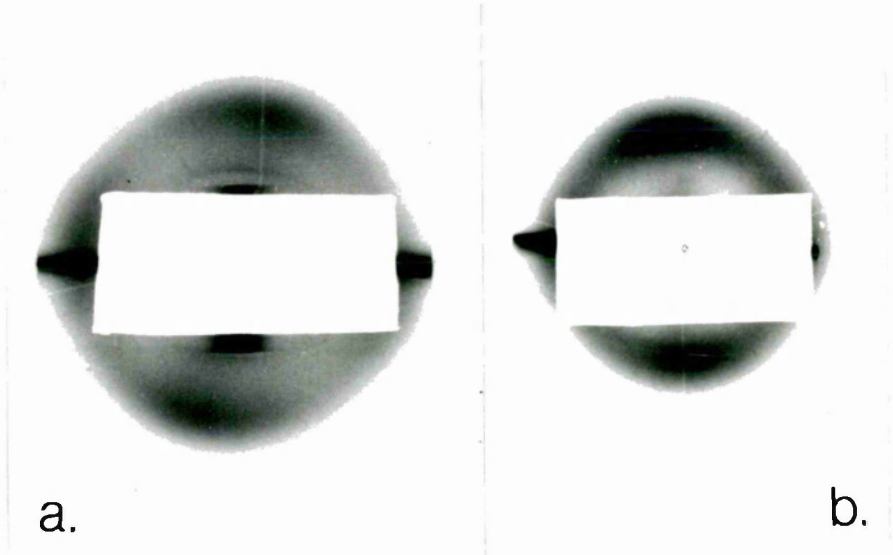

Figure 4.17 The first order equatorial X–ray diffraction ring from (a) an area of macular dystrophy cornea and (b) an area of normal adult human cornea. The fact that these exposures were obtained using different camera lengths has been compensated in the enlargement/printing procedure. The diameter of these rings is inversely related to the mean value for the interfibrillar spacing within the tissue.

this range of spacings, the observations indicate that the distribution of interfibrillar spacings in normal human cornea is symmetrical about the mean value. However, in macular dystrophy corneas, remembering that the diameter of the interfibrillar ring is inversely proportional to the spacing, the shape of the peak indicates that more interfibrillar spacings are smaller than the mean value than are larger than it.

In the schematic representation of the X–ray results obtained at various different positions across the cornea (figures 4.20 and 4.21) the boxes represent the areas of the cornea which were exposed to the X–ray beam in the macular dystrophy corneal button (figure 4.20) and the normal

human corneo–scleral disc (figure 4.21). In figure 4.20 the circle represents the edge of the macular dystrophy button. The corresponding area in the normal human cornea is approximately outlined in figure 4.21. The orientation of the corneas shown schematically in these figures is as *in vivo*. Subsequent analysis of the first order equatorial ring for each area gave a value for the most frequently occurring interfibrillar spacing within that area (throughout the whole thickness of the stroma). The number in each box gives this spacing in nm. The most frequently occurring spacings in the macular dystrophy cornea vary by as much as 19% around the mean value of 48.0nm (S.D.=$\pm$2.5). The spacings in the normal human cornea are more constant, varying by about 9% around the mean of 60.8nm (S.D.=$\pm$1.4).

An alternative representation of the macular corneal dystrophy data is obtained by measuring the distance between the centres of the densitometer peaks (taken as the mid–point at half peak height) rather than the distance between their highest points (figure 4.22). This, instead of giving a value for the most frequent spacing, produces a value which is the central point of a distribution, although not a mathematically normal distribution. The value therefore represents an overestimation of the mean and, as such, checks that the lower spacings found in macular dystrophy corneas are not dependant merely on the asymmetry of the densitometer scan. The values vary by about 17% around the mean value of 51nm (S.D.=$\pm$3.0). The data are still significantly lower than normal.

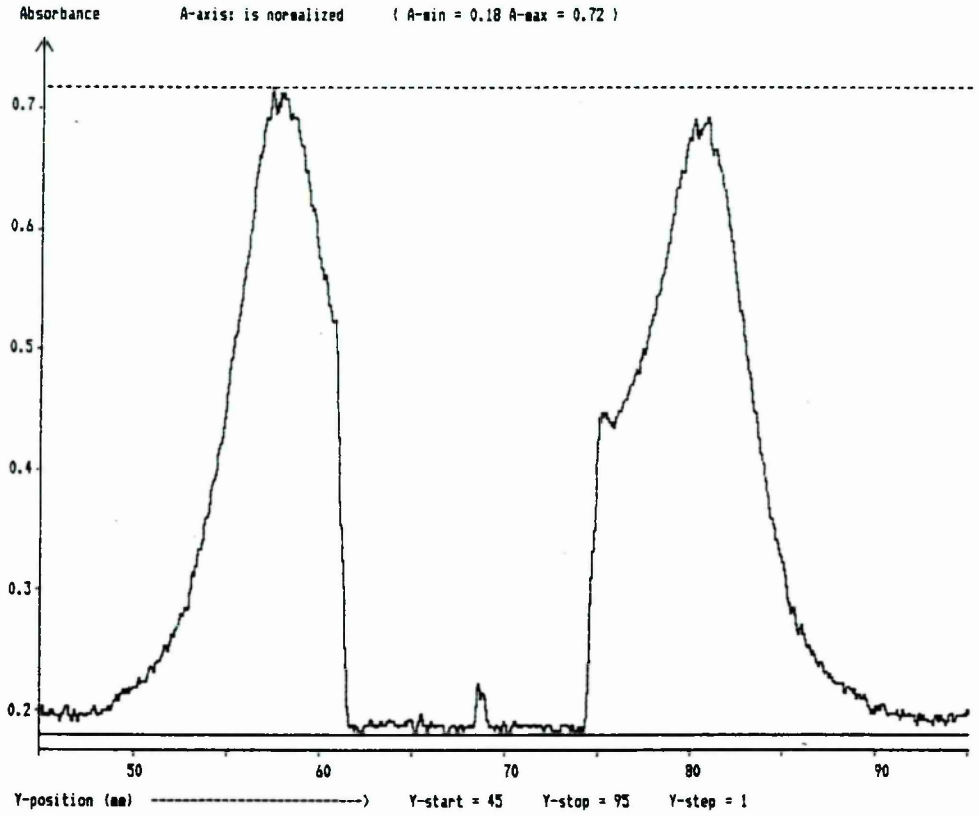

Figure 4.18 A laser densitometer scan across the first order equatorial reflection obtained from an area of normal human cornea. The reflection is shown in figure 4.17(b).

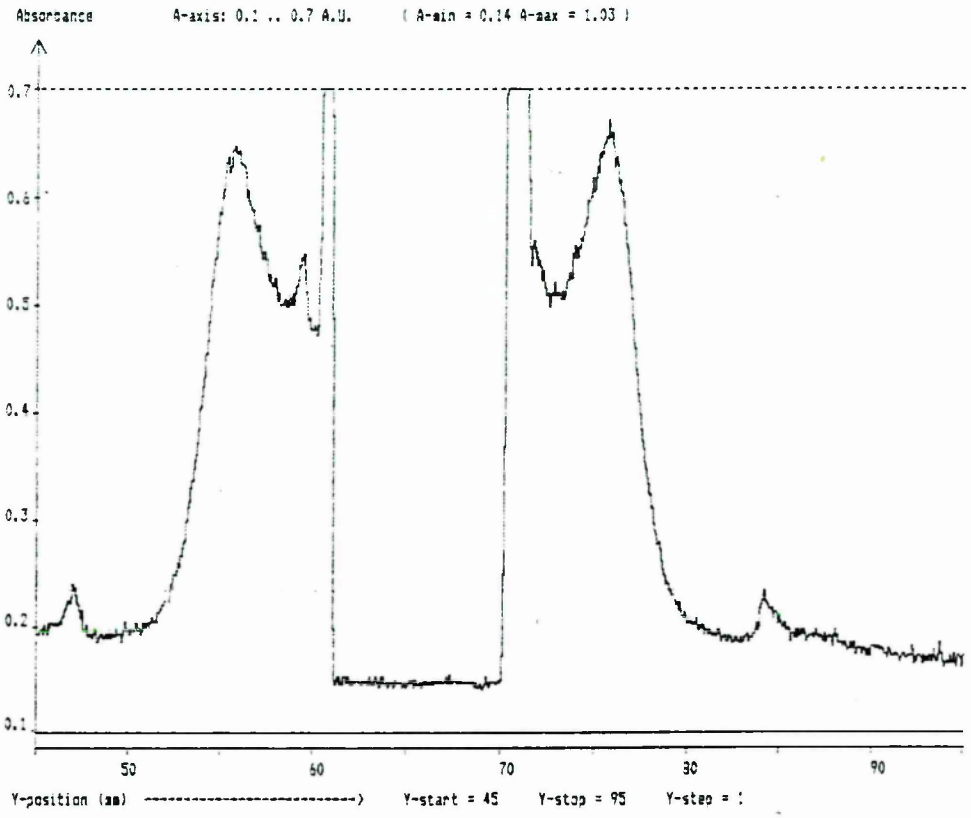

Figure 4.19 A laser densitometer scan across the first order equatorial reflection obtained from a macular dystrophy cornea. The reflection is shown in figure 4.17(a).

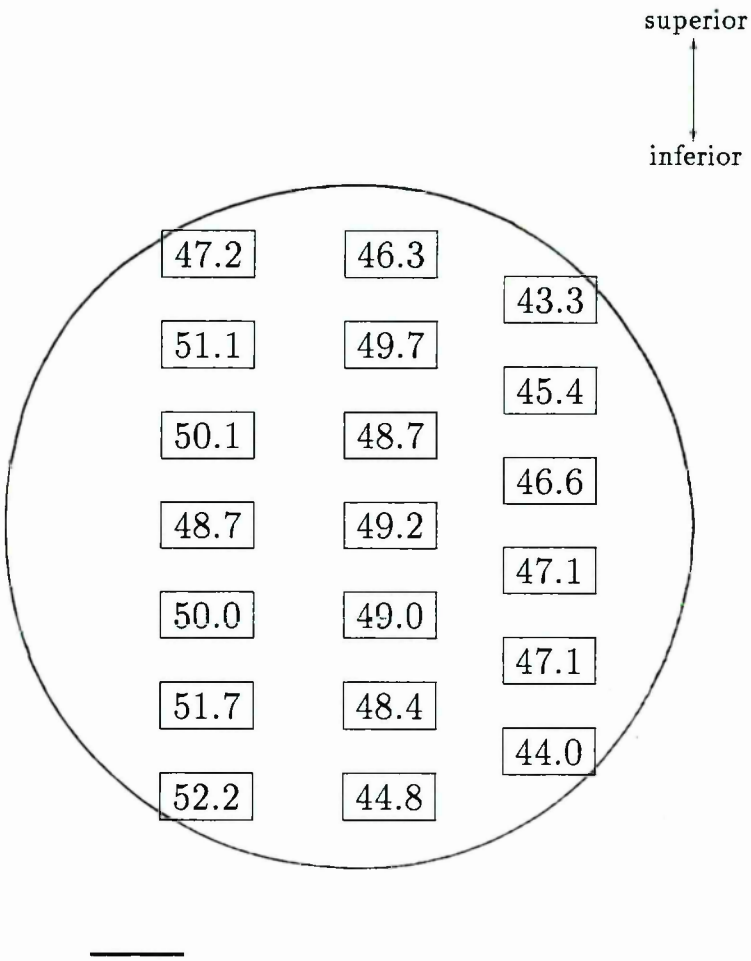

Figure 4.20 A schematic representation of the interfibrillar spacings which occur within macular dystrophy cornea 4. The circle represents the edge of the corneal button and the values are in nm (S.D.=±2.5nm); each one represents the most frequently occurring spacing within the area which outlines it, extended throughout the thickness of the cornea. Bar=1cm.

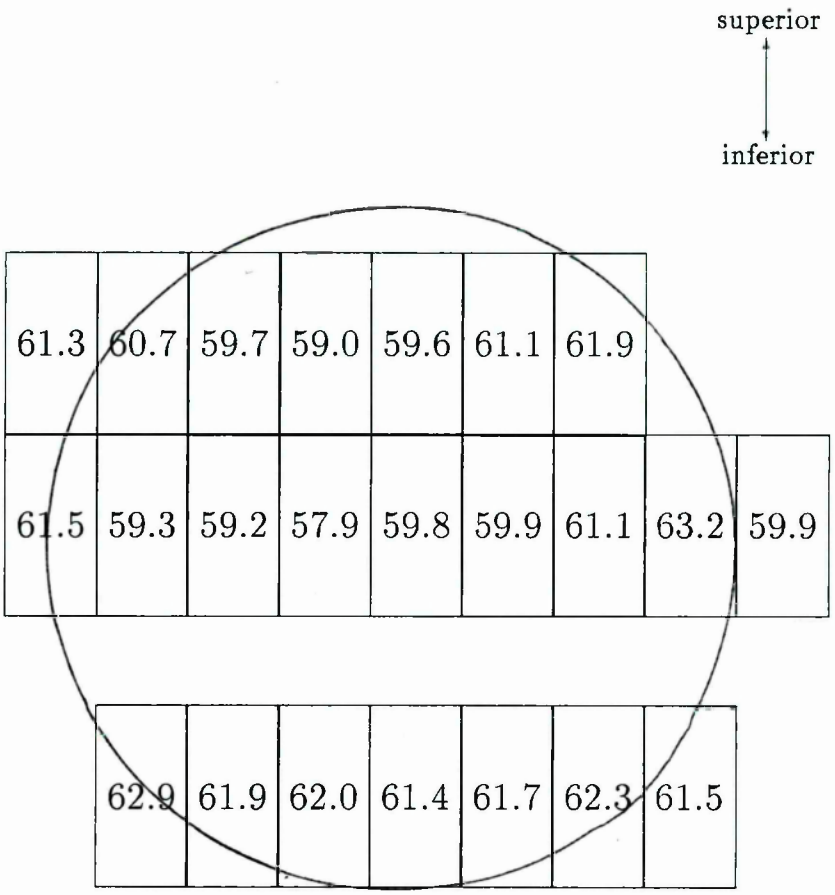

Figure 4.21 A schematic representation of the variation in interfibrillar spacings within a normal human cornea. The circle represents the area in the corneo–scleral disc which corresponds to the edge of a macular dystrophy button excised during penetrating keratoplasty (in this case button 4). The values are in nm (S.D.=±1.4nm); each one represents the most frequently occurring spacing within the area which outlines it extended throughout the thickness of the cornea. Bar=1cm.

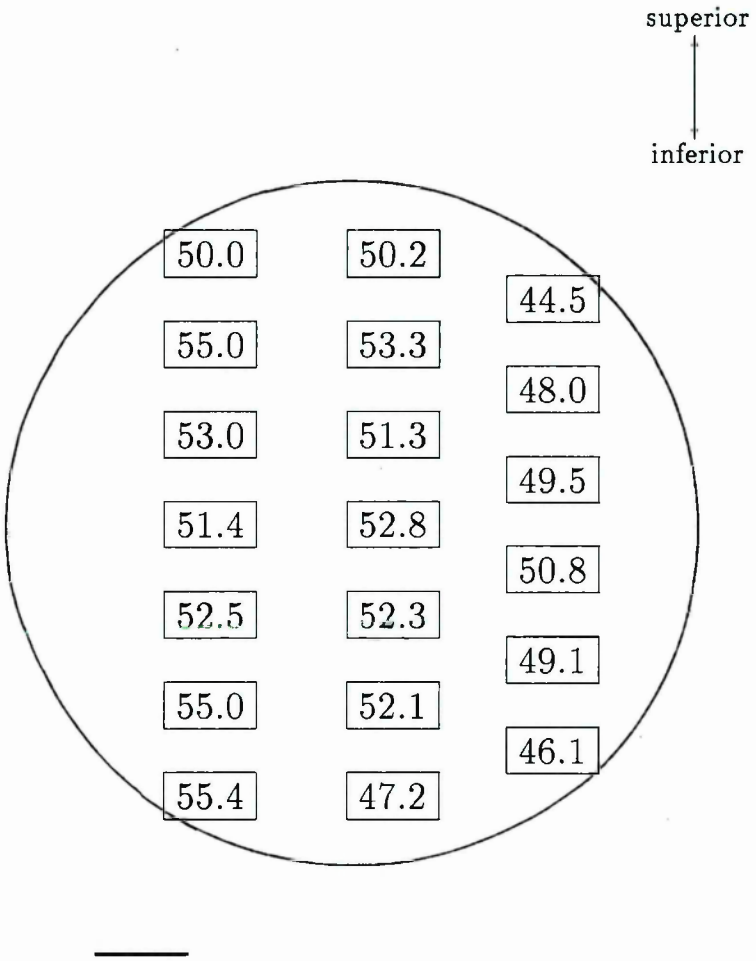

Figure 4.22 A schematic representation of the interfibrillar spacings which occur within macular dystrophy cornea 4. The circle represents the edge of the corneal button and the values are in nm (S.D.=±3.0nm); each one represents an overestimation of the mean spacing within the area which outlines it, extended throughout the thickness of the cornea. Bar=1cm.

The two subsequent orders of the equatorial diffraction pattern were obtained from two macular dystrophy corneas (specimens 1 and 3) and one normal, age–matched human cornea with exposure times of 20–30 minutes. The first subsequent order was obtained with a 15 minute exposure of another macular dystrophy cornea (specimen 8). Measurement of these reflections is thought to yield values for the average diameters of those collagen fibrils which give rise to the X-ray diffraction pattern. These values are given in table 4.8.

Specimen	Type	Diameter(nm)*	Diameter(nm)**	Average Diameter
1	II	29.4	30.1	29.7
3	I	30.7	31.8	31.3
8	I	30.0	–	30.0
Normal	–	30.8	30.7	30.75
Bovine†	–	40.2	35.1	37.65

*Using the first subsequent order reflection.
**Using the second subsequent order reflection.
† Data taken from Sayers et al., 1982.

Table 4.8 The mean collagen fibril diameter in macular dystrophy corneas (type I and type II) calculated by analysing the subsequent reflections (above the first order) of the low–angle equatorial diffraction pattern.

The data imply that fibril diameters in macular dystrophy corneas are not greatly altered from normal, especially when compared to the difference in size of corneal collagen between humans and, say, cattle. It should be noted, however, that the subsidiary reflections from macular dystrophy cornea were more diffuse than those from normal cornea. This implies that there may be some variation in the fibril diameter of macular dystrophy corneas (either between fibrils or along individual fibrils) but it will be necessary to collect more X–ray data before this suggestion can be verified.

4.3.5 Meridional X–Ray Diffraction

	Intensity		
Order	Macular 1	Macular 3	Normal*
1	16.3	26.4	30.3
2	0	0	0
3	50.9	65.8	61.8
4	10.1	7.3	11.6
5	25.0	16.3	19.1
6	0	0	0
7	7.0	0	0
8	12.8	6.3	6.0
9	13.2	–	6.5

* Taken from Meek et al., 1983

Table 4.9 The integrated meridional X–ray intensities from normal and macular dystrophy corneas. The macular dystrophy 1 intensities are presented with the fifth order arbitrarily assigned the value of 25 and the macular dystrophy 3 intensities are scaled to these by equating summed scattered intensities (see text). The normal data are scaled to the macular dystrophy 1 intensities by the same method. A zero value does not necessarily represent the complete absence of a reflection, just that its intensity was too low to be resolved by the densitometer (in this case anything below about 6.0).

The first nine integrated intensities from the low–angle meridional X-ray diffraction patterns from normal and macular dystrophy corneas are shown in table 4.9. The normal data have been scaled to the macular dystrophy 1 data by equating the summed scattered intensities using:

$$\sum_{n=1}^{9} I_{macular} = \sum_{n=1}^{9} I_{normal}$$

where n is the order of the reflection. Macular dystrophy 3 intensities were scaled to macular dystrophy 1 intensities by similarly equating the summed scattered intensities of the first eight orders; because of the camera length available on that experimental run, orders nine and above

were not recorded. It can be seen from table 4.9 that the intensities from macular dystrophy corneas are not greatly altered from normal . The R–factors resulting from the comparison of a set of macular dystrophy data with the set of normal data were lower than or equal to 0.18. These very low R–values indicate that the axial distribution of electron density along the collagen is not significantly altered in macular dystrophy corneas.

	Intensity	
Order	Cuprolinic blue	Control
1	0	21.6
2	0	0
3	26.6	47.3
4	19.1	16.3
5	25.0	25.0
6	29.0	34.2
7	15.0	18.1
8	0	21.9
9	21.2	51.8

Table 4.10 The integrated meridional X–ray intensities from macular dystrophy cornea 1 stained for proteoglycans with Cuprolinic blue. The data are scaled arbitrarily so as to equate fifth order intensities. As in table 4.9 a zero value represents an intensity too low to be resolved by the densitometer.

The meridional X-ray diffraction results obtained from macular dystrophy cornea 1, with and without Cuprolinic blue staining, are shown in table 4.10. These two data sets cannot be scaled together by equating summed scattered intensities because of the presence of extra stain material in the Cuprolinic blue treated specimen. However, inspection of the data revealed clear differences between the Cuprolinic blue–stained and control intensities (for example between orders 1, 8 and 9 in table 4.10). It was thus concluded that Cuprolinic blue staining produces real differences in the electron density of macular dystrophy corneal collagen. This means that sulphated proteoglycans are bound periodically

along at least some of the constituent collagen fibrils, but in the absence of any information about the phases of the reflections it is not possible to locate the axial positions of proteoglycan binding.

4.3.6 High–Angle X–Ray Diffraction

Specimen	Type	Hydration	Intermolecular distance (nm±0.04nm)
4	I	–	1.78
6	II	–	1.94
8	I	–	1.82
4	I	0	1.33
		0.5	1.79
		0.8	1.83
		1.6	1.83
		1.8	1.83
5	I	0	1.39
		2.8	1.97
		4.0	1.94
9	I	0	1.46
		6.8	2.01
Normal	–	0	1.32
		0.5	1.75
		0.8	1.80
		1.1	1.85
		1.3	1.85

Table 4.11 The average separation of collagen molecules within the fibrils of macular dystrophy corneas 4, 5, 6, 8 and 9 and a normal human cornea measured from the first order high–angle equatorial reflection. Patterns from specimens 4, 6 and 8 were recorded at near physiological hydration. Patterns were further recorded from specimes 4, 5 and 9 (plus a normal control) air–dried and at several stages of rehydration.

The high–angle X-ray diffraction patterns were obtained for macular dystrophy corneas 4, 6 and 8 at near physiological hydrations. Specimens 6 and 8 were required for future studies and hence were not dried down to

calculate the hydration. High–angle patterns were also taken of a normal human cornea and macular dystrophy corneas 4, 5, 7 and 9 air–dried and at several stages of rehydration[1]. Figure 4.23 shows the high angle X-ray diffraction pattern from (a) macular dystrophy cornea 4 and (b) a normal human cornea. The high angle patterns from macular dystrophy corneas 5, 6, 8 and 9 are similar to figure 4.23(a). The diameter of first order reflection was used to calculate the mean centre–to–centre spacing of molecules within macular dystrophy corneal collagen. The data are shown in table 4.11. The values for the separation of collagen molecules in the air–dried normal and macular dystrophy corneas compares well with the intermolecular separation in polyethylene glycol–dried bovine stromas which is 1.27±0.04nm (Fullwood et al., 1990). The intermolecular spacing of macular dystrophy corneas 4 and 5 is seen to increase from dry in a similar fashion to the normal human cornea.

The most striking features of the X-ray diffraction patterns from macular dystrophy corneas is the observation of two "extra reflections" (figure 4.23(a); small arrows). A densitometer scan across the high angle pattern of a macular dystrophy cornea (shown for macular dystrophy cornea 9 (H=0) in figure 4.24) identifies the position of the two extra rings, along with that of the 1st order equatorial reflection. These reflections are not present on high–angle X-ray diffraction patterns obtained from the normal human corneal stroma (figure 4.23(b)). The outer reflection is present on every high–angle X-ray diffraction pattern that was obtained from macular dystrophy corneas, irrespective of their hydration. The structure which gives rise to this outer reflection has a periodicity given in table 4.12. There is a remarkable consistency about the position of the outer ring in all thirteen X-ray diffraction patterns from five different macular dystrophy corneas at various states of hydration. The mean periodicity which gives rise to the outer reflection is 4.61Å with a standard deviation of only ±0.03Å. The corneal hydration of

[1]The three patterns from macular dystrophy cornea 7 were underexposed and, for this reason, did not yield intermolecular values. They did, however, contain two sharp "extra reflections" which are reported and discussed later.

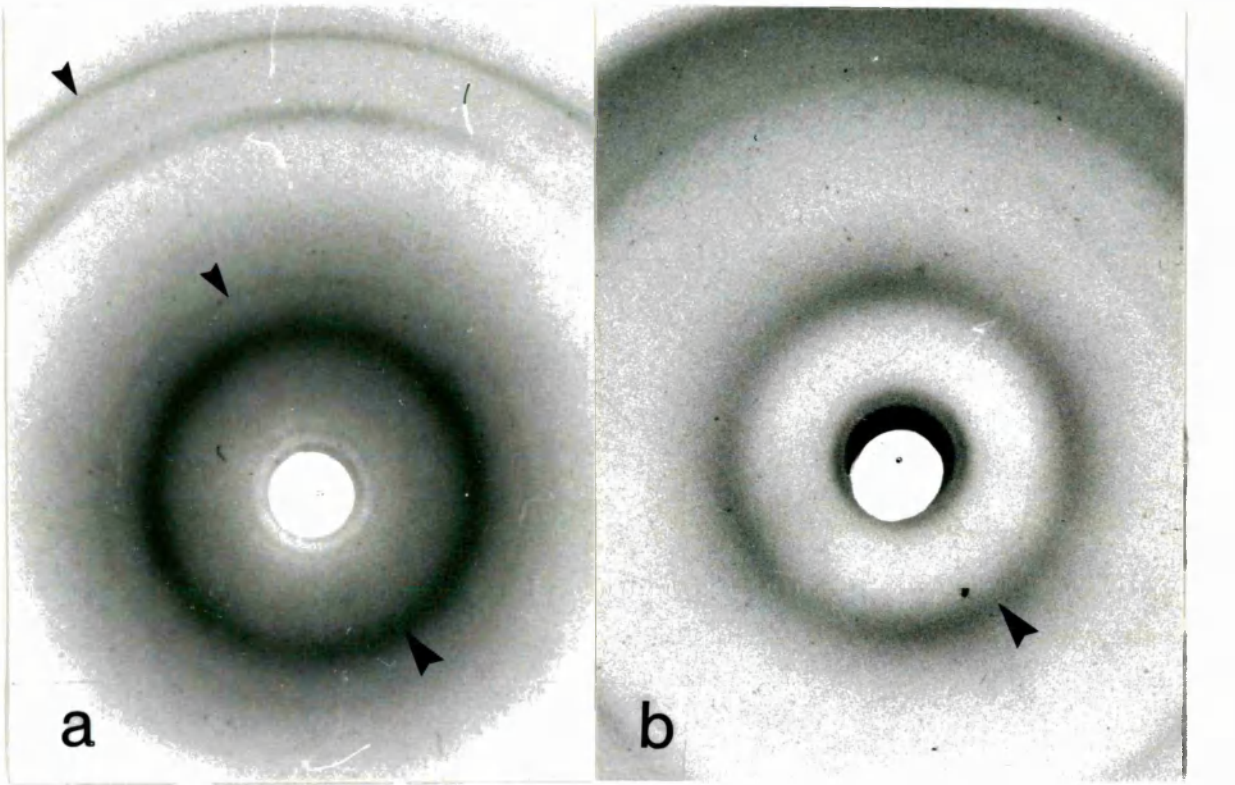

Figure 4.23 The high–angle synchrotron X-ray diffraction patterns from (a) macular dystrophy cornea 4 at H=0 and (b) a normal human cornea at H=0. The intermolecular reflection (large arrows) is present in both. It is larger than at physiological hydration due to the dehydrated state of the cornea, and hence close molecular packing in the collagen. The inner and outer "extra reflections" are observable on the macular dystrophy pattern. The asymmetric ring, just inside the outer extra reflection, is due to the mylar window of the cell holder. Figure 4.24 shows a densitometer scan across the high angle pattern of macular dystrophy cornea 9 at H=0.

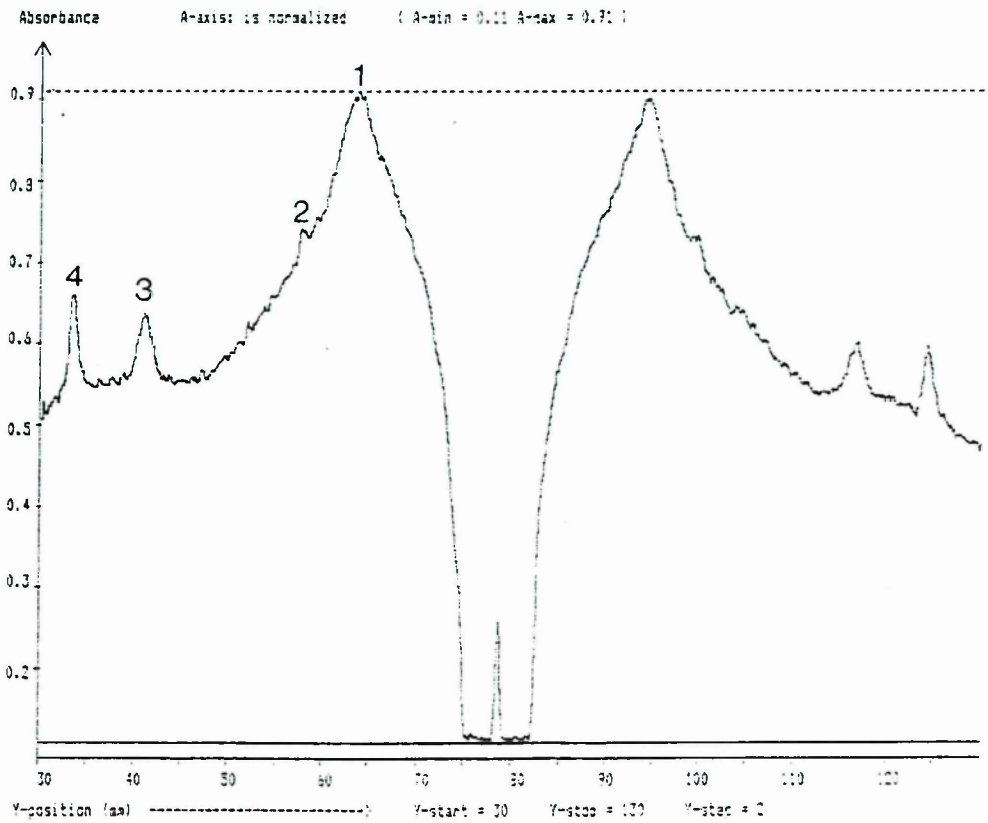

Figure 4.24 A densitometer scan across the high angle X-ray diffraction pattern from macular dystrophy cornea 9. This scan is used to define the positions of the various reflections.The pattern is symmetrical about a hole made in the centre of the X–ray film and the various reflections are denoted by numbers;

1. The 1st order equatorial
2. The inner "extra" reflection
3. The reflection arising from the mylar window of the cell holder
4. The outer "extra" reflection.

Patient	Type	H	d (outer) (Å)	d(inner) (Å)	I(outer:inner)
4	I	0	4.65	9.62	12:1
		0.5	4.65	9.67	19:1
		0.8	4.63	9.62	35:1
		1.6	4.64	–	–
		1.8	4.62	–	–
5	I	0	4.56	9.56	13:1
		2.8	4.59	–	–
		4.0	4.58	–	–
6	II	–	4.67	9.62	–
7	I	0.1	4.59	–	–
		0.5	4.60	–	–
		0.5	4.58	–	–
8	I	–	4.61	–	–
9	I	0	4.61	9.64	18:1

Table 4.12 The periodic spacings, within the five macular dystrophy stromas, which give rise to the two "extra reflections" in the high angle X-ray diffraction patterns. The periodic spacings giving rise to the outer ring (d(outer)) are in Å with a standard deviation of ± 0.03Å and those giving rise to the inner ring (d(inner)) are also in Å with a standard deviation of ± 0.04Å. The relative intensity of the two reflections (I(inner:outer)) is given as a ratio. Wherever possible the hydration (H) of the specimen is quoted.

macular dystrophy patient 5 rises from H=0 to H=4.0 causing the collagen intermolecular spacing to increase from 13.9Å to 19.4Å. Similarly the corneal hydration of macular dystrophy patient 4, in rising from H=0 to H=1.8 causes the collagen intermolecular spacing to rise from 13.3Å to 18.3Å. However in both these cases, where the stroma is obviously imbibing water, there is no significant change in the 4.61Å periodicity.

The inner "extra reflection" (figure 4.23(a)) is observable on five of the thirteen macular dystrophy X-ray diffraction patterns (the three patterns from patient 7 were underexposed and, for this reason, wouldn't have been expected to contain the inner ring) although on the pattern from

patient 6 it was too faint for its intensity to be recorded by the laser densitometer. The mean spacing which gives rise to the inner reflection is 9.62Å. It is clear from the X-ray diffraction patterns, and hence from the relative intensities of the two "extra reflections" (the intensity of each reflection is defined as the area under the peak multiplied by the circumference of the reflection) that the inner (9.62Å) reflection is only present when the cornea is below a certain level of hydration.

4.4 Oedematous Human Corneas

4.4.1 Scanning Electron Microscopy

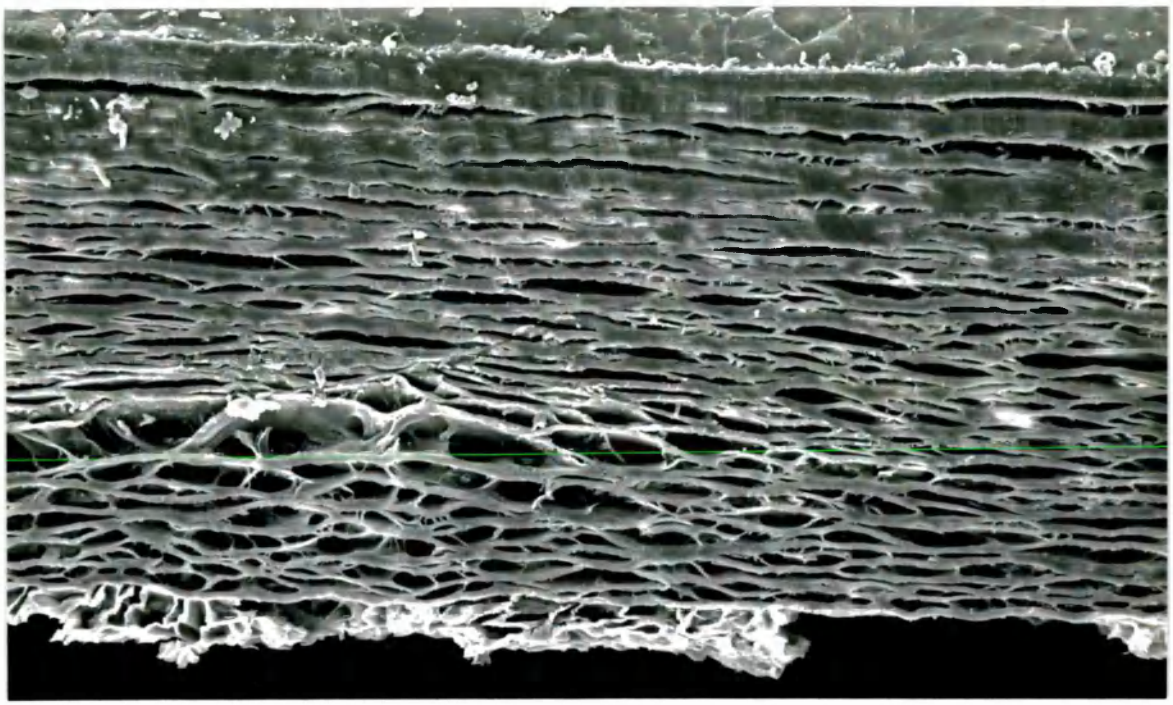

Figure 4.25 A low magnification scanning electron micrograph of a full thickness section of oedematous cornea 8. Interlamellar spaces are more prevalent in the posterior portion of the stroma. The epithelial cell layer is visible but the endothelium did not remain intact during processing.

A scanning electron micrograph showing a full thickness section of oedematous cornea 8 (figure 4.25) reveals the existence of intra–lamellar collagen–free areas. These areas are more prevalent in the posterior section of the oedematous stroma and could, *in vivo*, represent

water–filled "lakes" within the stroma. Of course, the possibility exists that the collagen–free areas are artifacts of the freezing process. A scanning electron microscopical study of the effects of freezing on bovine stromas at various hydrations (Fullwood, N.J., personal communication) demonstrated only minimal change in the stromal appearance between fresh and frozen corneas at physiological hydration; the appearance of collagen–free areas in the frozen specimens was very limited (see below). Small collagen–free areas were obseved in highly hydrated, frozen specimens but these were not so extensive as those in figure 4.25.

Higher magnification micrographs of normal stroma and oedematous stroma (figure 4.26) demonstrated that the individual collagen fibrils present in the normal stroma were not observable in the oedematous case. Since both specimens had been stored frozen it seems unlikely that this occurrence is artifactual.

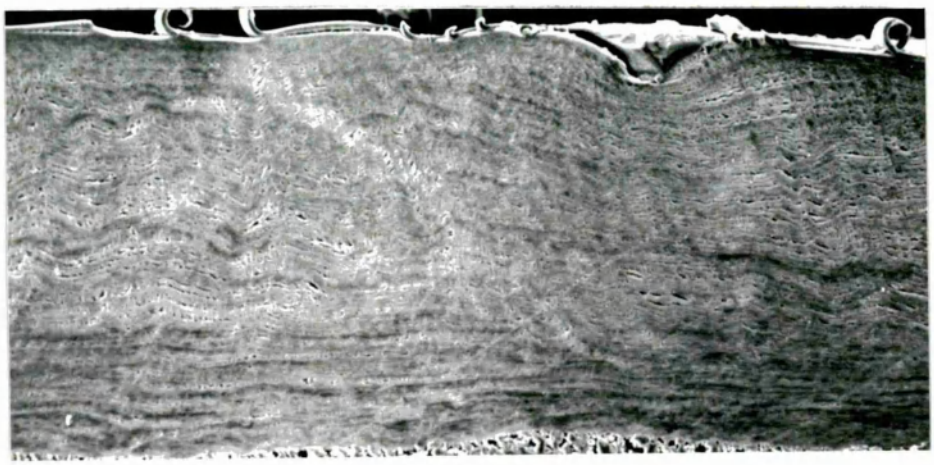

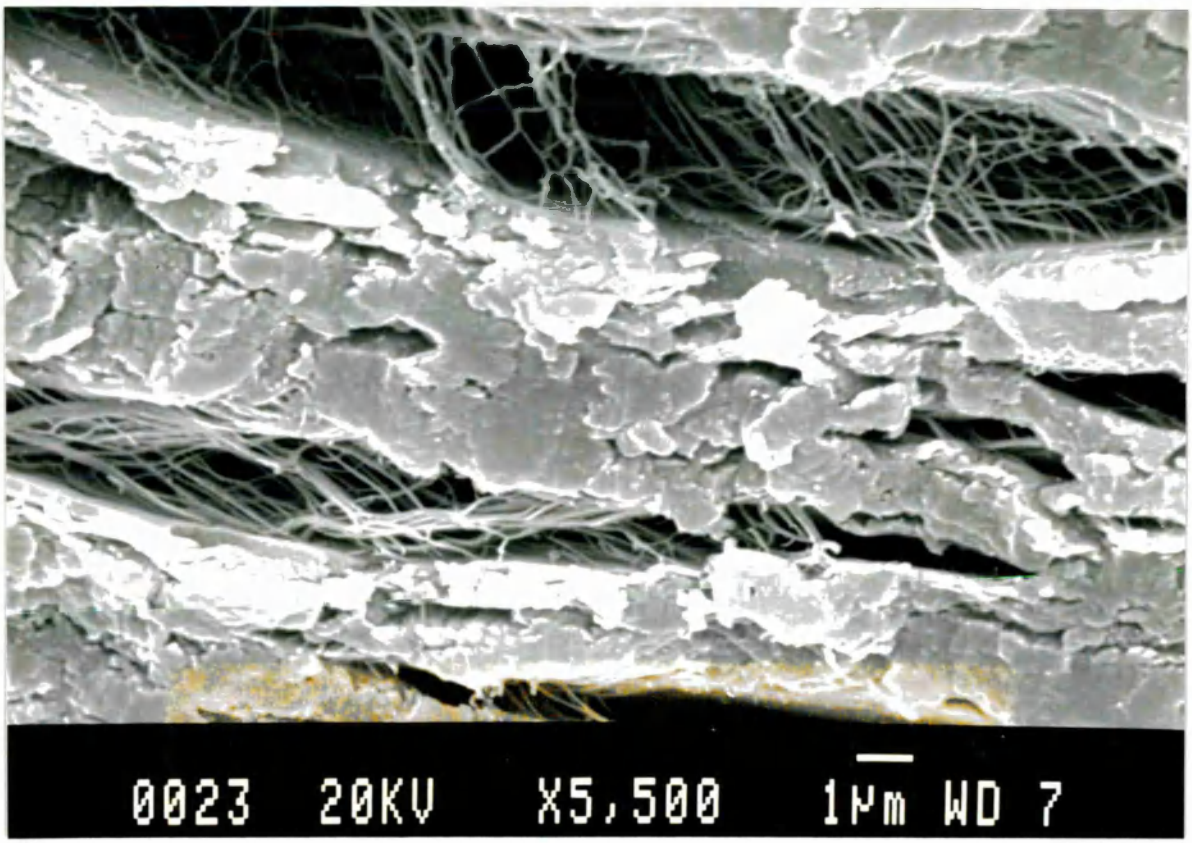

Figure 4.26 (a) A scanning electron micrographs of a cross–sectional area of normal corneal stroma. Individual fibrils are visible between the lamellae.
(b) A similar magnification scanning electron micrograph (overleaf) of oedematous stroma 8. In this case no individual fibrils are present between the lamellae.

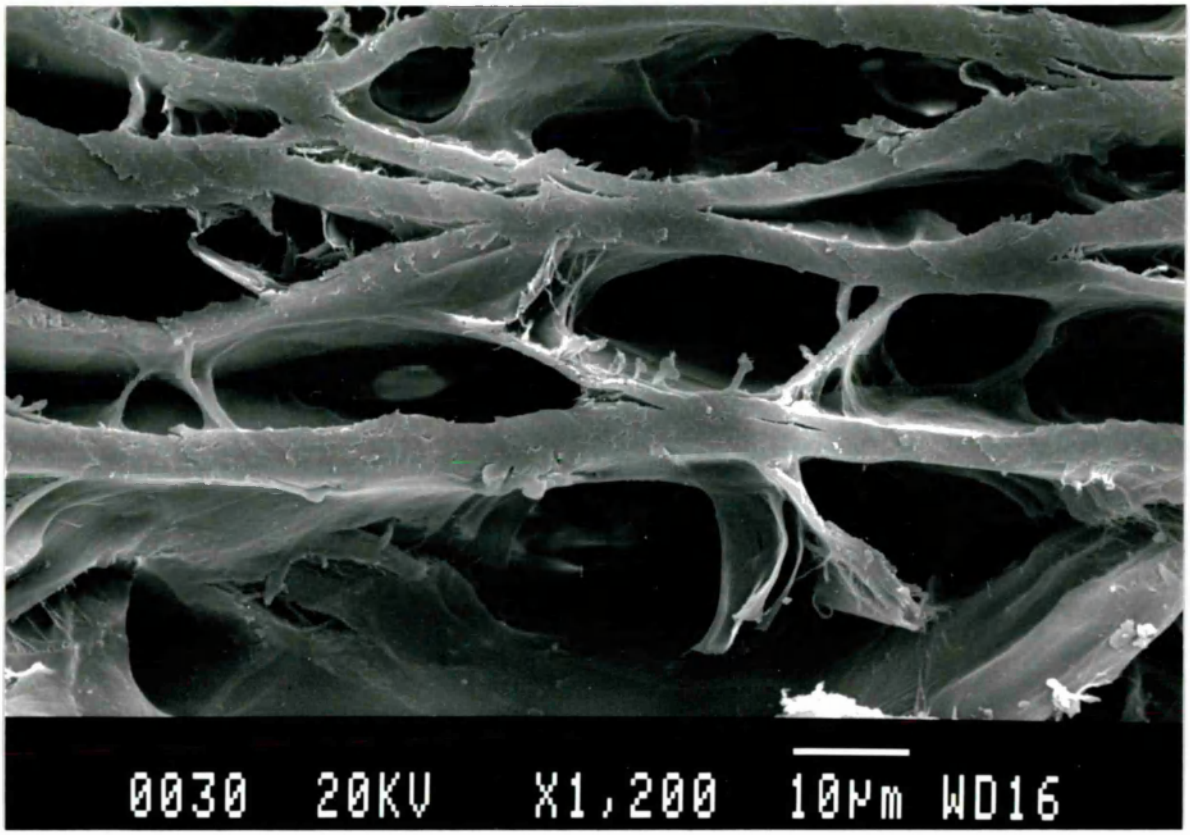
0030 20KV X1,200 10µm WD16

4.4.2 Transmission Electron Microscopy

The architecture of the oedematous stroma was disrupted with "wavy" lamellae (figure 4.27), small collagen–free areas (figure 4.28) and larger collagen–free "lakes" (figure 4.29) all observable in transmission electron micrographs of the tissues; separation of adjacent fibrils is also frequently observed (figure 4.30). The proteoglycan filaments in the collagen matrix of the oedematous tissue appeared normal in both size and electron density, but larger ones were occasionally visible in the collagen–free areas (figures 4.28 and 4.29). The proteoglycan content of the oedematous samples, as observed by the extent of Cuprolinic blue staining, varied, appearing to be normal in some areas and reduced in others. In several areas of the swollen tissue the proteoglycans seemed to associate with the collagen fibrils in a D–periodic fashion (figure 4.31). Also, in some areas, a disproportionately large number of proteoglycans were seen to associate with the collagen at the 'd/e' staining bands.

Enzyme digests were performed on two of the oedematous corneas. Samples from each were incubated with one of the glycosaminoglycanases (keratanase, chondroitinase AC or chondroitinase ABC) in a buffer, before treatment with Cuprolinic blue. The digests demonstrated no significant alteration in their proteoglycan content when compared to the control samples which had been treated identically with no enzyme in the buffer (figure 4.32).

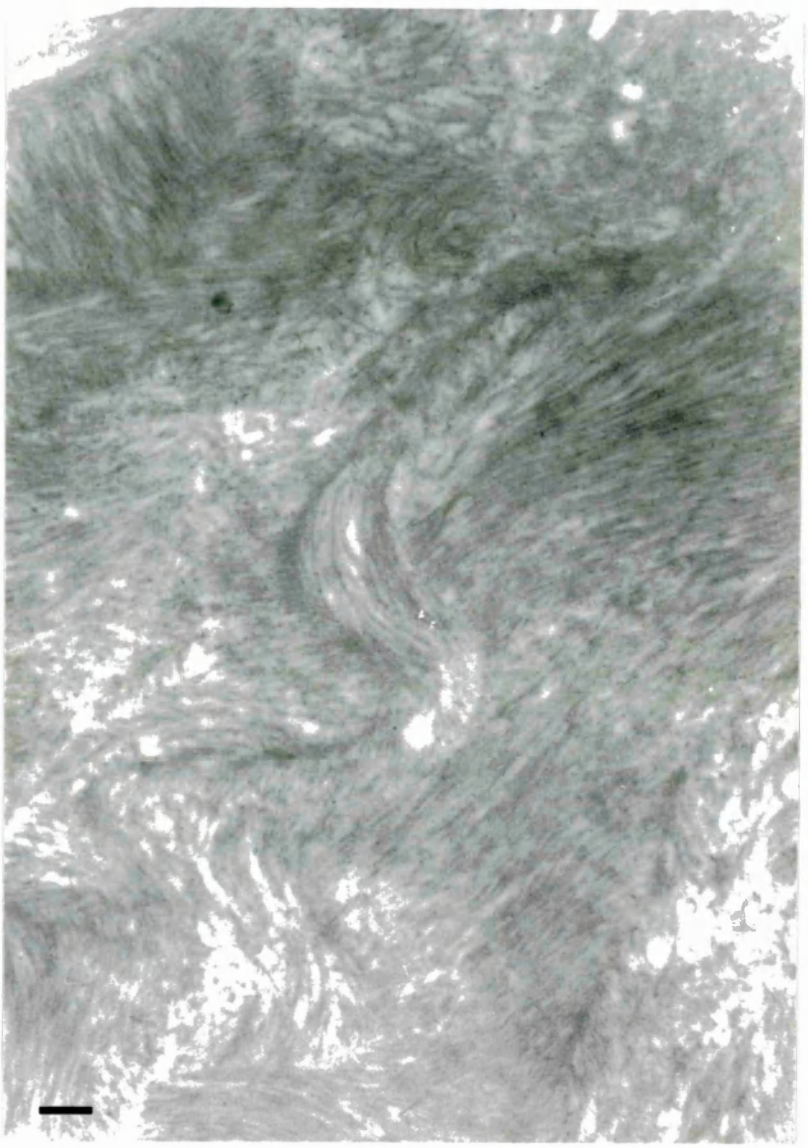

Figure 4.27 A transmission electron micrograph of an oedematous stroma stained for collagen with 2% uranyl acetate demonstrating the presence of disrupted "wavy" lamellae. Bar=350nm.

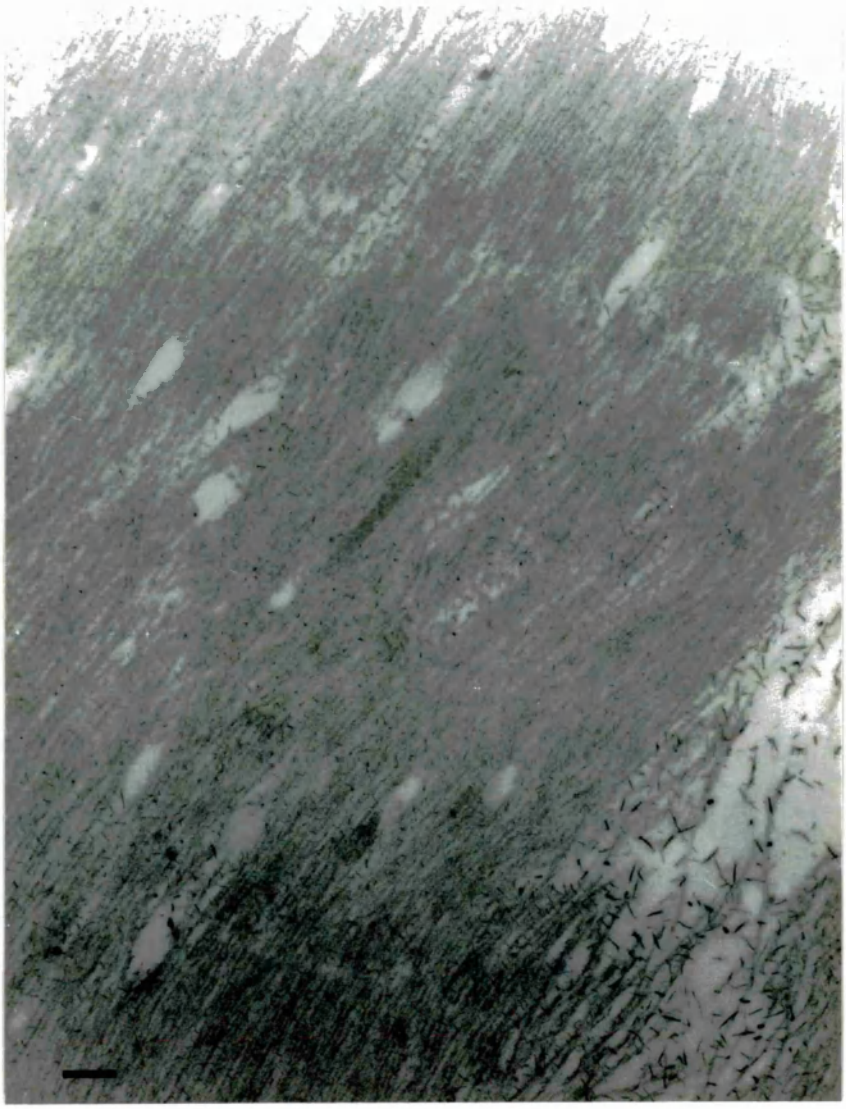

Figure 4.28 A transmission electron micrograph of an oedematous stroma, stained for collagen with 1% phosphotungstic acid and 2% uranyl acetate and for proteoglycans with Cuprolinic blue, demonstrating the presence of small collagen–free areas. Proteoglycan filaments within the collagen matrix appear fairly normal but larger ones are occasionally observed in the larger collagen–free areas. Bar=600nm.

Figure 4.29 A transmission electron micrograph of an oedematous stroma, stained for collagen with 1% phosphotungstic acid and 2% uranyl acetate and for proteoglycans with Cuprolinic blue, demonstrating the presence of larger collagen–free areas. The proteoglycan filaments in the collagen matrix appear fairly normal whilst larger ones are occasionally observed, along with fragments of collagen, in the disrupted areas. Bar=900nm.

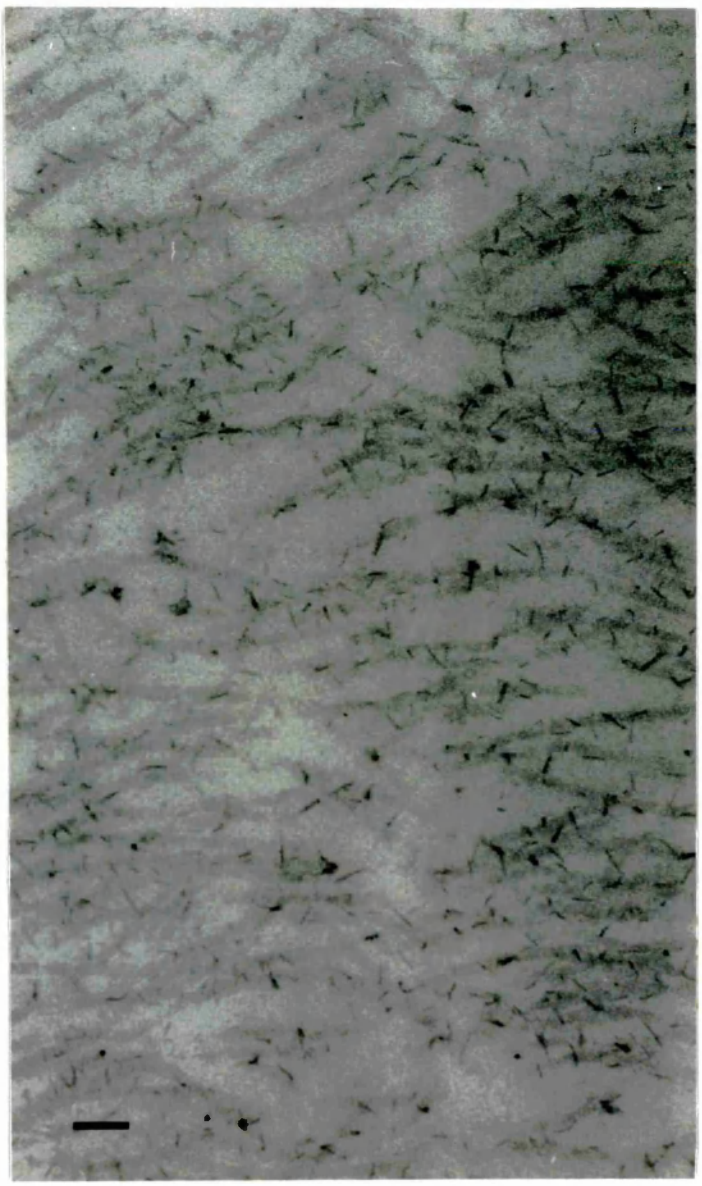

Figure 4.30 A transmission electron micrograph of an oedematous stroma, stained for collagen with 2% uranyl acetate and for proteoglycans with Cuprolinic blue, demonstrating the separation of individual adjacent fibrils. The proteoglycans appear normal in size and seem to remain associated with the collagen. Bar=80nm.

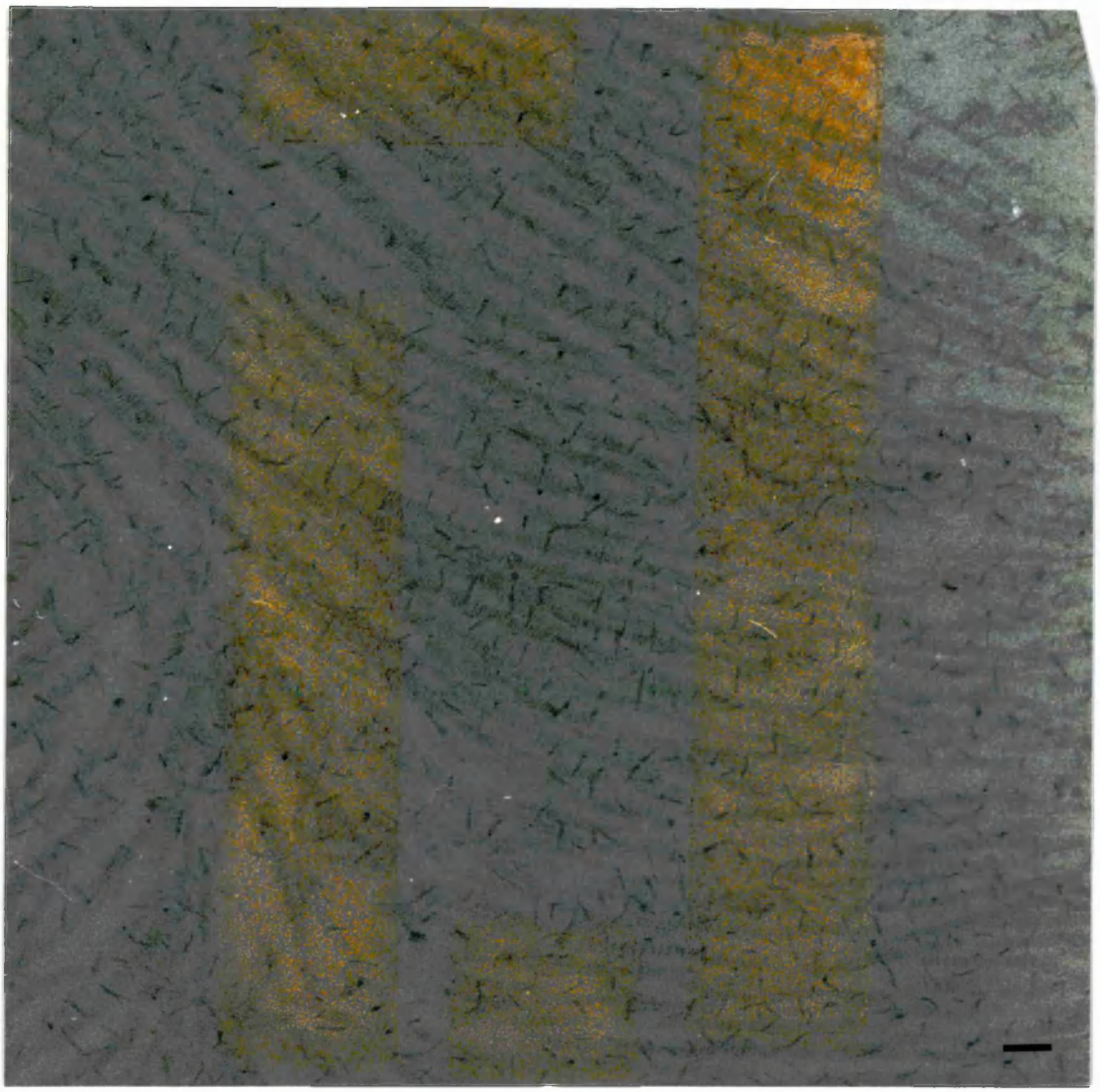

Figure 4.31 A transmission electron micrograph of an oedematous stroma stained for collagen with 1% phosphotungstic acid and 2% uranyl acetate and for proteoglycans with Cuprolinic blue. Proteoglycans are seen to associate with collagen fibrils in a D–periodic fashion. Bar=100nm.

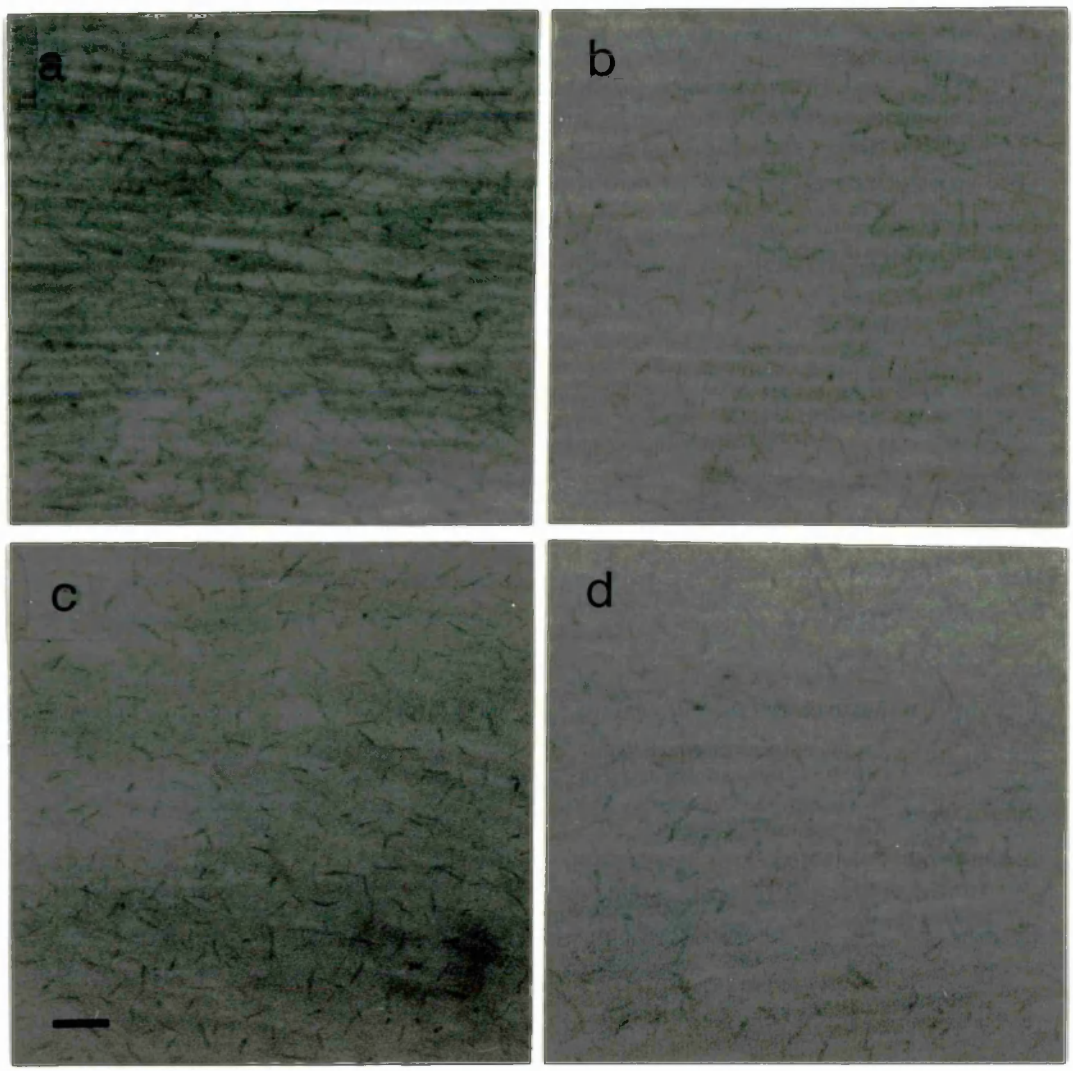

Figure 4.32 A composite figure consisting of transmission electron micrographs of an oedematous stroma which has been incubated with various glycosaminoglycanases prior to staining with 2% uranyl acetate for collagen and Cuprolinic blue for proteoglycans. (a) Control, (b) Keratanase, (c) Chondroitinase AC and (d) Chondroitinase ABC. Bar=100nm.

4.4.3 Equatorial X–Ray Diffraction

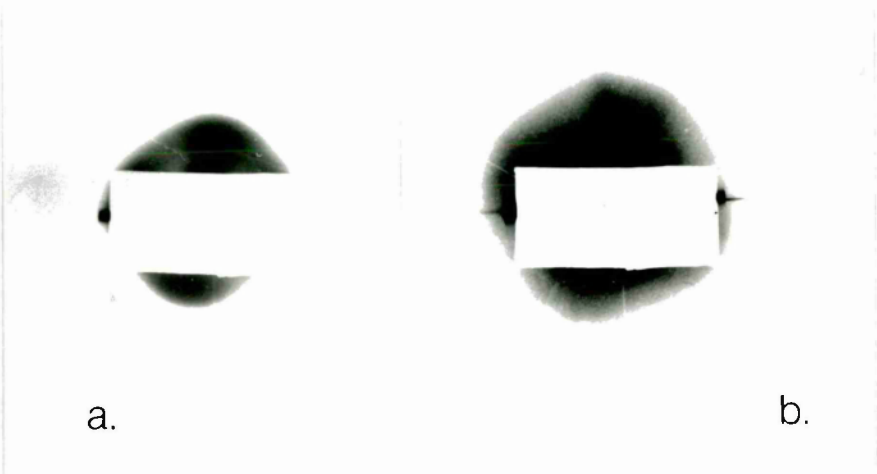

Figure 4.33 The first order equatorial reflection obtained from oedematous corneas (a)5 and (b)9.

Specimen	Hydration	Interfibrillar spacing (nm)
4	–	50.7±2
5	6.7	67.6±2
9	5.5	33.6±2 up to >75±2
Normal	–	60.8±2.9
Normal*	3.2	61.9±4.5
Normal†	3.2	61.7±5.3

* Taken from Gyi, et al., 1988.
†Fullwood, N. J., personal communication.

Table 4.13 The mean interfibrillar spacing, in nm, for three oedematous corneas and one normal control as derived from analysis of the first order equatorial reflection. The normal value is the mean of 20 values obtained from the X–ray scan of the normal stroma (figure 4.21). The normal data (*,n=4; †, n=14) are all near physiological hydration.

The first order equatorial reflection obtained from cornea 5 (figure 4.33) is a well defined ring which was obtained with an exposure time of 1 minute.

Specimen	Diameter(nm)*	Diameter(nm)**	Average diameter
4	31.7	34.6	33.2
5	34.5	–	34.5
Normal	30.8	30.7	30.75
Normal†	32.6	–	32.6

* Using the first subsequent equatorial reflection
** Using the second subsequent equatorial reflection
† Fullwood, N.J., personal communication.

Table 4.14 The mean collagen fibril diameter in two oedematous corneas and one normal control calculated by analysing the subsequent reflections (above the first order) of the low–angle equatorial diffraction pattern. The normal value† was obtained from four corneas (above H=2) which had been stored in a culture medium. There is no significant change in intermolecular spacing, and hence fibril diameter, above H=2 (Meek et al., 1991).

The ring is highly lobed, indicating a preferred orientation of collagen fibrils in mutually orthogonal directions, a feature of all human corneas (Meek et al., 1987). Cornea 4 exhibited a similar diffraction pattern but the corresponding interfibrillar spacing was reduced. Unfortunately, the hydration of this specimen is not known but it seems that the close fibril packing is the result of accidental post–operative specimen dehydration. The interfibrillar reflection from oedematous cornea 9 (figure 4.33) is very diffuse and required a 10 minute exposure. The reflection resembles a disc (rather than a ring) which extends into the backstop and represents a spread of interfibrillar spacings ranging from about 34nm to greater than 75nm. The data are given in table 4.13. The mean, centre–to–centre, collagen fibril separation is seen to be only marginally increased in the case of cornea 5.

Either of the two subsequent orders of the low–angle equatorial diffraction pattern from fresh cornea may be used to obtain an average value for the diameter of the approximately cylindrical collagen fibrils. The first subsequent order required a 10 minute exposure of cornea 5 and both

subsequent orders were obtained from cornea 4 with a 25 minute exposure. The values, given in table 4.14, demonstrate a slight increase in the diameter of the fibrils in oedematous cornea 5; even the suspected slightly dry cornea 4 has slightly swollen fibrils, an observation which is considered in greater detail in the discussion section. When compared to the data for the four normal corneas the slight increase in the diameters is not significant ($p>0.1$) within the experimental resolution of the system. The 10 minute exposure of oedematous cornea 9 was not long enough to record either of the subsequent reflections (above the first order reflection/disc) and hence contained no information about fibril diameters.

4.4.4 High–Angle X–Ray Diffraction

Specimen	Hydration	Intermolecular distance (nm±0.04nm)
2	–	1.88
4	–	1.90
6	5.6	1.81
7	4.6	1.87
8	6.1	1.82
9	5.5	1.93
10	3.9	1.82
Normal*	> 2	1.83±0.07

* Fullwood et al., personal communication.

Table 4.15 The average separation of collagen molecules within the fibrils of oedematous corneas measured from the first order high–angle equatorial reflection. The normal value (*) is a mean of 28 human corneas with a hydration greater than 2, above which the intermolecular separation does not increase with hydration (Meek et al., 1991).

The centre–to–centre lateral spacing of collagen molecules which make up the fibrils was calculated for seven oedematous specimens (table 4.15). There does appear to be a small increase (up to about 6%) in the intermolecular separation in some oedematous specimens, although this is within the experimental resolution of the system. A comparison of the

oedema data (n=7) with the normal data (n=28) reveals that there is no significant difference (p>0.2).

4.4.5 Meridional X–Ray Diffraction

	I(patient1)		I(patient6)		I(patient8)	
Order	CuB	Control	CuB	Control	CuB	Control
1	27.2	41.2	115.9	124.7	153.9	215.1
2	0	0	0	0	0	0
3	54.3	86.6	99.3	58.2	88.0	69.9
4	26.2	26.7	19.6	11.8	20.5	12.8
5	25	25	25	25	25	25
6	15.8	18.1	17.9	9.0	16.8	9.7
7	3.7	5.2	0	0	0	0
8	11.4	7.4	0	8.0	5.3	7.1
9	18.8	22.2	16.7	11.0	19.9	25.5
10	9.1	11.3	–	–	–	–

Table 4.16 The meridional intensities obtained from the stromas from three patients with oedematous corneas. Half the specimen was treated with Cuprolinic blue (CuB) and the other half was an unstained control.

The first 9 or 10 meridional orders in the low–angle X-ray diffraction pattern were recorded for a Cuprolinic blue stained half specimen and its unstained control half. Three of the oedematous corneas were used in this part of the investigation (patients 1,6 and 8). The integrated intensities, above background scatter, were obtained for these specimens and are given in table 4.16. The intensities are scaled to one another by arbitrarily equating the 5^{th} orders.

Assessing the similarity of the intensities for each of the patients gave R–values of; patient 1, R=0.15, patient 6, R=0.17 and patient 8, R=0.17. These values are sufficiently low to allow the conclusion that staining with Cuprolinic blue does not significantly alter the electron density along the collagen axis.

When the three control columns are compared to each other, significant differences become apparent between the intensities; R=0.31 (patient 1 with patient 6), R=0.30 (patient 1 with patient 8) and R=0.19 (patient6 with patient 8). This implies a difference in the axial electron density along the collagen axis in at least two out of the three fixed oedematous corneas.

4.4.6 Immunochemical Analysis

Specimen	Portion	Hydration	KS(μg/ml)	CS(μg/ml)
6	whole	5.5	1.8	6.0
	anterior		3.7	7.7
	posterior		1.6	7.4
7	whole	4.6	1.6	6.7
	anterior		2.3	5.0
	posterior		3.0	6.8
8	whole	6.1	4.7	7.9
	anterior		2.9	7.2
	posterior		4.6	7.5
9	whole	3.9	2.3	9.4
	anterior		1.5	6.9
	posterior		2.3	7.9
Normal	whole	3.4	10.2	7.7
	anterior		10.1	8.2
	posterior		5.8	6.0

Table 4.17 The keratan sulphate (KS) and chondroitin sulphate (CS) content of various portions of normal and variously hydrated oedematous human corneas. The glycosaminoglycan content is expressed as μg/ml of the wet tissue.

The keratan sulphate and chondroitin sulphate content, expressed as μg/ml. of the wet tissue, of the specimens from four oedematous corneas and a normal control are given in table 4.17. The keratan sulphate content has decreased markedly from normal in all four of the oedematous

specimens. The reduction in keratan sulphate content in the whole thickness corneal samples, for which the hydration is known, does not seem to correlate with the extent of stromal hydration or oedema. In three of the four oedematous corneas (patients 7,8 and 9) the anterior portion contains less keratan sulphate than the posterior portion. The anterior portion of the normal cornea, however, contains the larger proportion of antigenic keratan sulphate. There is no indication that the chondroitin sulphate content is altered in oedematous corneas.

4.5 Scheie's Syndrome

4.5.1 Transmission Electron Microscopy

The stroma of the Scheie's syndrome cornea contained numerous electron transparent holes. These disruptions to the regularity of the collagen matrix frequently contained, or were adjacent to, electron dense deposits (figures 4.34 and 4.35). The collagen fibrils appeared normal but, considering the sample had been stained with Cuprolinic blue, there was a distinct lack of proteoglycan filaments. Only very occasionally could proteoglycan–staining be observed in the stroma. Figure 4.36 demonstrates the presence of a fibrous long–spacing structure in the stroma; this has a periodicity in the region of 100nm and is probably of a collagenous nature.

Figure 4.34 A transmission electron micrograph of the Scheie's syndrome cornea stained for collagen with 1% phosphotungstic acid and 2% uranyl acetate and for proteoglycans with Cuprolinic blue. Disruptions in the collagen matrix are evident and frequently these contain electron dense material. Bar=200nm.

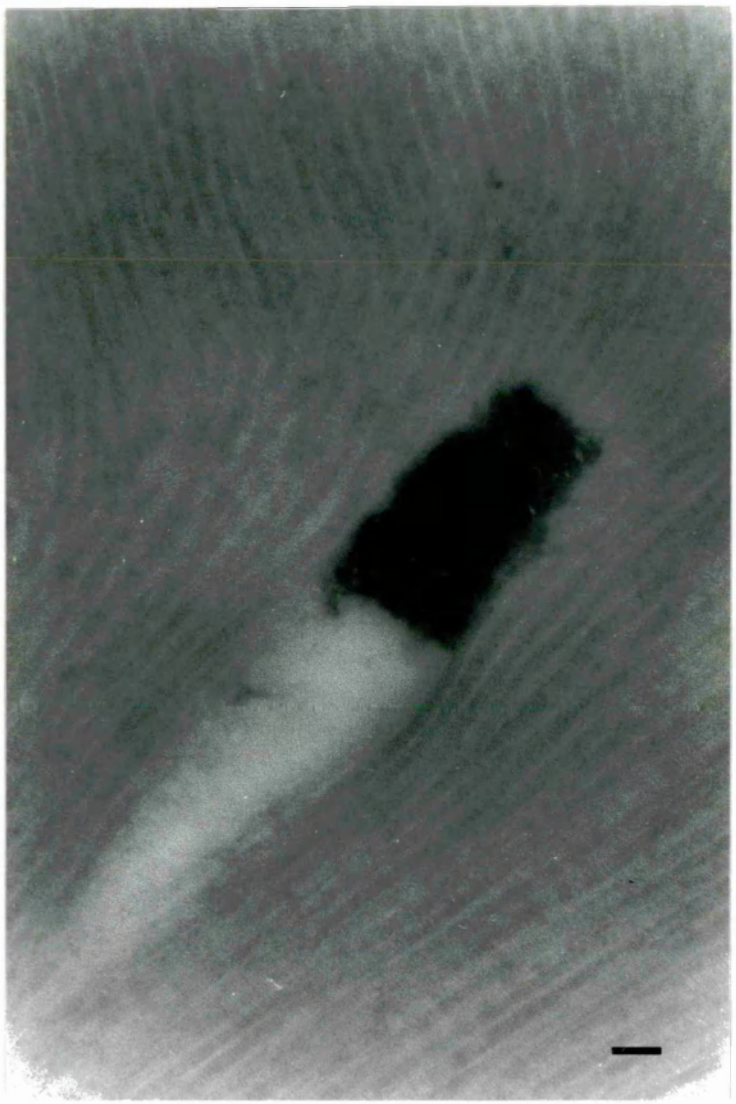

Figure 4.35 A transmission electron micrograph of the Scheie's syndrome cornea stained for collagen with 1% phosphotungstic acid and 2% uranyl acetate and for proteoglycans with Cuprolinic blue. This high magnification image demonstrates how the electron dense material disrupts the collagen fibrillar organisation. Bar=90nm.

Figure 4.36 A transmission electron micrograph of the Scheie's syndrome cornea stained for collagen with 1% phosphotungstic acid and 2% uranyl acetate and for proteoglycans with Cuprolinic blue. The collagen structure appears fairly normal in this image except for the lack of proteoglycan filaments. The extracellular matrix contains a type of fibrous long-spacing (probably collagenous) structure with a periodicity of about 100nm. Bar=200nm.

Chapter 5

Discussion

5.1 Human Sclera

It has been demonstrated that Cupromeronic blue staining, enhanced with sodium tungstate, modifies the meridional X–ray intensities from human sclera (section 4.2). The stain has similarly affected the intensities from rat tail tendons (Meek et al., 1985) and bovine cornea (Meek et al., 1986). To interpret the meridional changes which occur in sclera, it was necessary to scale the sets of data relative to each other. The fresh tendon data were scaled to the fresh sclera data by equating the summed scattered intensities on the assumption that the number of electrons per unit cross–sectional area coherently scattered from one D–period is the same in both structures. The Cupromeronic blue–stained sclera electron density was scaled to the electron density of its control by matching out the electron density in the overlap region of the respective collagen fibrils. This second assumption, namely that most proteoglycan binding occurs in the gap, rather than overlap, region of the fibrils, is consistent with the location of the stained filaments in the electron microscope (see figure 4.1).

Dermatan sulphate is the major proteoglycan in the sclera (Cöster & Fransson, 1981). X-ray diffraction has now revealed that it is attached at the same axial location (the 'd/e' bands) as occurs in rat tail tendon.

Using electron microscopy it has also been located at this site in skin (Scott & Haigh, 1985a), heart valve (Nako & Bashey, 1972), intervertebral disc (Scott & Haigh, 1986) and articular cartilage (Orford & Gardner, 1984). Proteoglycan/collagen binding in the cornea is more complex and although dermatan sulphate proteoglycans are bound at some 'd/e' bands (Scott & Haigh, 1985b; Meek et al., 1986; 1987) a proportion of the gap zones remain unoccupied. It has been suggested that the radial growth of collagen fibrils could be hindered by restricted access to the cross–linking sites, due to the proximity of the dermatan sulphate proteoglycans (Scott & Orford, 1981). This implies that tissues with less collagen–bound dermatan sulphate would contain fibrils with larger diameters, which is not the case in the cornea and sclera; sclera contains fibrils with much larger diameters. A possible explanation is that corneal keratan sulphate proteoglycans also play a role in restricting aggregation of collagen molecules and thus restrict the lateral growth of the fibrils.

The relationship between proteoglycans and collagen in the human sclera has been shown to be similar to that in rat tail tendon but different from that in bovine (Meek et al., 1986) and human cornea (Meek et al., 1987). This structural difference may be related to the functions of the tissues. The primary role of tendon and sclera is to resist mechanical stresses which attempt to extend the tissue. These stresses may be caused by external physical forces and motions (as in tendon) or intraocular pressure (as in sclera). Although the cornea also withstands the intraocular pressure, its consistency is not as firm as that of the sclera (Newell, 1982; Maurice, 1988). Its most important feature is its transparency, which seems to require a different collagen–proteoglycan organization.

The absence of dermatan sulphate proteoglycan at the 'd' band has been noted in demineralized bone collagen (Scott & Haigh, 1985a). This has led to the suggestion that its presence in non–calcified tissue sterically inhibits the nucleation of calcification.This seems an even more plausible hypothesis if the proteoglycans fill up not only the 'd' band but a large part of the gap zone as suggested by the X-ray diffraction results (see

figure 4.4). The deposition of calcium occurs in a number of connective tissue disorders including those of ocular tissues. In particular, it is sometimes present in pathological scleras, where it can occur throughout the whole thickness of the tissue (Yanoff & Fine, 1982). This calcification may be due to lack of some or all of the dermatan sulphate proteoglycans, or their abnormal arrangement with the collagen fibrils.

The high angle X-ray diffraction results obtained from normal human sclera show how collagen intermolecular spacing increases as a function of hydration (see figure 4.5) to a maximum value of about 1.7nm at a hydration of 2.5. The hydration range obtained by polyethylene glycol equilibration of normal human sclera (0.6–>5) is similar to the hydration range encountered when the same protocol is used to equilibrate bovine corneas, and shows that sclera has the ability to imbibe water above H=2.5; this probably causes the fibrils to move apart. However, it is not possible, since sclera does not produce an interfibrillar reflection, to use X-ray diffraction results to predict the distribution of water within the tissue; water could locate homogeneously between the fibrils or heterogeneously in "lakes". The molecules in bovine corneal collagen continue to move apart slowly beyond H=2.5, reaching a maximum value of about 1.9nm. In similar preparations of rat tail tendon, the collagen intermolecular spacing reaches a maximum value of about 1.65nm at around H=2.5, beyond which the tendon will not imbibe water (Meek et al., 1991). Human sclera, therefore, has similar *in vitro*, swelling properties to both cornea and tendon. The swelling characteristics of human sclera are very similar to those of bovine cornea, although sclera exhibits proportionally lower intermolecular spacings. The maximum intermolecular spacing for human scleral collagen, however, is closer to that of rat tail tendon collagen.

5.2 Normal Human Cornea

The transmission electron microscopical observations of Cuprolinic blue treated normal human cornea (see table 4.6) seem to suggest preferential association of proteoglycans in the region of the 'b' doublet on the collagen fibrils. This results in the presence of a strong, broad bar around the collagen 'b' bands on the histogram of proteoglycan occupation frequency (figure 4.7). Two other weaker, thinner bars are evident, at the 'a/e' and 'd' bands, but the relatively small sample size precludes any conclusions being drawn about this. The data do, however, point to a different proteoglycan binding than is observed in corneas from various other species (Scott & Haigh, 1988a). Meridional X-ray diffraction intensities obtained from human and bovine untreated corneas are not the same (Meek et al., 1983). This points to a difference in the axial electron density along the collagen fibrils which may be due, in part, to the different proteoglycan–collagen association. When human cornea is stained with Cupromeronic blue and the electron density profile is calculated, two areas of extra electron density are indeed observed at the 'b' doublet (Meek, K.M., unpublished result). These are attributed to the presence of collagen–bound proteoglycans. It should be pointed out, however, that this X-ray diffraction analysis employed the phases obtained for untreated normal human corneas (Meek et al., 1983). As it is not known what effect corneal staining has upon X–ray phases, the assumption that they remain the same is not necessarily true. Hence the correlation with the electron microscopical data should be regarded as tentative.

High–angle X-ray diffraction data demonstrate that the intermolecular separation of human corneal collagen, at hydrations approaching physiological hydration, is in the region of 1.85nm (see table 4.11). The corresponding separation of the molecules in bovine corneal collagen is about 1.8nm (Meek et al., 1991). Low–angle equatorial X-ray diffraction data show the diameter of the collagen fibrils in the human stroma to be

approximately 31nm (see table 4.8), whilst those in the bovine stroma are almost 38nm in diameter (Sayers st al., 1982). The implication, then, is that bovine corneal collagen fibrils contain more collagen molecules than do human corneal collagen fibrils.

5.3 Macular Corneal Dystrophy

Antigenic sulphated keratan sulphate in sera from two individuals without macular corneal dystrophy, analysed blind in a batch along with sera from macular corneal dystrophy patients 1–3, was present at normal and elevated levels (table 4.5). The keratan sulphate values (282 and 448 ng/ml) agreed well with previously published values (251±78 ng/ml) of serum keratan sulphate levels in 45 healthy volunteers (Klintworth et al., 1986), indicating that the monoclonal antibody was recognising the sulphated keratan sulphate epitopes after the transportation of the samples, either fixed or frozen, across the Atlantic.

Macular dystrophy patients 4, 5 and 8 are classified as having keratan sulphate negative (type I) macular corneal dystrophy due to the lack of antigenic keratan sulphate in both their corneas and sera. Also the lack of keratan sulphate in the cornea of patient 7 classified him as suffering from type I macular corneal dystrophy even though no serum was available for analysis. Patients 2, 3 and 9 were assumed to have type I macular corneal dystrophy, even though it was not possible to analyse their corneal tissue. However, since the contribution of corneal keratan sulphate to the serum is insignificant compared to that of cartilage keratan sulphate (Klintworth et al., 1986; Thonar et al., 1986) the corneas may possibly contain quantities of sulphated keratan sulphate. This possibility is supported by the discovery of a single macular corneal dystrophy patient with corneal keratan sulphate but negligible serum keratan sulphate (Edward et al., 1988).

Patient 6 is suffering from keratan sulphate positive (type II) macular corneal dystrophy due to the presence of antigenic keratan sulphate in both his serum and cornea. Patient 1 is also assumed to be suffering from type II macular corneal dystrophy. The amount of sulphated antigenic keratan sulphate in the serum from patient 1 is, however, greatly reduced from normal. Added to this is the fact that it was not possible to inhibit

totally the antibody from binding to the keratan sulphate. These results strongly suggest that the keratan sulphate epitope in the serum of patient 1 is slightly different to normal. The two most likely explanations are that the keratan sulphate side chains are undersulphated or shorter than normal. As previously stated, sulphated keratan sulphate present in the serum is thought to derive mostly from the normal turnover of cartilage proteoglycans (Thonar et al., 1985). So the presence of keratan sulphate in the serum of patient 1 does not necessarily mean that the cornea contains sulphated keratan sulphate.

The nine macular dystrophy patients come from seven different pedigrees in the United Kingdom. Of these nine, the immunohistochemical evidence has identified seven to be suffering from type I macular corneal dystrophy and two to be suffering from type II macular corneal dystrophy. This distribution is typical of macular corneal dystrophy since type I is by far the most prevalent form of the disease. In two recent studies it has accounted for 73% (Yang et al., 1988) and 80% (Edward et al., 1988) of macular corneal dystrophy patients according to the classification of Yang et al. (1988). Neither of the two brothers with macular corneal dystrophy (patients 2 and 4) contain antigenic sulphated keratan sulphate in their serum (the cornea of patient 4 also lacked keratan sulphate) and hence were both assumed to have type I macular corneal dystrophy. The brother and sister (patients 3 and 9) were also assumed to be suffering with type I macular corneal dystrophy due to negligible levels of serum keratan sulphate. These findings are consistent with the probability that siblings inherit the same type of macular corneal dystrophy.

It should be remembered that this immunohistochemical analysis, employing a monoclonal antibody, measures the keratan sulphate epitope and not absolute keratan sulphate mass. The possibility cannot be ruled out that keratan sulphate proteoglycans are present in samples where they are not detected by the antibody. These samples, cornea or serum, could contain keratan sulphate chains which, for some reason, are less antigenic than those in other samples. Possible reasons for reduced antigenicity

include shorter, or less highly sulphated, keratan sulphate side chains.

The transmission electron microscopical appearance of the macular dystrophy stromas exhibits a close similarity in the distribution of electron transparent lacunae to previous micrographs obtained using conventional staining (Klintworth & Vogel, 1964; Morgan, 1966; Klintworth, 1982). However, the techniques employed here were directed to staining collagen (and sometimes proteoglycans) and hence the internal detail of the keratocytes (figure 4.9) is less well visualized than in other published micrographs. These previous electron microscopical studies seem to have made little mention of the packing of the collagen fibrils in macular dystrophy corneas. However, the observations by Morgan (1966) show fibrils, in between the lacunae and keratocytes, with a fairly homogeneous distribution. This appears to contradict the electron optical observations (figures 4.9 and 4.10) which suggest some variation in the macular corneal dystrophy collagen fibril packing. This variation is noticed to occur both within and between individual corneas. Mogan (in 1966) could not comment on possible packing differences between individual fibrils since all the electron microscopy was carried out on a single specimen. Since the macular corneal dystrophy specimens studied here were prepared using identical methods it seems that the observed differences are inherent in the tissue and are not due to variations in the preparative process.

The same structural abnormalities are apparent in high–magnification micrographs taken of specimens which had been stored at $-40°C$ prior to electron microscopy preparation (corneas 1,2,3 and 5) and those which had been processed from fresh (corneas 4,6 and 8)[1]. This is an important observation. It demonstrates that freezing the specimens has no noticeable effect (on a small scale) on either the collagen structure or the proteoglycan character and distribution in the macular dystrophy cornea. Any artifactual ice–crystal formation would, therefore, seem to be

[1]Cornea 4 was stored in a saturated atmosphere (H_2O) for approximately 48 hours prior to electron microscopy preparation whilst corneas 6 and 8 were immersed in the fixative/staining solution within minutes of removal of the button.

predominantly interlamellar. This conclusion relates to the excised, *in vitro*, stroma. It can not be used to assess the chances of stromal healing after cryosurgical, lamellar keratoplasty techniques. Even though the data lead to the assumption that ice crystal formation does not affect the fine structure of the stroma, freezing procedures kill the majority of keratocytes (Lee et al., 1985) which play a major role in resynthesis of the extracellular matrix after wounding.

The abnormal features of macular dystrophy corneas, namely the presence of distinct electron transparent lacunae within the matrix and the proliferation of unusually large proteoglycan filaments, should now be regarded as being typical of the disease. Since the stromal architecture of macular dystrophy corneas, as observed in high–magnification transmission electron micrographs, seems to be unaffected by freezing it seems reasonable to assume that this is also the case for other corneas.

Cuprolinic blue staining has demonstrated several different kinds of proteoglycan filaments within macular dystrophy corneas. Large electron dense filaments are located predominantly clustered in zones free of any collagen fibrils along with smaller proteoglycans. The keratan sulphate proteoglycans in the keratan sulphate negative (type I) macular dystrophy corneas contain glycosaminoglycan side chains which are either undersulphated or shorter than normal. These would not be expected to react with the Cuprolinic blue stain under the conditions employed. Macular dystrophy cornea 1 was classified as being keratan sulphate positive (type II) macular corneal dystrophy due to the presence of antigenic keratan sulphate in the stroma. However, since the sulphated keratan sulphate level was much lower than normal, these proteoglycans may not stain with Cuprolinic blue. Hence all the proteoglycan filaments present in micrographs of the macular dystrophy stromas are likely to be of the chondroitin sulphate or dermatan sulphate variety. This was confirmed in corneas 1 and 4 where incubation with chondroitinase ABC digested almost all of the proteoglycan filaments, both small and large. Chondroitin sulphate proteoglycans, by definition, contain glucuronic acid

and do not contain iduronic acid. The chondroitin sulphate proteoglycans in the cornea however, do contain some iduronic acid and hence are generally referred to as being chondroitin/dermatan sulphate proteoglycans. The apparent lack of susceptibility of the proteoglycans in macular dystrophy cornea 4 to chondroitinase AC, an enzyme which is able to cleave the dermatan sulphate chain wherever glucuronic acid residues are present, implies that they contain a proportion of iduronic acid. Even so, since the glucuronic acid residues are still likely to make up a significant percentage of the uronic acid residues in the dermatan sulphate chains, some degradation of the proteoglycan filaments by the chondroitinase AC might have been expected. However, this did not seem to occur and the possibility cannot be ruled out that the aggregation of dermatan sulphate chains renders the glucuronic acid residues inaccessible to the action of the enzyme. Alternatively, cleavages may indeed occur within the dermatan sulphate chains but somehow the fragments generated remain within the aggregate via interaction with undegraded segments.

The large Cuprolinic blue–stained proteoglycan filaments are more electron–dense, several times wider and up to 12 times as long as the "small" proteoglycans. These facts suggest that they are proteoglycan assemblies rather than individual molecules, although there is no direct biochemical evidence available relating to this possibility. A group of unusually large proteoglycan filaments have been observed in micrographs obtained from mouse interphotorecepter matrix which had been stained with Cuprolinic blue (Tawara et al., 1988). These filaments were assumed to consist of chondroitin sulphate–type proteoglycans which had formed into large macromolecular aggregates. It is also known that dermatan sulphate proteoglycans occasionally self–associate via their side chains (Fransson, 1976; Cöster et al., 1981; Fransson et al., 1982). Why the chondroitin/dermatan sulphate proteoglycans apparently do this in macular dystrophy corneas, where they are oversulphated (Nakazawa et al., 1984) and presumably more negatively charged, as yet remains

unclear. The occasional large proteoglycan filament which remains after the chondroitinase ABC digest of macular dystrophy cornea 4 could possibly be of the keratan sulphate variety; a minute amount was detected in the cornea of the patient even though he was classified as a type I patient. It is, however, more likely to be a chondroitin/dermatan sulphate proteoglycan which escaped the action of the enzyme.

The clinical features of macular corneal dystrophy have long been assumed to be, in some way, related primarily to the abnormal sulphation of keratan sulphate. Because this undersulphation seems to be the primary defect in macular corneal dystrophy, most of the previous work has concentrated on this aspect of the disease. This study has demonstrated that there are also considerable abnormalities in the character and distribution of the chondroitin/dermatan sulphate proteoglycans. This fact should not be overlooked. The stromal defects, which are probably the cause of corneal opification, may well be due to by the presence abnormal keratan sulphate proteoglycans. However, the abnormal chondroitin/dermatan sulphate proteoglycans may have an equal, or even greater, contribution to the existence of a pathological stromal matrix.

Measurements of the collagen fibril diameters in embedded sections of macular dystrophy tissue gave a value of 24nm, which is identical to that reported for a wide range of vertebrates including humans with normal vision (Craig & Parry, 1981). It is accepted, however, that these measurements represent collagen fibrils in a laterally shrunken state (Craig et al., 1986) and indeed, the X-ray diffraction measurements have indicated substantially larger collagen fibril diameters in hydrated corneas (Sayers et al., 1982; Worthington & Inoyue, 1985). It is clear that the disruptive procedures necessary for conventional electron microscopy, along with the fact that practical limitations place a restriction on the number of areas which can be examined, make it difficult to draw any quantitative conclusions about structural dimensions of the fibrils and the collagen matrix. This information may be obtained by analysis of the low–angle equatorial X-ray diffraction pattern.

The X-ray diffraction measurements on macular dystrophy and normal corneas have confirmed that the mean fibril diameter is about 30nm in both tissues. The mean centre–to centre fibrillar spacing for the five macular dystrophy corneas studied by equatorial X-ray diffraction was found to be reduced by varying amounts (see table 4.7). The data show that, although the distance between fibril surfaces could vary throughout the tissue, the *average* distance between the fibril surfaces is reduced from about 32nm in normal corneas to between 13nm and 22nm in macular dystrophy corneas. The electron–optical images showing varying degrees of close packing amongst the fibrils in macular dystrophy corneas can thus be reconciled with the equatorial X–ray data; electron microscopy preparation represents a more or less uniform shrinkage of collagen diameters and spacings by about 20%. Also, the meridional X–ray data seem to confirm that the occurrence, in electron micrographs, of some areas in macular dystrophy corneas where the proteoglycans run parallel to the collagen is not artifactual. If the distance between fibril surfaces, which has to accommodate extrafibrillar proteoglycans, is substantially reduced, their normal "mesh–like" organisation will presumably be affected. Whether these "parallel proteoglycans" are a primary cause or secondary effect of the close collagen packing is open to speculation. The equatorial X–ray data demonstrate that a (larger than normal) range of spacings and diameters exists in the macular dystrophy stroma. This is consistent with the appearance of apparently normal areas of collagen and proteoglycans in several macular dystrophy electron micrographs.

It is interesting that the X-ray diffraction data from macular dystrophy cornea 1 (see table 4.7) showed the same fibril diameter and interfibrillar spacing at two different hydrations (partially dehydrated and near physiological hydration). This indicates that the additional water goes elsewhere than into the fibrils themselves or between adjacent fibrils. It is most likely that the congregations of abnormal highly–charged sulphated proteoglycans draw the water into the collagen–free lacunae in which they are located.

The spacings of the collagen fibrils, as measured by X–ray diffraction, in various areas throughout macular dystrophy cornea 4 are not all equal (see figure 4.20). There does not, however, seem to be an obvious pattern to the variation. All of the twenty measurements of the interfibrillar spacing are below 60.8nm, the mean value obtained from the X-ray diffraction scan of the normal adult human cornea. This value compares very well with a previously published value of 61.9nm for adult human cornea near physiological hydration (Gyi et al., 1988). The mean of the interfibrillar spacings from macular dystrophy cornea 4 is 48.0nm which represents a reduction in the average interfibrillar spacing of about 22%; the spread of the reductions within the macular dystrophy cornea ranging from 14% to 29%.

The superiority of the synchrotron source, as compared with conventional laboratory based X–ray sets, is highlighted by the results obtained in these corneal scanning experiments. It would not have been possible to obtain such data using a conventional X–ray source since the required exposure times would each be of the order of several hours. With such long exposures it would be difficult to maintain the hydration of the tissue throughout the course of such an experiment. Even if this were to be achieved the preservation of the unfixed specimen over a period of several days would present additional complications.

Clinical studies have shown that the central cornea is, on average, about 20% thinner than normal in macular corneal dystrophy (Ehlers & Thorkild, 1978; Donnenfeld et al., 1986). The extent of thinning varied between individuals, the thickness being reduced by between 15% and 26% in one study of four patients (Ehlers & Thorkild, 1978) and by between 12% and 29% in another study of six individuals (Donnenfeld et al., 1986). Unfortunately, the pachymetric measurements of the pre–surgical corneal thickness from patient 4 are unavailable. However, his brother (patient 2) demonstrated bilateral corneal thinning; 27% in his right eye and 19% in his left. Due to this fact, and from a survey of the literature, it can be assumed with a reasonable degree of confidence that macular dystrophy

cornea 4 was typical of macular dystrophy corneas in that it was thinner than normal by about 20%. The percentage reduction in the interfibrillar distances in this case ties in very well with the assumed percentage reduction in the corneal thickness. The correlation between corneal thinning and close packed collagen fibrils was demonstrated for macular dystrophy cornea 1. In this case the central corneal thickness, prior to surgery, was measured to be 0.37mm as opposed to the normal value obtained by this surgeon of 0.52mm. This is consistent with a reduction in thickness of about 29%. The average interfibrillar separation in her cornea was measured by X-ray diffraction to be about 43nm as opposed to the measured value for the normal human cornea of about 61nm. This indicates that the distance between fibrils is also reduced by about 29%. These results strongly suggest that the corneal thinning seen in macular corneal dystrophy patients is due to an abnormal, heterogeneous, close–packed arrangement of the individual, normal diameter collagen fibrils. The percentage values obtained imply that the presence of lacunae in the matrix has minimal effect on the stromal thickness as a whole.

Of the six macular dystrophy patients whose corneas were used in the high–angle X-ray diffraction experiments, five were classed as keratan sulphate negative (type I) and one was classed as keratan sulphate positive (type II) (see table 4.6). The increase in intermolecular spacing of macular dystrophy cornea 4 with hydration (13.3Å–18.3Å; table 4.11) was in tandem with the increase of an air–dried normal human cornea (13.2Å–18.5Å; table 4.11) over a similar hydration range. This finding is in line with previous data (table 4.8), which point to the existence of a normal collagen fibril structure in macular dystrophy stromas.

The 4.61Å Bragg spacing is unique to macular dystrophy corneas. It has not been observed in corneal high–angle patterns from a variety of species, neither was it present on the patterns from the normal human corneas studied for this thesis nor on patterns from 28 human corneas which had been stored in various culture media for some time (Fullwood, N.J., personal commumication). Moreover, high–angle X-ray diffraction

studies on pathologic human corneas (7 oedematous (table 4.15) and 21 keratoconus (Fullwood, N.J., personal communication) failed to reveal the outer "extra reflection". Occasionally observed on the diffraction pattern from macular dystrophy stromas is the inner (9.62Å) reflection; this appears and becomes progressively more intense at lower hydrations. These two reflections could well be contributed to by the first and second order reflections of the same, or similar, regularly repeating structures. Accepting this assumption leaves two problems to be addressed. What are the identities of the periodic structures? Why does the intensity of the first order (inner ring) increase with decreasing hydration?

The evidence, albeit circumstantial, points towards a proteoglycan structure as the origin of the two "extra reflections". The glycosaminoglycan side chains of proteoglycan molecules consist of a polydisaccharide linked 1–3, 1–4, and the disaccharide repeat distance is usually in the range 9.5Å–9.7Å (Atkins et al., 1974; Sheehan et al., 1975). This could account for the 9.62Å structure which occurs in dehydrated macular dystrophy corneas. A 9.5Å reflection, arising from the pitch of the collagen triple helix, is observed in X-ray diffraction patterns obtained from rat tail tendon (Brodsky et al., 1988). However, it seems reasonable to discount the collagen pitch as the origin of the 9.62Å reflection, since the reflection only occurs in corneas with macular corneal dystrophy, and macular corneal dystrophy is primarily a proteoglycan defect.

The corneal stroma contains two main types of proteoglycan; one consists of a protein core to which is covalently linked one or two side chains consisting of keratan sulphate, the other has a side chain which is a mixture of chondroitin sulphate and dermatan sulphate (Gregory et al., 1982). It seems that the abnormal sulphation of corneal proteoglycans in macular dystrophy renders the outer reflection visible at all hydrations. However, the data presented here are not sufficient to allow direct identification of the proteoglycan population, if any, responsible for its appearance. A 4.61Å periodic structure causes a reflection which is extremely sharp and intense in the high-angle pattern obtained from

macular dystrophy corneas. One can hypothesise that either this is due to the unsulphation of the keratan sulphate glycosaminoglycans, the oversulphation of the chondroitin/dermatan sulphate glycosaminoglycans, or a combination of both. Presumably unsulphation of the keratan sulphate glycosaminoglycans would cause the two monosaccharides within a disaccharide to look more similar to each other than is the situation in normal cornea. Thus, one could envisage a structure with an electron density tending towards that of a monosaccharide repeat, with a periodicity 4.61Å, which would give rise to the strong outer ring. The deficiency of hydrophillic sulphate groups on the keratan sulphate glycosaminoglycans would make the outer "extra reflection" less dependant upon stromal hydration. Indeed, this is the case. The keratan sulphate disaccharide repeat could, via its first order, contribute to the 9.62Å reflection. However, the reflection's strong dependance on corneal hydration suggests a greater involvement of the chondroitin/dermatan sulphate side chains with their hydrophillic sulphate groups. Normal human cornea does not display the 9.62Å reflection, even when completely dry. The fact that macular dystrophy corneas do may well be due to aggregation of the chondroitin/dermatan sulphate proteoglycans. This phenomenon could conceivably lead to an increased number of coherently scattering disaccharide repeat distances, especially at low hydrations. The two types of disaccharides within the chondroitin/dermatan sulphate chain would lead to discontinuities in the regularity and a diffuse 9.62Å reflection. This would be further compounded by increased chondroitin–6–sulphate synthesis (Klintworth & Smith, 1977) and the presence of small amounts of oversulphated disaccharide repeats (Nakazawa et al., 1984). The enhanced intensity of the inner ring at low hydrations implies that the glycosaminoglycan structure is being altered. It can, therefore, be inferred that, as concluded by Atkins et al. (1974), water (and not just sulphate groups) may influence the structure of the glycosaminoglycans.

High angle patterns obtained from the corneas of individuals with corneal

oedema, keratoconus, Scheie's syndrome and Reis–Bücklers' dystrophy did not contain the "extra reflections". The presence of the outer "extra reflection" in the X-ray diffraction patterns from macular dystrophy corneas does not depend upon the specimens' state of hydration; neither does it depend on the type of disease under investigation. It thus represents a possible alternative, non–invasive method of post–operatively confirming a diagnosis of macular corneal dystrophy.

5.4 Oedematous Human Corneas

The conventional scanning electron microscopy techniques used in this investigation allow only limited, *in vivo*, information to be gained as to the stromal/lamellar structure because of the unknown extent of freezing processes and/or preparative artifacts. There do, however, seem to be less individual fibrils present in the oedematous case (figure 4.26). This could well be due to aggregation of collagen fibrils, possibly facilitated by the reduced number of collagen–associated proteoglycans leading to lower negative charge on adjacent fibrils. The majority of the extra stromal water seems to be located in the posterior portion of the stroma. The presence of collagen–free areas, especially in the posterior stroma, is so extensive that it seems that, even if a proportion of these are an artifactual response to freezing, the oedematous stroma could well contain its extra stromal water as a "lake" system or network.

Transmission electron micrographs of the oedematous stromas treated with Cuprolinic blue demonstrated reduced proteoglycan staining and a disproportionately high association of proteoglycan filaments with the 'd/e' collagen staining bands. In all connective tissues so far studied in this way, the 'd/e' zone is the attachment site for chondroitin/dermatan sulphate proteoglycans while the keratan sulphate proteoglycans associate with the 'a' or 'c' bands (Scott & Haigh, 1988a). Therefore, a depletion of keratan sulphate proteoglycans in the oedematous stroma is indirectly inferred. Large Cuprolinic blue stained filaments, observed mainly in collagen–free areas (figures 4.28 and 4.29), could well represent proteoglycan aggregates. Even though the glycosaminoglycan digests were not conclusive, comparison with the macular corneal dystrophy work added to the reduced keratan sulphate content of the oedematous corneas suggests that chondroitin/dermatan sulphate proteoglycans are involved. Micrographs from the areas of the oedematous stroma which demonstrate D–periodic affiliation of proteoglycans with collagen also bear a striking resemblance to micrographs of keratanase–incubated rabbit stroma which

had been treated with Cupromeronic blue (Scott & Haigh, 1985a). The keratan sulphate proteoglycans in the rabbit cornea had been digested away leaving chondroitin/dermatan sulphate proteoglycans to take up the stain. It is not clear why various glycosaminoglycanase digests of the oedematous stroma did not reveal a significant difference in the proteoglycan population. Perhaps, on this occasion, the enzymes failed to fully penetrate the tissue. There is an inherent problem with glycosaminoglycan digestions of cornea, in that if there is an obvious difference between the enzyme digested tissue sample and its control, then it can be assumed that the enzyme has worked. However, if the reverse occurs, and there is no obvious difference, no absolute conclusions can be drawn about the content and structure of the sample since there is no way of knowing, for certain, if the enzyme was able to penetrate the tissue.

In the analysis of the meridional intensities from macular corneal dystrophy stromas it was concluded that normal corneal collagen has more of its binding sites occupied by proteoglycans since its meridional orders are more greatly modified by Cuprolinic blue staining. Extrapolating this hypothesis, and taking into account the fact that staining oedematous corneas with Cuprolinic blue results in no significant change to the meridional intensities, allows us to infer that the binding of stain to the proteoglycans associated with the collagen in oedematous corneas is severely reduced. This may be due to the removal of proteoglycans from their normal binding sites or to a reduced stain–binding capacity, although it is difficult to envisage how the latter could come about. Meek et al. (1986) have shown that in bovine cornea only a small proportion of the proteoglycans are regularly associated with the collagen. Previous reports have shown a glycosaminoglycan depletion in oedematous corneas (Anseth, 1969; Cintron, 1989; Kangas et al., 1990) but have not indicated from where the glycosaminoglycans have been lost. The fact that the meridional orders exhibit no significant change when stained with Cuprolinic blue clearly demonstrates that the missing proteoglycans include a significant proportion of those which were originally associated

with the collagen fibrils. Evidence exists for the preferential loss of keratan sulphate proteoglycans from the oedematous stroma (Cintron, 1989; Kangas et al., 1990). Some of the transmission electron micrographs of oedematous corneas obtained in this study suggested that a larger proportion of chondroitin/dermatan sulphate proteoglycans remain bound to the collagen. The meridional X-ray diffraction results from oedematous human corneas do not preclude this suggestion but reveal that the reduction in chondroitin/dermatan sulphate proteoglycan binding is not negligible. If a large percentage of chondroitin/dermatan sulphate proteoglycans had remained bound to the collagen then a noticeable alteration in the meridional intensities would have been expected due to the periodic nature of the chondroitin/dermatan sulphate collagen association. One hypothesis is that oedematous corneas lose both keratan sulphate and chondroitin/dermatan sulphate proteoglycans due to leakage caused by the infiltration of water. However, a larger proportion of chondroitin/dermatan sulphate proteoglycans remain, possibly due to their stronger binding to the collagen (Gyi, 1988) and/or faster turnover rate of chondroitin/dermatan sulphate proteoglycans which occurs in oedematous corneas (Anseth, 1969).

The meridional intensities from the fixed, unstained, control oedematous corneas are not the same. Since by far the biggest difference between the control data sets is that of the first order meridional intensity, it seems that the major difference in the electron density of the corneas is in the region of the step between the gap and overlap zones. This could be due to a different response to the fixation process, although this seems unlikely. Extraction of a collagenous component from the gap zone of bovine corneal collagen renders the first order meridional intensity more intense (Wall et al., 1988). It is possible that a similar process is occurring, in varying degrees, in the oedematous stromas, caused by the influx of the extra water.

The data for the intermolecular separation of collagen in oedematous corneas (table 4.15) demonstrate a small, but not significant, increase in

four out of seven cases. Similarly, the intermolecular separation in bovine stromal collagen has recently been shown to increase by only about 6% between H=3.2 and H=5 when the corneas are swollen *in vitro* (Meek et al., 1991). This is in line with work by Kaye et al., (1982) who suggested that swelling of individual fibrils in oedematous corneas did not occur. The intermolecular spacing is restricted to a maximum of about 1.9nm, in bovine and human corneal collagen, probably because of the extension of intermolecular cross–links. Reduced keratan sulphate levels within oedematous stromas may contribute to the slight increase in intermolecular spacings noticed in some of the oedematous corneas. Collagen fibrils from human articular cartilage exhibit higher intermolecular separations in areas of the tissue where the extrafibrillar proteoglycan concentration is low (Katz et al., 1986). The conclusion from the X–ray data presented here is that a marginal increase in intermolecular spacing can occur, probably caused by the fibrils imbibing a small proportion of the extra stromal water, and this may lead to a small increase in the diameter of the collagen fibrils which is within the experimental resolution of the system. The majority of the extra stromal water imbibed during oedema, however, does not seem to locate itself within the fibrils. It seems reasonable, therefore, to assume that it exists in some type of extrafibrillar compartment or "lake" system.

The interfibrillar reflection from oedematous cornea 9 was interesting. Obtaining the reflection called for an exposure time which was an order of magnitude greater than that required for the corresponding reflection from other corneas. The fact that the fibrillar ultrastructure of this cornea is very weakly diffracting suggests that, compared to other corneas, some of the order has been lost. Also the fact that the reflection is very diffuse points to the presence of a diffracting structure which is highly disordered. The picture, then, is one of an extracellular matrix with collagen fibrils in disarray due to the influx of water. However, specimen 5, which was more hydrated, did not produce an interfibrillar ring that implied such a great deal of structural disruption. If we assume that all the extra water

imbibed by cornea 5 is homogeneously distributed between the fibrils, the volume increase of a unit cell would be substantially greater than the results imply. It can therefore be concluded that most of the water goes into "lakes". Two main types of stromal swelling can now be envisaged. The formation of large (mostly interlamellar) "lakes" would leave considerable parts of the extracellular matrix relatively undisturbed and able to produce an X-ray diffraction pattern (as seems to be the case in oedematous cornea 5). A less heterogeneous distribution of water would lead to the occurrence of many more small (mostly intralamellar) "lakes", the separation of adjacent fibrils and hence a more widespread stromal disruption. This structure would be more weakly diffracting (as seems to be the case in oedematous cornea 9). Both types of disruption seem to occur, to a greater or lesser extent, in oedematous corneas. At present it is not clear why one type predominates in a particular specimen since the basis of cohesive strength of the corneal lamellae is still poorly understood (Maurice & Monroe, 1990). The idea of various sized stromal "lakes" in oedematous corneas, arrived at by considering the X-ray diffraction evidence, is reinforced by the electron microscopical observations of the swollen extracellular matrix (figures 4.25, 4.28) and 4.29).

The average diameter of collagen fibrils in the stroma (table 4.14) is not significantly changed in oedematous cornea 5 and cornea 4, which possibly had dried down slightly from its oedematous state prior to the investigation. The suggestion that cornea 4 had become slightly dehydrated by losing water from its interfibrillar space and not its intrafibrillar space need not be a paradox. A recent study (Meek et al., 1991) demonstrated that the corneal stroma swells initially by imbibing water into the fibrils themselves, and only when the fibrils are fully hydrated does water go exclusively into the interfibrillar space. This preferential retention of stromal water within the fibrils would explain the apparently contradictory findings from cornea 4.

The immunochemical identification of glycosaminoglycans in corneal tissue from a normal human is in line with previous studies (Klintworth et

al., 1986). The bisection of the cornea indicates that the posterior section contains less keratan sulphate than does the anterior portion. This is contrary to the observation of a posteriorly increasing keratan sulphate gradient within the bovine cornea (Anseth, 1961, Bettelheim & Goetz, 1976; Castoro et al., 1988) and the hypothesis that keratan sulphate is the glycosaminoglycan which is preferentially synthesised in conditions of restricted oxygen supply (Scott & Haigh, 1988b). It should be remembered however, that the bisection of the cornea into anterior and posterior sections was not exact and invariably differed from cornea to cornea. The discrepancy with previously published work could also be explained by the fact that the present analysis is measuring the keratan sulphate epitope and not absolute keratan sulphate mass. The possibility cannot be ruled out that there are keratan sulphate proteoglycans present in the posterior portion of the normal cornea which, for some reason, contain keratan sulphate side chains which are less antigenic than those in the anterior portion. Possible reasons for this reduced antigenicity include shorter, or less highly sulphated, keratan sulphate side chains. The technique used to quantify chondroitin sulphate levels contains no such dependance on antigenicity. The reduction of the keratan sulphate levels occurs in all four of the whole thickness sections of oedematous corneas. The reduction of the ratio of corneal keratan sulphate to chondroitin sulphate in various oedematous corneas (Klintworth et al., 1986) can now, based on the results presented in this thesis, be attributed specifically to a reduction in keratan sulphate content with constant chondroitin sulphate levels.

5.5 Scheie's Syndrome

I was fortunate that the opportunity arose to briefly examine a Scheie's syndrome cornea. Fortunate on two counts; firstly because of the rarity (estimated 2 live births per million) of the condition and secondly because the disorder (deficiency of α–L–iduronidase) conceivably lent itself well to investigation using Cuprolinic blue. The specimen had been the subject of a previously published ultrastructural analysis (Zabel et al., 1988) and, not surprisingly, some of the findings echo the previous ones. The previous work did not, however, employ Cuprolinic blue staining. Disruptions of the collagen architecture, similar to those observed here, were reported (Zabel et al., 1988). The presence of fibrous long–spacing collagen in the Scheie's syndrome stroma supported the observations of others (Tabone et al., 1978; Zabel et al., 1988). Zabel and colleagues (1988) further postulated that the existence of fibrous long–spacing collagen in the corneal stroma is unique to Scheie's syndrome; indeed I have not observed it in any other pathologic stroma. Also postulated by Zabel et al., (1988) was the existence of 39nm diameter collagen fibrils in the Scheie's syndrome stroma. My electron microscopical investigation did not reveal any such structures, although maybe a more extensive study would. Equatorial X-ray diffraction would not be expected to identify such fibrils unless they were very populous within the stroma. Zabel et al, (1988) reported collagen fibrils (measured in the transmission electron microscope) to have diameters in the range 21–24nm. The authors contrast their values to a normal range of diameters, quoted as 24–28nm (Kenyon et al., 1972) and seem to suggest that their value is abnormally low. This evidence, however, does not seem to conclusively show that the majority of the collagen fibrils in the cornea of a Scheie's syndrome patient are thinner than normal. Firstly the diameter ranges appear to overlap, and, more importantly, the diameter of collagen fibrils in the transmission electron microscope is dependant upon the type of processing used; for example it has been reported as ~25–26nm (Jakus,

1954) and, more recently, ~22–24nm (Craig & Parry, 1981).

The extracellular matrix of this specimen was reported to contain deposits of electron dense material (Zabel et al., 1988) although no suggestion was made as to its possible identity. This 'storage material'(figure 8; Zabel et al., 1988) appeared diffuse and relatively homogeneous. The deposits observed in this study were much denser and well defined (figures 4.34 and 4.35); they appeared to be different entities to those observed by Zabel et al. (1988). The overall impression gained from the micrographs (including figures 4.34 and 4.35) was that the darkly–stained material was, at least in part, the cause of the stromal disruption. The possibility exists that these dense deposits represent the excessive chondroitin/dermatan sulphate material, which accumulates in the Scheie's syndrome cornea, and has, for some reason, condensed and taken up the tungstate enhanced–Cuprolinic blue stain. These deposits appear different to the large chondroitin/dermatan sulphate deposits present in macular dystrophy corneas which are assumed to be proteoglycan aggregates. This difference could come about because there is possibly a greater excess of chondroitin/dermatan sulphate glycosaminoglycan in Scheie's syndrome corneas than macular dystrophy corneas. This might be expected since the former is a storage defect due to the deficiency of a catabolic enzyme, whilst the latter is a storage deficiency of an anabolic (keratan sulphate related) enzyme which leads to possible oversulphation of chondroitin dermatan sulphate. There is no evidence of an α–L–iduronidase defect in macular corneal dystrophy.

Chapter 6

Conclusions

The intention, at the beginning of this project, was to establish a general ultrastructural picture of the normal human corneal stroma, and to observe any aberrations which accompany the reduction in transparency in specific ocular disorders. I will briefly outline what I believe to be the more interesting developments during the course of the study.

It has been demonstrated that the intimate relationship between collagen fibrils and proteoglycan macromolecules in the corneal stroma, when disturbed, has a profound effect of the ability of the tissue to function correctly. Of course, it is not possible, on the basis of these studies alone, to conclusively decide if the observed alterations in the proteoglycan–collagen arrangement are a cause of the disruption or an effect due to deformation of the extracellular matrix by unrelated processes. Of the two main pathologies investigated, it appears that the existence of proteoglycan abnormalities in the stroma is the initial cause of stromal disruption in one case and the effect of an unrelated process in the other.

It seems, from prior knowledge of the pathology of macular corneal dystrophy, that it is a condition in which the primary proteoglycan defect (abnormal synthesis of keratan sulphate proteoglycans) eventually leads to the clinical symptoms of the disease. This, I think, has long been

assumed. However, this study has demonstrated that the abnormalities in the keratan sulphate proteoglycans may not be *directly* responsible for the stromal disruption, and that abnormalities in the chondroitin/dermatan sulphate proteoglycans are just as, if not more, widespread. The fact that some mammalian corneas retain their transparency without any stromal keratan sulphate (Scott & Haigh, 1988b) suggests that the chondroitin/dermatan sulphate proteoglycans may play the greater role in influencing fibrillar architecture. The chondroitin/dermatan sulphate defect, in macular dystrophy, (abnormal distribution, oversulphation and aggregation) may therefore be a major cause of stromal disruption. The chondroitin/dermatan sulphate defect may eventually be shown to be a result of the undersulphation of keratan sulphate proteoglycans via a feedback mechanism. Nevertheless, it still represents a very important stage in the chain of events leading to the opacification of macular dystrophy corneas, a stage which has, to date, been underrated. The presence of large chondroitin/dermatan sulphate proteoglycans (along with a lack of keratan sulphate) in healing scar cornea (Hassell et al., 1983) offers an interesting, alternative, explanation of the ultrastructural stromal manifestations in macular dystrophy. It may be the case that the macular dystrophy stroma is being disrupted by "unknown" factors and the presence of large amounts of large chondroitin/dermatan sulphate proteoglycans indicates the cornea is"working overtime" in order to facilitate repair. The proteoglycan defects in the stroma of oedematous human corneas are almost certainly the result of the stromal influx of water. The data suggest that the chondroitin/dermatan sulphate proteoglycans are more strongly bound to the collagen than the keratan sulphate proteoglycans. The results seem to demonstrate the limitations of the stromal proteoglycans in ultimately preserving the architecture of the corneal stroma in the face of adversity.

The equatorial X-ray diffraction data, from the oedematous stromas, demonstrated the existence of various sized collagen–free "lakes". This was supported by the scanning and transmission electron microscopical

observations, although it should be remembered that the specimens were stored frozen and may have been susceptible to stromal deformations due to ice crystal formation. The suspicion of reduced corneal keratan sulphate associated with oedema, based on transmission electron microscopy, was reinforced by the immunochemistry. It was also very interesting to occasionally see large proteoglycans in collagen–free areas within the oedematous stroma. These observations possibly represent another case of chondroitin/dermatan sulphate aggregates in a pathological corneal stroma. The additional observation of chondroitin/dermatan sulphate possibly deposited in the stroma of the Scheie's syndrome cornea, added to the fact that it has recently been reported to form aggregates in the corneal stroma of patients with Reis–Bücklers' dystrophy (Chang et al., 1991), emphasizes its importance in the scheme of things.

6.1 Future Work

This study is not complete. Much interest remains in this field and there are several obvious aspects which deserve greater investigation.

The meridional X-ray diffraction intensities from Cuprolinic blue stained normal human cornea and the unstained controls could be analysed to obtain the axial electron densities, and hence specifically locate the proteoglycans in the tissue. The analysis could be preceded by incubation of the tissue with specific glycosaminoglycanases to differentiate between the proteoglycan populations. This analysis would require derivation of the appropriate phases.

The keratan sulphate proteoglycans should be located, possibly by immunoelectron microscopy, either within the oedematous stroma or at its boundaries.

A clinico–pathologic study could be initiated, where the ultrastructure of

the opaque versus cloudy areas within a macular dystrophy cornea could be compared. It would also be interesting to histologically observe cartilage and/or tendon (if they became naturally available) from a macular dystrophy patient to see the extent of the proteoglycan abnormalities throughout the body. Biochemical techniques need to be implemented to decide if the chondroitin/dermatan sulphate proteoglycans in macular corneal dystrophy actually do self–associate and elucidate the mechanism of aggregation. Immunolabelling of the core protein of keratan sulphate should be carried out (possibly in conjunction with Cuprolinic blue staining) in the case of macular dystrophy in order to observe its distribution, and shed light on the suggestion that it can exist in deposits with the abnormal keratan sulphate proteoglycans. Glycosaminoglycan digests of fresh macular dystrophy corneas need to be performed before the high–angle X-ray diffraction pattern is obtained to try and establish what structures are responsible for the presence of the "extra" reflections. This will present slight problems due to the need for a whole thickness cornea sample to be placed in the beam and the questionable penetration of the enzyme. It would, presumably, be obvious if the enzyme had worked but not if it hadn't. One could, therefore, not confidently discount a proteoglycan structure as the origin of the reflections.

Chapter 7

Publications

This research has led directly to the publication of five papers and five refereed abstracts. In addition, one manuscript is currently under consideration.

Papers

Quantock, A.J. & Meek, K.M. (1988) Axial electron density of human scleral collagen: location of proteoglycans by X–ray diffraction. Biophys. J., **54**, 159.

Meek, K.M., Quantock, A.J., Elliott, G.F., Ridgway, A.E.A., Tullo, A.B., Bron, A.J. & Thonar, E.J–M.A. (1989) Macular corneal dystrophy: the macromolecular structure of the stroma observed using electron microscopy and synchrotron X–ray diffraction. Exp. Eye Res., **49**, 941.

Quantock, A.J. & Meek, K.M. (1990) Proteoglycan distribution in the corneas of individuals with bullous keratopathy. Biochem Soc. Trans., **18**, 958.

Quantock, A.J., Meek, K.M., Ridgway, A.E.A., Bron, A.J. & Thonar, E.J–M.A. (1990) Macular corneal dystrophy: reduction in both corneal thickness and collagen interfibrillar spacing. Curr. Eye Res., **9**(4), 393.

Quantock, A.J., Meek, K.M., Brittain, P., Ridgway, A.E.A. & Thonar, E.J-M.A. (1991) Alteration of the stromal architecture and depletion of keratan sulphate proteoglycans in oedematous human corneas: Histological, immunochemical and X-ray diffraction evidence. Tissue and Cell (in press)

Refereed Abstracts

Quantock, A.J., Meek, K.M. & Wall, R.S. (1988) Collagen–proteoglycan interactions in pathological corneas. Proc. Int. Soc. Eye Res. Vol. V, 30.

Meek, K.M., Elliott, G.F., Gyi, T.J., Quantock, A.J. & Wall, R.S. (1988) X-ray diffraction studies on corneal collagen. Proc. Int. Soc Eye Res. Vol. V, 58.

Quantock, A.J., Meek, K.M., Elliott, G.F., Wall, R.S. & Gyi, T.J. (1989) Collagen–proteoglycan interactions in pathological corneas. Invest. Ophthalmol. and Vis. Sci. (supp.), **30**(3), 190.

Quantock, A.J., & Meek, K.M. (1990) Proteoglycan distribution in the corneas of individuals with bullous keratopathy. Proc. Int. Soc. Eye Res. Vol. VI, 196.

Quantock, A.J., Meek, K.M., Elliott, G.F., Ridgway, A., Tullo, A., Bron, A.J. & Thonar, E. (1991) Ultrastructural studies of the corneal stroma in macular dystrophy. Documenta Ophthalmologica (in press).

Manuscript under consideration

Quantock, A.J., Meek, K.M. & Thonar, E.J–M.A. Analysis of the high–angle synchrotron X-ray diffraction patterns from macular dystrophy corneas? Submitted to Cornea.

Chapter 8

References

Adachi, E. & Hayashi, T. (1987) Comparison of axial banding patterns of type V collagen and type I collagen. Coll. Rel. Res., **7**, 27.

Anseth, A. (1961) Studies on corneal polysaccharides: III. Topographic and comparative biochemistry. Exp. Eye Res., **1**, 106.

Anseth, A. (1969) Studies on corneal polysaccharides: V. Changes in corneal glycosaminoglycans in transient stromal edema. Exp. Eye Res., **8**, 297.

Aspden, R.M. & Hukins, D.W.L. (1981) Collagen organization in articular cartilage determined by X–ray diffraction and its relationship to tissue function. Proc. Roy. Soc. London, series B, **212**, 299.

Atkins, E.D.T., Isaac, D.H., Nieduszynski, I.A., Phelps, C.F. & Sheehan, J.K. (1974) The polyuronides: their molecular architecture. Polymer, **15**,263.

Axelsson, I. & Heinegård, D. (1975) Fractionation of proteoglycans from bovine corneal stroma. Biochem. J., **145**, 491.

Bach, G., Friedman, R., Weissmann, B. & Neufeld, E.F. (1972) The defect in the Hurler and Scheie syndromes: Deficiancy of α–L–iduronidase. Proc. Natl. Acad. Sci. U.S.A., **69**(8), 2048.

Balazs, E.A. (1965) *In*: The Amino Sugars Vol. 2A. (eds. Balazs, E.A. & Jeanloz, R.W.), 444, Academic Press, London.

Bansal, M.K., Ross, A.S.A. & Bard, S.B.L. (1989) Does chondroitin sulphate have a role to play in the morphogenesis of the chick primary corneal stroma? Dev. Biol., **133**, 185.

Bettelheim, F. & Goetz, D. (1976) Distribution of hexosamines in bovine cornea. Biochem. J., **15**, 301.

Birk, D.E. & Trelstad, R.L. (1984) Extracellular compartments in matrix morphogenesis; collagen fibril, bundle and lamellar formation by corneal fibroblasts. J. Cell. Biol., **99**, 2024.

Birk, D.E., Finch, J.M., Babiarz, J.P. & Linsenmayer, T.F. (1986) Collagen type I and type V are present in the same fibrl in the avian corneal stroma. Coll. Rel. Res., **2**, 541.

Borcherding, M.S., Blacik, L.J., Sittig, R.A., Bizzell, J.W., Breen, M. & Weinstein, H.G. (1975) Proteoglycans and collagen fibre organisation in human corneoseleral tissue. Exp. Eye Res., **21**, 59.

Bradshaw, J.P., Miller, A. & Wess, T.J. (1989) Phasing the meridional diffraction pattern of type I collagen using isomorphous derivatives. J. Mol. Biol., **205**, 685.

Brodsky, B.E.F., Eikenberry, K.C., Belbruno, K.C. & Sterling, K. (1982) Variations in collagen fibril structure in tendon. Biopolymers, **21**, 935.

Brodsky, B., Tanaka, S. & Eikenberry, E.F. (1988) X–ray diffraction as a tool for studying collagen structure. *In*: Collagen, Volume 1; Biochemistry (ed. Nimni, M.E) 95, CRC Press Inc., Boca Raton, Florida.

Buckley, R.J. (1987) The Cornea *In*: Clinical Ophthalmology (ed. Miller, S.) 129, I.O.P. Publishing Ltd., Bristol.

Burgeson, R.E. (1988) Do banded collagen fibres contain two or more collagen types. ISI Atlas of Science: Biochemistry, 88.

Castoro, J.A., Bettelheim, A.A. & Bettelheim, F.A. (1988) Water concentration gradients across bovine cornea. Invest. Ophthalmol. Vis. Sci., **29**, 963.

Chandross, R.J. & Bear, R.S. (1973) Improved profiles of electron density distribution along collagen fibrils. Biophys. J., **13**, 1030.

Chang, I., Sawaguchi, S., Yue, B. & Sugar, J. (1991) Sulphated proteoglycans in corneas of Reis–Bucklers dystrophy. Invest. Ophthalmol. Vis. Sci. (Supp.), **32**(4), 1004.

Chapman, J.A., Tzaphilidou, M., Meek, K.M. & Kadler, K.e. (1990) The collagen fibril – A model system for studying the staining and fixation of a protein. Electron Microsc. Rev., **3**, 143.

Cintron, C. (1989) *In*: Healing processes in the cornea. (eds. Beverman, R.W., Crossen, C.E. & Kaufman, H.E.) 105, Gulf Publishing Company, Houston, Texas.

Cintron, C., Hassinger, L.C., Kublin, C.L. & Cannon, D.J. (1978) Biochemical and ultrastructural changes in collagen during corneal wound healing. J. Ultrastruct. Res., **65**(1), 13.

Cöster, L. & Fransson, L.A. (1981) Isolation and characterisation of dermatan sulphate proteoglycans from bovine sclera. Biochem. J., **193**, 143.

Craig, A.S. & Parry, D.A.D. (1981) Collagen fibrils of the vertebrate corneal stroma. J. Ultarstruct. Res., **74**, 232.

Craig, A.S., Robertson, J.G. & Parry, D.A.D. (1986) Preservation of corneal collagen fibril structure using low temperature procedures for electron microscopy. J. Ultrastruct. Mol. Struct. Res., **96**, 172.

Donn, A. (1966) Cornea and sclera. Arch. Ophthalomol., **75**, 261.

Edward, D.P., Yue, B.Y.J.T., Sugar, J., Thonar, E.J–M.A., SundarRaj, N., Stock, E.L. & Tso, M.O.M. (1988) Heterogeneity in macular corneal

dystrophy. Arch. Ophthalmol., **106**, 1579.

Eikenberry, E.F. & Brodsky, B. (1980) X–ray diffraction of reconstituted collagen fibres. J.Mol. Biol., **144**, 397.

Fatt, I. (1978) The cornea *In*: Physiology of the Eye. An Introduction to the Vegetative Functions. (ed. Fatt, I.) 92, Buterworths, London.

Fitton-Jackson, S. (1957) The fine structure of developing bone in the embryonic fowl. Proc. Roy. Soc. London, series B., **146** 270.

Fullwood, N.J., Meek, K.M., Malik, N.S. & Tuft, S.J. (1990) A comparison of proteoglycan arrangement in normal and keratoconus human corneas. Biochem. Soc. Trans., **18**, 961.

Garner, A. (1969) Histochemistry of corneal macular dystrophy. Invest. Ophthalmol., **8**, 515.

Ghosh, M. & McCulloch, C. (1973) Macular corneal dystrophy. Can. J. Ophthalmol., **8** 515.

Gipson, I.K., Spurr-Michaud, S.J. & Tisdale, A.S. (1987) Anchoring fibrils form a complex network in human and rabbit cornea. Invest. Ophthalmol. Vis. Sci., **28**, 212.

Goldman, J.N. & Kuwabara, T. (1968) Histopathology of corneal edema. *In*: Corneal Edema (ed. Dohlman, C.H.) vol8 (3), 561, Little, Brown & Company, Boston.

Goodfellow, J.M., Elliott, G.F. & Wollgar, A.E. (1978) X–ray diffraction studies of the corneal stroma. J. Mol. Biol., **119**, 237.

Gregory, J.D., Coster, L. & Damle, S.P. (1982) Proteoglycans of rabbit corneal stroma. Isolation and partial characterisation. J. Biol. Chem., **257**, 6965.

Gregory, J.D., Damle, S.P., Covington, H.I. & Cintron, C. (1988) Developmental changes in proteoglycans of rabbit corneal stroma. Invest.

Ophthalmol. Vis. Sci., **28** (9), 1413.

Gyi, T.J. (1988) A comparison of the structure of the corneal stroma in a variety of animal species. Ph.D. Thesis, Open University.

Gyi, T.J., Meek, K.M. & Elliott, G.F. (1988) The interfibrillar spacings of collagen fibrils in the corneal stroma; a species study. Int. J. Biol. Macromol., **10**, 265.

Harding, J.J., Crabbe, M.J.C. & Panjwani, N.A. (1980) Corneal collagen. Colloques Int. Cent. Natl. Rech. Sci., **287**, 51.

Hardingham, T.E., Beardmore-Gray, M., Dunham, G. & Ratcliffe, A. (1986) Cartilage proteoglycans. *In*: Functions of the Proteoglycans. CIBA Foundation Symposium 24 (eds., Evered, D. & Whelan, J.) 30, John Wiley & Sons, Chichester, UK.

Hart, R.W. & Farrell, R.A. (1969) Light scattering in the cornea. J. Opt. Soc. Amer., **59**, 766.

Hassell, J.R., Newsome, D.A., Krachmer, J.H. & Rodrigues, M. (1980) Macular corneal dystrophy: failure to synthesise a mature keratan sulphate proteoglycan. Proc. Natl. Acad. Sci. USA, **77**, 3705.

Hassell, J.R., Newsome, D.A., Nakazawa, K., Rodrigues, M. & Krachmer, J. (1982) Defective conversion of a glycoprotein precursor to keratan sulphate proteoglycan in macular corneal dystrophy. *In*: Extracellular Matrix (eds., Hacks, S. & Wang, J.), 397, Academic Press, New York.

Hassell, J.R., Cintron, C., Kublin, C. & Newsome, D.A. (1983) Proteoglycan changes during restoration of transparency in corneal scars. Arch. Biochem. Biophys., **222**, 362.

Hassell, J.R., Hascall, V.C., Ledbetter, S., Caterson, B., Thonar, E., Nakazawa, K. & Krachmer, J. (1984) Corneal proteoglycan biosynthesis and macular corneal dystrophy. *In*: In Cell and Development Biology of the Eye. Hereditary and Visual Development. (eds., Sheffield, J.B. &

Hilfer, S.R.) 101, Springer-Verlag, New York.

Hay, E.D., & Revel, J.P. (1969) Fine structures of the developing avian cornea. *In*: Monographs in Developmental Biology, vol 1 (eds., Wolsky, A. & Chen, P.A.) S. Karger, Basel.

Heinegård, D., Björne-Persson, A., Cöster, L., Franzén, A., Gardell, S., Malmstrom, A., Paulsson, M., Sandfalk, R. & Vogel, K. (1985) The core proteins of large and small interstitial proteoglycans from various connective tissues form distinct subgroups. Biochem. J., **230**, 181.

Hirsch, M., Nicolas, G. & Pouliquen, Y. (1989) Interfibrillar structures in fast-frozen, deep-etched and rotary-shadowed extracellular matrix of the rabbit corneal stroma. Exp. Eye Res., **49**, 311.

Hodge, A.J. & Schmitt, F.O. (1960) The charge profile of the tropocollagen macromolecule and the packing arrangement in native–type collagen fibrils. Proc. Natl. Acad. Sci. USA, **46**, 186.

Hodge, A.J. & Petruska, J.A. (1963) *In*: Aspects of Protein Structure (ed., Ramachandran, G.N.) 289, Academic Press, New York.

Hulmes, D.J.S., Miller, A., White, S.W & Brodsky-Doyle, B. (1977) Interpretation of the meridional X–ray diffraction pattern from collagen fibres in terms of the known amino acid sequence. J. Mol. Biol., **110**, 643.

Hulmes, D.J.S., Miller, A., White, S.W., Timmings, P.A. & Berthet–Colominas, C. (1980) Interpretation of the low–angle meridional neutron diffraction patterns from collagen fibres in terms of the amino acid sequence. Int. J. Biol. Macromol., **2**,338.

Jakus, M.A. (1954) Studies on the cornea, I. The fine structure of the rat cornea. Am. J. Ophthalmol., **38**, 40.

Jonasson, F., Johannsson, J.H., Garner, A. & Rice, N.S.C. (1989) Macular corneal dystrophy in Iceland. Eye., **3**, 446.

Kanai, A. & Kaufman, H.E. (1973) Electron microscope studies of swollen

corneal stroma. Ann. Ophthalmol., **5**, 178.

Kanai, A., Waltman, S., Polack, F.M. & Kaufman, H.E. (1971) Electron microscope study of hereditary corneal edema. Invest. Ophthalmol., **10**(2), 89.

Kangas, T.A., Edelhauser, H.F., Twining, S.S & O'Brien, W.J. (1990) Loss of stromal glycosaminoglycans during corneal edema. Invest. Ophthalmol. Vis. Sci., **31**(10), 1994.

Kanski, J.J. (1984) Disorders of the cornea and sclera. *In*: Clinical Ophthalomology, 2nd edition (ed. Kanski, J.) 87, Butterworth & Co. Ltd., London.

Katz, E.P., Wachtel, E.J. & Maroudas, A. (1986) Extrafibrillar proteoglycans osmotically regulate the molecular packing of collagen in cartilage. Biochim. Biophys. Acta, **882**, 136.

Kaye, G.I., Edelhauser, H.F., Stern, M.E., Cassai, N.D., Weber, P. & Dische, Z. (1982) Further studies of the effect of perfusion with a calcium free medium on the rabbit cornea: Extraction of stromal componants. *In*: The structure of the Eye (ed. Hollyfield, J.G.) 271, Elsevier, Amsterdam.

Kenyon, K.R., Topping, T.M., Green, W.R. & Maumenee, M.E. (1972) Ocular pathology of the Maroteaux–Lamy syndrome (systemic mucopolysaccharidosis type VI). Am. J. Ophthalmol., **73**, 718.

Klintworth, G.K. (1980) Research into the pathogenesis of macular corneal dystrophy. Trans. Ophthalmol. Soc. UK., **100**, 186.

Klintworth, G.K. (1982) Macular corneal dystrophy – a localized disorder of mucopolysaccharide metabolism. Prog. Clin. Biol. Res., **82**, 69.

Klintworth, G.K. & Vogel, F.S. (1964) Macular corneal dystrophy: an inherited acid mucopolysaccharidosis storage disease of the corneal fibroblast. Am. J. Path., **45**, 565.

Klintworth, G.K. & Smith, C.F. (1977) Macular corneal dystrophy: Studies of sulphated glycosaminoglycans in corneal explant and confluent stromal cell cultures. Am. J. Path., **89**, 167.

Klintworth, G.K. & McCracken, J.S. (1979) Corneal diseases. *In*: Electron microscopy in human medicine (ed., Johannessen, J.V.) vol 6, 239, McGraw Hill Book Co., New York.

Klintworth, G.K. & Smith, C.F. (1980) Abnormal product of corneal explants from patient with macular corneal dystrophy. Am. J. Pathol., **101**, 143.

Klintworth, G.K. & Smith, C.F. (1983) Abnormalities of proteoglycans syntheized by corneal organ cultures derived from patients with macular corneal dystrophy. Lab. Invest., **48**, 603.

Klintworth, G.K., Meyer, R., Dennis, R., Hewitt, A.T., Stock, E.L., Lenz, M.E. Hassell, J.R., Stark, W.J., Kuettner, K.E. & Thonar, E.J-M.A. (1986) Macular corneal dystrophy – lack of keratan sulphate in serum and cornea. Ophthalmic Paediatri. Gen., **7**, 139.

Klug, H.P. & Alexander, L.E. (1974) *In*: X–ray diffraction procedures for polycrystaline and amorphous materials. Whiley, New York.

Lapiere, Ch. M., Nusgens, B, Pierard, G.E. (1977) Interaction between collagen type I and type III in conditioning bundles organization. Connect. Tissue Res., **5**, 21.

Lee, T.J., Wan, W.L., Kash, R.L., Kratz, K.L. & Schanzlin, D.J. (1985) Keratocyte survival following a controlled–rate freeze. Invest. Ophthalmol. Vis. Sci., **26**, 1210.

Maurice, D.M. (1957) The structure and transparency of the cornea. J. Physiol. (London), **136**, 263.

Maurice, D.M. (1969) The cornea and the sclera. *In*: The Eye.(ed. Davson, H.), 489, Academic Press, New York.

Maurice, D.M. (1984) The cornea and the sclera. *In*: The Eye 3rd edition, Vol. 1B, (ed. Davson, H.), 1, Academic Press, New York.

Maurice, D.M. (1988) Mechanics of the cornea *In*: The Cornea: Transactions of the World Congress on the Cornea III. (ed. Cavanagh, H.D.) Raven Press Ltd., New York.

Maurice, D.M. & Monroe, F. (1990) Cohesive strength of corneal lamellae. Exp. Eye Res., **50**, 59.

Meek, K.M. & Chapman, J.A. (1985) Glutaralderhyde induced changes in the axially–projected fine structure of collagen fibrils. J. Mol. Biol., **185**, 359.

Meek, K.M., Chapman, J.A. & Hardcastle, R.A. (1979) The staining pattern of collagen fibrils: Improved corrolation with sequence data. J. Biol. Chem., **254**(21), 10710.

Meek, K.M., Elliott, G.F., Sayers, Z., Whitburn, S.B. & Koch, M.H.J. (1981a) Interpretation of the meridional X-ray diffraction pattern from collagen fibrils in corneal stroma. J. Mol. Biol., **149**, 477.

Meek, K.M., Elliott, G.F., Sayers, Z. & Whitburn, S.B. (1981b) The distribution of electron density in corneal collagen fibrils. Curr. Eye Res., **1**, 281.

Meek, K.M., Elliott, G.F., Hughes, R.A. & Nave,C. (1983) The axial electron density in collagen fibrils from human corneal stroma. Curr. Eye Res., **2**(7), 471.

Meek, K.M., Scott, J.E. & Nave, C. (1985) An X-ray diffraction analysis of rat tail tendons treated with Cupromeronic blue. J. Microsc., **139**, 205.

Meek, K.M., Elliott, G.F. & Nave, C. (1986) A synchrotron X-ray diffraction study of bovine cornea stained with Cuprolinic blue. Coll. Rel. Res., **6**, 203.

Meek, K.M., Blamires, T., Elliott, G.F., Gyi, T.J. & Nave, C. (1987a)

The organisation of collagen fibrils in the corneal stroma; a synchrotron X-ray diffraction study. Curr. Eye Res., **6**(7), 841.

Meek, K.M., Elliott, G.F., Gyi, T.J. & Wall, R.S. (1987b) The structure of normal and keratoconus human corneas. Ophthalmic Res., **19**, 6.

Meek, K.M., Fullwood, N.J., Cooke, P.H., Elliott, G.F., Maurice, D.M., Quantock, A.J., Wall, R.S. & Worthington, C.R. (1991) Synchrotron X-ray diffraction studies of the cornea with implications for stromal hydration. Biophys. J., in press.

Miller, E.J. (1988) Collagen types: Structure, distribution and functions. *In*: Collagen, Volume I; Biochemistry. (ed. Nimni, M.E.) 139, CRC Press Inc., Boca Raton, Florida.

Miller, S.J.H. (1990) *In:* Parsons' Diseases of the Eye. (18^{th} edition), 4, Churchill Livingstone.

Mishima, S. (1968) Corneal thickness. Survey of Ophthalmology, **13**, 57.

Mishima, S. & Kudo, T. (1967) *In vitro* incubation of rabbit cornea. Invest. Ophthalmol., **6**, 329.

Morgan, G. (1966) Macular dystrophy of the cornea. Br. J. Ophthalmol., **50**, 57.

Murata, Y., Yoshioka, H., Iyama, K. & Usuka, G. (1989) Distribution of type VI collagen in the bovine cornea. Ophthal. Res., **21**, 67.

Nakao, K. & Bashey, R.I. (1972) Fine structure of collagen fibrils as revealed by ruthenium red. Exp. Mol. Pathol., **17**, 6.

Nakayasu, K., Tanaka, M., Konomi, H. & Hayashi, T. (1986) Distribution of types I, II, III, IV and V collagen in normal and keratoconus corneas. Ophthalmic Res., **18**, 1.

Nakazawa, K., Hassell, J.R., Hascall, V.C., Lohmander, S., Newsome, D.A. & Krachmer, J. (1984) Defective processing of keratan sulphate in

macular corneal dystrophy. J. Biol. Chem., **259**, 13751.

Newell, F.W. (1982) *In*: Ophthalmology; principles and concepts, 5th edition. (ed. Newell, F.W.) The C.V. Mosby Company, St. Louis, U.S.A.

Newsome, D.A., Foidart, J.M., Hassell, J.R., Krachmer, J.H., Rodrigues, M.M. & Katz, S.I. (1981) Detection of specific collagen types in normal and keratoconus corneas. Invest. Ophthalmol. Vis. Sci., **20**, 738.

Newsome, D.A., Gross, J. & Hassell, J.R. (1982) Human corneal stroma contains three distinct collagens. Invest. Ophthalmol. Vis. Sci., **22**, 376.

Newsome, D.A., Hassell, J.R., Rodrigues, M.M., Rahe, A.E. & Krachmer, J.H. (1982) Biochemical and histological analysis of 'recurrent' macular corneal dystrophy. Arch. Ophthalmol., **100**, 1125.

Nimni, M.E. & Harkness, R.D. (1988) Molecular structure and functions of collagen. *In*: Collagen, Volume 1; Biochemistry. (ed. Nimni, M.E.) 1, C.R.C. Press Inc., Boca Raton, Florida.

Orford, C.R. & Gardner, D.L. (1984) Proteoglycan association with collagen 'd' band in hyline articular cartilage. Connect. Tissue Res., **12**, 345.

Parry, D.A.D. (1988) The molecular and fibrillar structure of collagen and its relationship to the mechanical properties of connective tissue. Biophys. Chem., **29**, 195.

Poole, A.R. (1986) Proteoglycans in health and disease; structures and functions. Biochem. J., **236**, 1.

Pratt, B.M. & Madri, J.A. (1985) Immunolocalization of type IV collagen and laminin in nonbasement membrane structures of murine corneal stroma: a light and electron microscopic study. Lab. Invest., **52**, 650.

Ramachandran, G.N. (1967) Structure of collagen at the molecular level. *In*: Tretise on collagen. Volume 1 (ed. Ramachandran, G.N.) 102,

Academic Press, New York.

Sayers, Z., Koch, M.H.J., Whitburn, S.B., Meek, K.M., Elliott, G.F. & Harmsen, A. (1982) Synchrotron X-ray diffraction study of corneal stroma. J. Mol. Biol., **160**, 593.

Schwartz, W. (1953) Elektronenmicroskopische untersuchungen uber die differenzierung der cornea und sklera fibrillen des menschen. Z. Zellforsch, **38**, 78.

Scott, J.E. (1980) Collagen–proteoglycan interactions. Localization of proteoglycans in tendon by electron microscopy. Biochem. J., **187**, 887.

Scott, J.E. (1984) The periphery of the developing collagen fibril. Quantitative relationships with dermatan sulphate and other surface–associated species. Biochem. J., **218**, 229.

Scott, J.E. (1988a) Proteoglycan–fibrillar collagen interactions. Biochem. J., **252**, 313.

Scott, J.E. (1988b) Fibrillar collagen–proteoglycan interactions. ISI Atlas of Science: Biochemistry, 139.

Scott, J.E. & Orford, C.R. (1981) Dermatan sulphate rich proteoglycan associates with rat tail tendon collagen at the 'd' band in the gap region. Biochem. J., **197**, 213.

Scott, J.E. & Haigh, M. (1985a) Proteoglycan–type I collagen interactions in bone and non–calcifying connective tissues. Biosci. Rep., **5**, 71.

Scott, J.E. & Haigh, M. (1985b) "Small" proteoglycan–collagen interactions. Keratan sulphate proteoglycan associates with rabbit corneal collagen fibrils at the 'a' and 'c' bands. Biosci. Rep., **5**, 765.

Scott, J.E. & Haigh, M. (1986) Proteoglycan–collagen interactions in intervertabral disc. A chondroitin sulphate proteoglycan associates with collagen fibrils in rabbit annulus fibrosus at the 'd'–'e' bands. Biosci. Rep., **6**, 879.

Scott, J.E. & Haigh, M. (1988a) Identification of specific binding sites for keratan sulphate proteoglycans and chondroitin/dermatan sulphate proteoglycans on collagen fibrils in cornea by the use of Cupromeronic blue in 'critical electrolyte concentration' techniques. Biochem. J., **253**, 607.

Scott, J.E. & Haïgh, M. (1988b) Keratan sulphate and the ultrastructure of cornea and cartilage: a 'stand in' for chondroitin sulphate in conditions of oxygen lack? J. Anat., **158**, 95.

Scott, J.E., Orford, C.R. & Hughes, E.W. (1981) Proteoglycan–collagen arrangements in developing rat tail tendon. An electron microscopical and biochemical investigation. Biochem. J., **195**, 573.

Sheehan, J.K., Atkins, E.D.T. & Nieduszynski, I.A. (1975) X–ray diffraction studies on connective tissue polysaccharides. Two dimensional packing schemes for threefold hyaluronate chains. J. Mol. Biol., **91**, 153.

Smith, J.W. & Frame, J. (1969) Observations on the collagen and protein polysaccharide complex of rabbit corneal stroma. J. Cell Sci., **4**, 421.

Stinson, R.H., Bartlett, M.W., Kurg, T., Sweeny, P.R. & Hendricks, R.W. (1979) Experimental confirmation of calculated phases and electron density profile for wet native collagen. Biophys. J., **26**, 209.

Stuhlsatz, H.W., Muthiah, P.L. & Greiling, H. (1972) Occurrance of dermatan sulphate in calf cornea. Scand. J. Clin. Lab. Invest., **29**(supp.), 123.

Tabone, E., Grimaud, J.A., Peyrol, S., Grandperret, D. & Durand, L. (1978) Ultrastructural aspects of corneal fibrous tissue in the Scheie syndrome. Virchows Arch. B (Cell Path.), **27**, 63.

Teng, C.C. (1966) Macular dystrophy of the cornea – a histochemical and electron microscopical study. Am. J. Ophthalmol., **62**, 436.

Tomlin, S.G. & Worthington, C.R. (1956) Low–angle X–ray diffraction

patterns of collagen. Proc. Roy. Soc. Ser. A, **235**, 189.

Thonar, E.J–M.A., Lenz, M.E., Klintworth, G.K., Caterson, B., Pachman, L.M., Glickman, P., Katz, K., Huff, J. & Kuettner, K.E. (1985) Quantification of keratan sulphate in blood as a marker of cartilage catabolism. Arthritis Rheum., **28**, 1367.

Thonar, E.J–M.A., Meyer, R.F., Dennis, R.F., Lenz, M.E., Maldonando, B.A., Hassell, J.R., Hewitt, A.T., Stock, E.L., Kuettner, K.E. & Klintworth, G.K. (1986) Absence of normal keratan sulphate in the blood of patients with macular corneal dystrophy. Am. J. Ophthalmol., **102**, 561.

Veis, A. & Payne, K. (1988) Collagen fibrillogenesis. *In*: Collagen, Volume I; Biochemistry. (ed. Nimni, M.E.) 113, C.R.C. Press Inc., Boca Raton, Florida.

Velasco, A. & Hidalgo, J. (1988) Ultrastructural demonstration of proteoglycans in adult rat cornea. Tissue and Cell, **20**(4), 567.

Vogel, K.G. & Heinegård, D. (1983) *In*: Glycoconjugates (Eds. Chester, M.A., Heinegård, D., Lundbland, A. & Svensson, S.) 830, Rahms, Lund.

Vogel, K.G., Paulsson, M. & Heinegård, D. (1984) Specific inhibition of type I and type II collagen fibrillogenesis by the small proteoglycan of tendon. Biochem. J., **223**, 587.

Wall, R.S., Elliott, G.F., Gyi, T.J., Meek, K.M. & Brandford–White, C.J. (1988) Bovine corneal stroma contains a structural glycoprotein located in the gap region of the collagen fibrils. Biosci. Rep., **8**(1), 77.

Winterhalter, K.H. (1988) 8^{th} Int. Congress On Eye Research, San Francisco; Workshop proceedings (unpublished).

Worthington, C.R. & Inoyue, H. (1985) X–ray diffraction study of the cornea. Int. J. Biol. Macromol., **7**, 2.

Yang, J., SundarRaj, N., Thonar, E.J–M.A. & Klintworth, G.K. (1988)

Immunohistochemical evidence of heterogeneity in macular corneal dystrophy. Am. J. Ophthalmol., **106**, 65.

Yanoff, Y. & Fine, B.S. (1982) *In*: Ocular Pathology. A Text and Atlas. 2nd edition. Harper and Row, Philadelphia.

Young, R.D. (1985) The ultrastructural organization of proteoglycans and collagen in the human and rabbit scleral matrix. J. Cell Sci., **74**, 95.

Young, R.D., Powell, J. & Watson, P.G. (1988) Ultrastructural changes in scleral proteoglycans precede destruction of the collagen fibril matrix in necrotizing scleritis. Histopathology, **12**, 75.

Yttborg, J. & Dohlman, C.H. (1965) Corneal edema and intraocular pressure. Arch. Ophthalmol., **74**, 477.

Zabel, R.W., MacDonald, I.M., Mintsioulis, G. & Addison, D.J. (1989) Scheie's syndrome: An ultrastructural analysis of the cornea. Ophthalmol., **96**(11), 1631.

Zimmerman, D.R., Trueb, B, Winterhalter, K.H., Witmer, R. & Fischer, R.W. (1986) Type VI collagen is a major componant of the human cornea. F.E.B.S. Lett., **197**, 55.